US Army Corps of Engineers

AD-A214 990

ENVIRONMENTAL LABORATORY

Unclassified

SECURITY CLASSIFICATION OF THIS PAGE

REPORT DOCUMENTATION PAGE

Form Approved OMB No. 0704-0188

1a. REPORT SECURITY CLASSIFICATION Unclassified	1b. RESTRICTIVE MARKINGS
2a. SECURITY CLASSIFICATION AUTHORITY	3. DISTRIBUTION/AVAILABILITY OF REPORT Approved for public release; distribution unlimited.
2b. DECLASSIFICATION/DOWNGRADING SCHEDULE	
4. PERFORMING ORGANIZATION REPORT NUMBER(S)	5. MONITORING ORGANIZATION REPORT NUMBER(S) Miscellaneous Paper EL-79-6
6a. NAME OF PERFORMING ORGANIZATION Louisiana State University 6b. OFFICE SYMBOL (If applicable)	7a. NAME OF MONITORING ORGANIZATION USAEWES Environmental Laboratory
6c. ADDRESS (City, State, and ZIP Code) Baton Rouge, LA 70803-6405	7b. ADDRESS (City, State, and ZIP Code) 3909 Halls Ferry Road Vicksburg, MS 39180-6199
8a. NAME OF FUNDING/SPONSORING ORGANIZATION US Army Corps of Engineers 8b. OFFICE SYMBOL (If applicable)	9. PROCUREMENT INSTRUMENT IDENTIFICATION NUMBER
8c. ADDRESS (City, State, and ZIP Code) Washington, DC 20314-1000	10. SOURCE OF FUNDING NUMBERS See reverse. PROGRAM ELEMENT NO. / PROJECT NO. / TASK NO. / WORK UNIT ACCESSION NO.

11. TITLE (Include Security Classification)
Military Hydrology; Report 14, Breach Erosion of Earth-Fill Dams and Flood Routing (BEED) Model

12. PERSONAL AUTHOR(S)
Singh, Vijay P.; Scarlatos, Panagiotis D.

13a. TYPE OF REPORT	13b. TIME COVERED	14. DATE OF REPORT (Year, Month, Day)	15. PAGE COUNT
Report 14 of a series	FROM _____ TO _____	August 1989	128

16. SUPPLEMENTARY NOTATION
Available from National Technical Information Service, 5285 Port Royal Road, Springfield, VA 22161.

17 COSATI CODES			18. SUBJECT TERMS (Continue on reverse if necessary and identify by block number)
FIELD	GROUP	SUB-GROUP	Computer modeling, Erosion, Dams, Flooding, Dam break, Reservoirs

19. ABSTRACT (Continue on reverse if necessary and identify by block number)

A computer model has been developed for simulation of breach erosion of earth-fill dams (BEED). The model incorporates the processes of surface erosion and slope sloughing to simulate breach enlargement. Depletion of reservoir water is approximated by a volume continuity equation, while broad-crested weir hydraulics is used to describe flow over and through the breach. Due to the implicit form of these equations, an iterative solution is proposed with convergence achieved within only a few iterations. The BEED model is written in both FORTRAN 77 and BASIC computer languages. Testing of the model using historical data of the failures of Teton and Huaccoto Dams showed that timing, shape, and magnitude of the predicted outflow hydrograph were adequately simulated by this model. The same is true for the dimensions of the terminal breach. A sensitivity analysis indicated that internal friction angle and the relation for surface erosion were the major factors affecting the model results.

20. DISTRIBUTION/AVAILABILITY OF ABSTRACT ☒ UNCLASSIFIED/UNLIMITED ☐ SAME AS RPT ☐ DTIC USERS	21. ABSTRACT SECURITY CLASSIFICATION Unclassified
22a. NAME OF RESPONSIBLE INDIVIDUAL	22b. TELEPHONE (Include Area Code) / 22c. OFFICE SYMBOL

DD Form 1473, JUN 86 *Previous editions are obsolete*

SECURITY CLASSIFICATION OF THIS PAGE
Unclassified

10. SOURCE OF FUNDING NUMBERS (Continued).

DA Project No. 4A762719AT40
Task Area BO, Work Unit 052

PREFACE

The work described in this report was conducted for the Environmental Laboratory (EL) of the US Army Engineer Waterways Experiment Station (WES), under the Scientific Services Program, Short Term Analysis Service Order No. DAAG 29-81-D-001, issued by Battelle, Research Triangle Park, NC. The work was sponsored by the Headquarters, US Army Corps of Engineers (HQUSACE), under Department of the Army Project No. 4A762719AT40, Task Area BO, Work Unit 052. Mr. Austin A. Owen was the HQUSACE Technical Monitor.

The study was conducted and the report prepared by Dr. Vijay P. Singh, Department of Civil Engineering, Louisiana State University (LSU), Baton Rouge, LA, and Dr. Panagiotis D. Scarlatos, Louisiana Water Resources Research Institute, also of LSU. The authors wish to acknowledge the assistance of Mr. Cesar A. Quiroga in computer programming and Mrs. Susan Sartwell in preparation of the draft manuscript. The report was edited by Ms. Jessica S. Ruff of the WES Information Technology Laboratory.

The contract was monitored at WES by Messrs. Mark R. Jourdan and John G. Collins, Environmental Constraints Group (ECG), Environmental Systems Division (ESD), EL, under the general supervision of Mr. Malcolm Keown, Chief, ECG; Dr. Victor E. LaGarde III, Chief, ESD; and Dr. John Harrison, Chief, EL. Technical review was provided by Dr. Richard Weiss, ECG, and Mr. Jourdan.

COL Dwayne G. Lee, EN, was Commander and Director of WES during preparation of the report. Dr. Robert W. Whalin was Technical Director.

This report should be cited as follows:

Singh, Vijay P., and Scarlatos, Panagiotis D. 1989. "Military Hydrology; Report 14, Breach Erosion of Earth-Fill Dams and Flood Routing (BEED) Model," Miscellaneous Paper EL-79-6, prepared by Louisiana State University, Baton Rouge, LA, for US Army Engineer Waterways Experiment Station, Vicksburg, MS.

CONTENTS

LIST OF TABLES

LIST OF FIGURES

MILITARY HYDROLOGY

BREACH EROSION OF EARTH-FILL DAMS AND FLOOD ROUTING (BEED) MODEL

PART I: INTRODUCTION

Background

1. Under the Meteorological/Environmental Plan for Action, Phase II, approved for implementation on 26 January 1983, the US Army Corps of Engineers (USACE) has been tasked to implement a Research, Development, Testing, and Evaluation program that will (a) provide the Army with environmental effects information needed to operate in a realistic battlefield environment and (b) provide the Army with the capability for near-real time environmental effects assessment on military materiel and operations in combat. In response to this tasking, the Directorate for Research and Development, USACE, initiated the AirLand Battlefield Environment (ALBE) Thrust program. This new initiative will develop the technologies to provide the field Army with the operational capability to perform and exploit battlefield effects assessments for tactical advantage.

2. Military hydrology, one facet of the ALBE Thrust, is a specialized field of study that deals with the effects of surface and subsurface water on planning and conducting military operations. In 1977, the Headquarters, USACE, approved a military hydrology research program; management responsibility was subsequently assigned to the Environmental Laboratory, US Army Engineer Waterways Experiment Station, Vicksburg, MS.

3. The objective of military hydrology research is to develop an improved hydrologic capability for the Armed Forces with emphasis on applications in the tactical environment. To meet this overall objective, research is being conducted in four areas: (a) weather-hydrology interactions, (b) state of the ground, (c) streamflow, and (d) water supply.

4. Previously published Military Hydrology reports are listed inside the back cover. This report is the fifth that contributes to the streamflow modeling area. Streamflow modeling is oriented toward the development of procedures for rapidly forecasting streamflow parameters, including discharge,

velocity, depth, width, and flooded area from natural and man-induced hydrologic events. Specific work efforts include (a) the development of simple and objective streamflow forecasting procedures suitable for Army Terrain Team use, (b) the adaptation of procedures to automatic data processing equipment available to Terrain Teams, (c) the development of procedures for accessing and processing information included in digital terrain data bases, and (d) the development of streamflow analysis and display concepts.

Purpose and Scope

5. The work reported herein is an effort in the "Induced Floods as Linear/Area Obstacles" work unit of Department of the Army Project No. 4A762719AT40. The objective of the work unit is to provide the Armed Forces improved capabilities for forecasting the downstream flood flow impacts resulting from controlled or uncontrolled (dam breach) releases for single or multiple dams.

6. The purpose of this study was threefold:

   a. To develop a mathematical model for the simulation of gradual erosion processes of an earth dam so that the flash-flood hydrograph can be predicted.

   b. To route the released water mass through a certain distance downstream by means of an existing numerical technique.

   c. To conduct a sensitivity analysis for the various parameters involved.

7. The first phase included development of a numerical model, both for mainframe and microcomputer facilities, as well as analytical solutions for simplified versions thereof for prediction of the flash-flood hydrograph. In the second phase, the solutions provided in the first phase were used as upstream boundary conditions for the Muskingum-Cunge method with variable parameters that will route the flood wave through the receiving downstream channel. In the third phase, the combined model was applied under various conditions, and the results were compared and analyzed.

Dam Failure

8. Devastating flash floods resulting from sudden dam failure involve potential hazard to both human life and property. Jansen (1980) states that

there have been approximately 2,000 dam failures around the world since the 12th century. About 10 percent of those failures occurred during the 20th century, causing loss of more than 8,000 lives and damage costs of millions of dollars. A recent example is the failure of Stava Valley Dam in Italy on 19 July 1985, which resulted in 200 fatalities and the destruction of 20 houses and 3 hotels.

9. The International Commission on Large Dams census of 1962 registered 9,315 dams with heights greater than 15 m or between 10 and 15 m if water storage exceeds 1,000,000 m^3. However, according to Gruner (1967), the total number of dams that impose risk of serious damage in case of failure may well exceed 150,000. The US Army Corps of Engineers (1975) classified about 20,000 dams in the United States as potentially dangerous in the event of a failure. In spite of these impressive statistics, little is known about the triggering and controlling mechanisms of dam failure.

10. The majority of dams are man-made earth-filled dams. Their failure can be attributed to a single factor or to a combination of various factors such as unexpectedly large inflows, inadequate foundation, differential settlement, landslides, earthquakes, poor design or construction, deficient materials, improper management, or acts of war. The mode of failure depends both on the cause and the characteristics of the individual dam. Historical earth-dam failure data indicate that the time taken for the reservoir to empty after the dam was breached has varied from 15 min to more than 5 hr (Singh and Snorrason 1982). This is an indication that dam failure is a time-dependent and not an instantaneous process.

11. The failure processes on an earth dam are generally classified in one of the following categories: internal erosion due to piping, progressive erosion of the downstream face due to seepage, or overtopping of the crest and subsequent enlargement from erosion of an initially developed breach. Statistics based on information from several sources (Lou 1981) show that about 40 percent of failures are caused by piping or seepage, 30 percent by overtopping due to inadequate spillway capacity, 10 percent by landslides, and 20 percent by other causes classified as miscellaneous. The ability to predict dam breaching is essential for a reliable estimation of the released water hydrograph. The shape, duration, and magnitude of the dam-breach flood hydrograph affect the results of flood routing on its downstream course. Accuracy

of these results is very important for flood forecasting, contingency evacuation planning, and management decisions for dam safety.

12. The dam-break problem can be divided into two parts: dam failure processes and routing of the released mass of water downstream. The two parts can be solved separately. Of course, the sequence of the solution cannot be changed, since the results of the first part must be used as upstream boundary conditions for the study of the second part.

13. Failure of an earth dam is a very complicated, unsteady, nonhomogeneous, three-dimensional phenomenon that is still not fully understood. The size, shape, and location of the initial breach is usually unknown. The erosion processes during breach enlargement involving suspended sediment transport, layer by layer and/or mass erosion, and sloughing of the slopes are very dynamic processes that have not been defined theoretically as yet. On the other hand, routing of the flood wave downstream becomes complicated by rapid changes of the morphology of the receiving channel or basin due to scouring or shoaling, inadequate information regarding friction factors, and water mass losses due to infiltration or local storage. Another process contributing to the complexity of the problem is the presence of solid materials, in the form of mud and debris, which are carried downstream by the flowing water.

14. In spite of these difficulties, it is possible to idealize the system and to develop a mathematical model for dam break/flood routing simulation by making proper assumptions and simplifications. The accuracy of this model will be compatible with the validity of its approximations. Due to the large number of controlling physical parameters, the uncertainty of the governing processes, and the idealization of the physical system, it is essential for the sake of safety to predict the most severe conditions to be expected by conducting a sensitivity analysis. This will also provide information about the importance of each individual quantity or process within the entire dam break/flood routing simulation model.

PART II: LITERATURE REVIEW

15. Although dam break and flood routing might be coupled processes, they will be treated separately for simplicity throughout this study.

Dam-Break Mathematical Modeling

16. In spite of the importance of the subject, very few attempts have been made to mathematically model the gradual failure of an earth dam. All of the existing models are based on the principles of hydraulics, hydrodynamics, and sediment transport, but each model has its own characteristic features. A general discussion of these models is given in the following paragraphs.

Cristofano

17. The first attempt to simulate the mechanics of gradual dam breach erosion was perhaps done by Cristofano (1965), who equated the force of water flowing over the breach to the friction resistance force acting on the wetted perimeter of the breach. After some manipulation, he derived a differential equation relating the rate of change of water discharge to the rate of change of the vertical and lateral erosion within the notch. However, the application of this equation was cumbersome for manual computation and was also discontinuous in certain cases. Cristofano simplified his approach, and the following analytical expression was obtained:

$$\frac{Q_s}{Q_b} = K_c \exp\left(-\frac{\ell \tan \phi}{h}\right) \tag{1}$$

where

Q_s = sediment discharge

Q_b = water discharge through the breach

K_c = proportionality constant

ℓ = length of the breach in the flow direction

ϕ = developed angle of repose of the soil

h = hydraulic head at any given time

18. The applicability of Cristofano's model is limited by the assumption of a trapezoidal breach of constant width where the side slopes and the longitudinal slope of the breach bottom are equal to the developed angle of internal friction. There also is an uncertainty in the estimation of the proportionality constant K_c. The solution requires a trial-and-error procedure. The model was applied by the Bureau of Reclamation to Hyrum Dam, Utah, and by the Tennessee Valley Authority to Brown's Ferry Nuclear Power Plant.

Harris and Wagner

19. Harris and Wagner (1967) treated the dam failure problem as a parabolic breach subjected to erosion. The sediment transport was estimated by the Schoklitsch bed-load formula. The flow through the breach was assumed as spillway overflow, while tailwater effects were neglected. The model requires specification of breach dimensions and slope, in addition to sediment grain size and critical value of discharge for initiation of sediment motion. The applicability of the model is limited by the uncertainty of the values of various parameters involved and by neglecting tailwater effects and sloughing.

Brown and Rogers

20. Brown and Rogers (1977, 1981) reported on the Bureau of Reclamation computer program BRDAM, which was based on the work of Harris and Wagner (1967). The model, which is capable of simulating erosion from either overtopping or piping, was applied to the failure of Teton Dam, Idaho. Its limitations are similar to those of the original model of Harris and Wagner.

Fread

21. Extensive research on dam-breach flash flooding was accomplished by Fread (1977, 1978, 1980, 1981) using the National Weather Service computer program DAMBRK, which can handle rectangular, triangular, or trapezoidal breach shapes. The breaching of the dam commences after the water elevation within the reservoir exceeds a specific value, and the breach bottom enlarges at a predetermined linear rate. In the total outflow discharge, both broad-crested weir flow over the breach and flow through spillway outlets are incorporated. The DAMBRK program was applied to five historic dam-break flood cases. Although the results after calibration were satisfactory, the model cannot be applied for predictive purposes due to the requirement of a priori definitions of failure time duration and terminal shape and size of the breach. Therefore, this model is useful only for the estimation of a spectrum

of possible flooding events, not for prediction of the one most likely to occur.

Lou

22. Lou (1981) presented a model for estimation of the outflow hydrograph generated by a gradual earth-dam rupture. His model was based on the continuity and momentum equations of unsteady flow solved by Priessmann's four-point finite-difference scheme. The inertia terms of the momentum equation were neglected. For the sedimentation processes, Lou initially used DuBoy's bed-load equation along with Einstein's theory for suspended sediment transport. However, this approach, when applied to dam-erosion cases, experienced instability problems. Thus, he proceeded with a simplified sediment transport expression that he called a transport function. It was derived from the assumption that embankment erosion was proportional to the kinetic energy of the flowing water and was expressed by the following equation:

$$M = e_i t_d u^4 \tag{2}$$

where

M = mass of eroded soil

e_i = erodibility index

t_d = failure duration time

u = water velocity through the breach

23. Applicability of the model as a predicter is very limited since the duration of failure time and the erodibility index are almost impossible to predetermine. The model was calibrated and tested using the transport function approach for the failure cases of Teton Dam, Idaho, and Mantaro Dam, Peru. The results were satisfactory.

Ponce and Tsivoglou

24. Ponce and Tsivoglou (1981) developed a gradual dam-breach model using the St. Venant system of equations, which they solved numerically by the Priessmann's finite-difference scheme. The sediment routing was done by an Exner-type equation where the bed-load function was that of Meyer-Peter and Mueller (Simons and Senturk 1976). Regarding the breach morphology, they introduced a regime-type relation between top width of the breach and flow rate. This relation was applied from inception to peak flow, after which the breach was kept constant. The weakness of this model is the determination of

the rate of growth of the breach width and the neglect of the sloughing effects. The model was tested on actual data of the failure of the natural embankment that formed Mantaro Dam in Peru.

Fread

25. The latest development on breach erosion for earth-fill dams is the BREACH model presented by Fread (1984). This is an iterative numerical model based on broad-crested weir flow over the breach and quasi steady-state uniform flow along the downstream face breach channel. In development of the model, tailwater effects were included. Sediment transport was treated by the Meyer-Peter and Mueller bed-load formula. The innovative aspect of the model is the introduction of slope stability, although the theoretical derivation is for dry soil conditions. The simulation of erosion assumes that the breach slope is parallel to the downstream face slope of the dam. The applicability of the model for predictive purposes is restricted by the uncertainty of the values of critical shear stress for initiation of erosion and terminal breach width, which are required as input data by the model. The model was applied to the failures of Teton Dam, Idaho, and Mantaro Dam, Peru.

Classification and comparison of models

26. All of the existing models have some advantages and disadvantages regarding computational efficiency and realistic description of the physical processes. When they were applied to historical dam-failure cases, all of the models showed an acceptable degree of accuracy. Of course this is due partially to the fact that a number of parameters can be calibrated to improve simulation results. The basic philosophy for mathematical modeling of dam-break problems is the coupled treatment of the two phases involved, i.e., reservoir water and sediment from the dam body. Governing equations and the number and nature of physical and empirical parameters determine the suitability of the model for prediction.

27. Similarities and differences of the various models are given in Table 1. This illustrates the evolution and expansion of the technology of earth-dam failure simulation during the last 20 years, from the simple conceptual model of Cristofano to the most sophisticated BREACH model of Fread. Improvement of the existing state of the art can be achieved by reducing the number of parameters needing calibration and by introducing more realistic assumptions for both water discharge and sediment transport mechanisms.

Table 1

Mathematical Models for Dam-Breach Erosion

Model (Year of Publication)	Hydrodynamic Approach	Sediment Transport	Solution Algorithm	Breach Morphology	Characteristic Parameters	Other Features
Cristofano (1965)	Broad-crested weir hydraulic relation	Empirical relation	Manual-iterative	Constant width	Proportionality constant, angle of repose	No tailwater effects, no sloughing
Harris and Wagner (1967)	Broad-crested weir hydraulic relation	Schoklitsch bed-load formula	Numerical	Parabolic shape	Grain size, critical discharge value, breach dimensions and slope	No tailwater effects, no sloughing
BRDAM (Brown and Rogers 1977, 1981)						
DAMBRK (Fread 1977)	Broad-crested weir hydraulic relation	Linear pre-determined rate of erosion	Numerical-iterative	Rectangular, triangular, trapezoidal	Failure duration time, terminal size and shape of breach	No sloughing
Lou (1981)	St. Venant system of equations	Empirical relation	Preissmann's four-point finite difference	Regime-type relation between top width and flow rate	Coefficients of the regime relation, critical shear stress	No sloughing
Ponce and Tsivoglou (1981)		Meyer-Peter and Mueller bed-load formula				
BREACH (Fread 1984)	Broad-crested weir hydraulic relation	Meyer-Peter and Mueller bed-load formula	Numerical-iterative	Rectangular changing to trapezoidal	Critical shear stress-grain size-cohesion friction angle	Tailwater effects and sloughing are included

Note: Bracket indicates that models are included in the same category due to their similarities.

Breach Characteristics

28. One of the weak points in the studies of earth-dam failures is the breach morphology. Breach shapes and dimensions have been documented in many cases, but predictive correlations are very limited. The same is true of the failure duration time. Information on pertinent earth-dam breach characteristics for 52 cases is given in Table 2 (Ponce 1982; Singh and Snorrason 1982; MacDonald and Langridge-Monopolis 1984).

29. Singh and Snorrason (1982) analyzed the historic data for 20 dams and provided information on the three breach parameters: width of breach, initial hydraulic head for failures caused by overtopping, and failure duration time.

30. Ponce (1982) presented a preliminary analysis of certain parameters relevant to the breach morphology. For his analysis he used the breach Froude number F :

$$F = \frac{Q_p}{B\left(gd^3\right)^{1/2}} \tag{3}$$

and a shape factor S_F , defined as

$$S_F = \frac{Bd}{B_D Z_o} \tag{4}$$

where

Q_p = peak outflow discharge
B = top width of the breach
g = acceleration due to gravity
d = depth of breach
B_D = top width of dam
Z_o = initial height of dam

By plotting the data from 29 historical cases (Figure 1), Ponce derived the relation

$$F = 0.20 S_F^{-0.39} \tag{5}$$

Table 2

Physical Characteristics and Breach Historical Data from Dam Failures

Name and Country of Dam (Reference Number)	Year Built/ Failed	Height m	Crest Width m	Dam Slopes Vertical: Horizontal*	Storage m^3	Peak Outflow Discharge m^3/sec	Breach Width, m (Top/Bottom/Average)	Breach Depth m	Time of Failure hr
Apishapa, USA (1)	1920/1933	34	4.9	1:3/1:2	2.25×10^7	6.85×10^3	91.5/ 81.5/ 86.5	30.5	2.5
Baldwin Hills, USA (2)	1951/1963	49	19	1:2/1:1.8	1.10×10^6	1.1×10^3	23 / 10 / 16.5	27.5	1.3
Bradfield, England (3)	1863/1864	29	--	--	3.20×10^6	1.15×10^3	-- / -- / --	--	< 0.5
Break Neck Run, USA	1877/1902	7	--	--	4.9×10^4	9.2	-- / -- / 30.5	7	3
Buffalo Creek, USA	1972/1972	14	128	1:1.6/1:1.3	6.10×10^5	1.42×10^3	153 / 97 /125	14	0.5
Bullock Drew Dike, USA	1971/1971	5.8	4.3	1:2/1:3	1.13×10^6	--	13.6/ 11.0/ 12.3	5.8	--
Canyon Lake, USA	1938/1972	6	--	--	9.85×10^5	--	-- / -- / --	--	0.10
Cheaha Creek, USA	1970/1970	7	4.3	1:3/1:2.5	6.9×10^4	--	-- / -- / --	--	5.5
Coedty, England	1924/1925	11	--	--	3.1×10^5	--	67 / 18.2/ 42.5	--	--
Eigiau, England (10)	1908/1925	10.5	--	--	4.52×10^6	4.0×10^2	-- / -- / --	--	--
Elk City, USA	1925/1936	9	--	1:3/1:2	7.4×10^5	--	45.5/ -- / --	9	--
Frindale, Canada	1910/1912	10.5	--	--	--	--	39.5/ -- / --	4.6	< 0.5
Euclides de Cunha, Brazil	1958/1977	53	--	--	1.36×10^7	1.02×10^3	131 / -- / --	53	7.3
Frankfurt, Germany	1975/1977	10	--	--	3.5×10^5	$7.9 \times 10_2$	9.2/ 4.6/ 6.9	10.0	2.5
French Landing, USA (15)	1925/1925	12	2.5	1:2/1:2.5	--	9.3×10^2	41 / -- / --	14.2	0.58
Frenchman Creek, USA	1952/1952	12.5	6	1:3/1:2	2.10×10^7	1.41×10^3	67 / 54.4/ 60.4	12.5	--
Frias, Argentina	1940/1970	--	--	1:1/1:1	--	--	62 / -- / --	15	0.25
Goose Creek, USA	1903/1916	6	3	1:1.5/1:1.5	1.06×10^7	5.65×10^2	30.5/ 22.3/ 26.4	4.1	0.5
Grand Rapids, USA	1874/1900	7.5	3.7	1:1.5/1:1.5	2.22×10^5	--	12.2/ 6.0/ 9.1	7.5	< 0.5
Hatchtown, USA	1908/1914	19	6	1:2/1:2.5	1.48×10^7	2.1×10^3	180 /140.4/160.2	19.0	3
Hatfield, USA	1908/1911	6.8	--	--	1.23×10^7	3.4×10^3	-- / -- / 91.5	6.8	2
Hebron, USA	1913/1914	11.5	3.7	1:3/1:1.5	--	--	61 / 30.4/ 45.7	15.3	2.25
Johnston City, USA	1921/1981	4.3	1.8	1:4.75/1:2.75	5.75×10^5	--	13.4/ 2 / 7.7	5.2	--
Kaddam, India	1957/1958	12.5	--	--	2.14×10^8	--	30 / -- / --	15.2	1
Kelly Barnes, USA	1948/1977	11.5	6	1:1/1:1	5.05×10^5	6.8×10^2	35 / 18 / 26.5	11.5	0.5
Lake Avalon, USA	1894/1904	14.5	--	--	7.75×10^6	2.32×10^3	-- / -- /137	14.5	2
Lake Barcroft, USA	1913/1972	21	--	--	3.12×10^6	--	23 / -- / --	11	> 1
Lake Frances, USA	1899/1899	15	5	1:3/1:2	8.65×10^5	--	30 / 10.4/ 20.2	15	1
Lake Latonka, USA	1965/1966	13	--	--	1.59×10^6	2.9×10^2	-- / -- / 33.5	13	3
Laurel Run, USA	-- /1977	13	--	--	3.85×10^5	1.05×10^3	-- / -- / --	--	--
Little Deer Creek, USA	1962/1963	26	--	--	1.73×10^6	1.33×10^3	23 / -- / --	21.4	0.33
Lower Two Medicine, USA	1913/1964	11	--	--	1.96×10^7	1.8×10^3	-- / -- / --	--	--
Lyman, USA	1913/1915	20	3.7	1:2/1:2	4.95×10^7	--	107 / 87 / 97	20	--
Mammoth, USA	1916/1917	21.3	--	--	1.36×10^8	2.52×10^3	-- / -- / 9.2	21.3	3
Manchhu II, India	--/1979	60	6	1:3/1:2	1.10×10^8	--	540 / -- / --	60	2.0
Melville, USA	1907/1909	11	3	1:3/1:1.5	--	--	40 / -- / --	11	--
Nanaksagar, India	1962/1967	16	--	--	2.1×10^8	9.7×10^2	-- / -- / 46	16	12
North Branch, USA	--/1977	--	--	--	--	2.9×10^2	-- / -- / --	--	--
Oakford Park, USA	--/1903	6	2.6	--	--	--	23 / -- / --	4.6	1

(Continued)

* Entries are presented as upstream/downstream.

Table 2 (Concluded)

Name and Country of Dam (Reference Number)	Year Built/ Failed	Height m	Crest Width m	Dam Slopes Vertical: Horizontal	Storage m^3	Peak Outflow Discharge m^3/sec	Breach Width, m (Top/Bottom/Average)	Breach Depth m	Time of Failure hr
Oros, Brazil (40)	1960/1960	35.5	--	--	6.5×10^8	1.15×10^4	200 / -- / --	35.5	--
Otto Run, USA	-- /1977	--	--	--	--	6.0×10^2	-- / -- / --	--	--
Rito Manzanares, USA	-- /1975	7.3	3.7	1:1.34/1:1.34	2.46×10^7	--	19 / -- / --	7.3	--
Salles Oliveira, Brazil	1966/1977	35	--	--	2.59×10^4	7.2×10^3	-- / -- /168	35.2	
Sandy Run, USA	-- /1977	8.5	--	--	5.68×10^6	4.35×10^2	-- / -- / --	--	--
Schaeffer, USA	-- /1921	30.5	4.6	1:3/1:2	3.92×10^6	4.5×10^3	210 / -- / --	27.5	0.5
Sheep Creek, USA	1969/1970	17	6	1:3/1:2	1.43×10^4	--	30.5/ 13.5/ 22	17	--
Sherburne, USA	1892/1905	10.5	--	--	4.2×10^4	9.6×10^2	46 / -- / --	--	--
Sinker Creek, USA	1910/1943	21	--	--	3.33×10^6	--	92 / 49.2/ 70.6	21.0	2
South Fork, USA	-- /1977	--	--	--	--	1.22×10^2	-- / -- / --	--	--
Spring Lake, USA	1887/1889	5.5	2.5	1:0.75/1:0.75	1.35×10^5	--	20 / 9 / 14.5	5.5	--
Teton, USA	1972/1976	93	10.5	1:3/1:2.5	3.56×10^8	6.6×10^4	-- / -- / 46	79	4
Wheatland No. 1, USA (52)	1893/1969	13.6	6	--	1.15×10^7	--	46 / 41 / 43.5	13.5	1.5

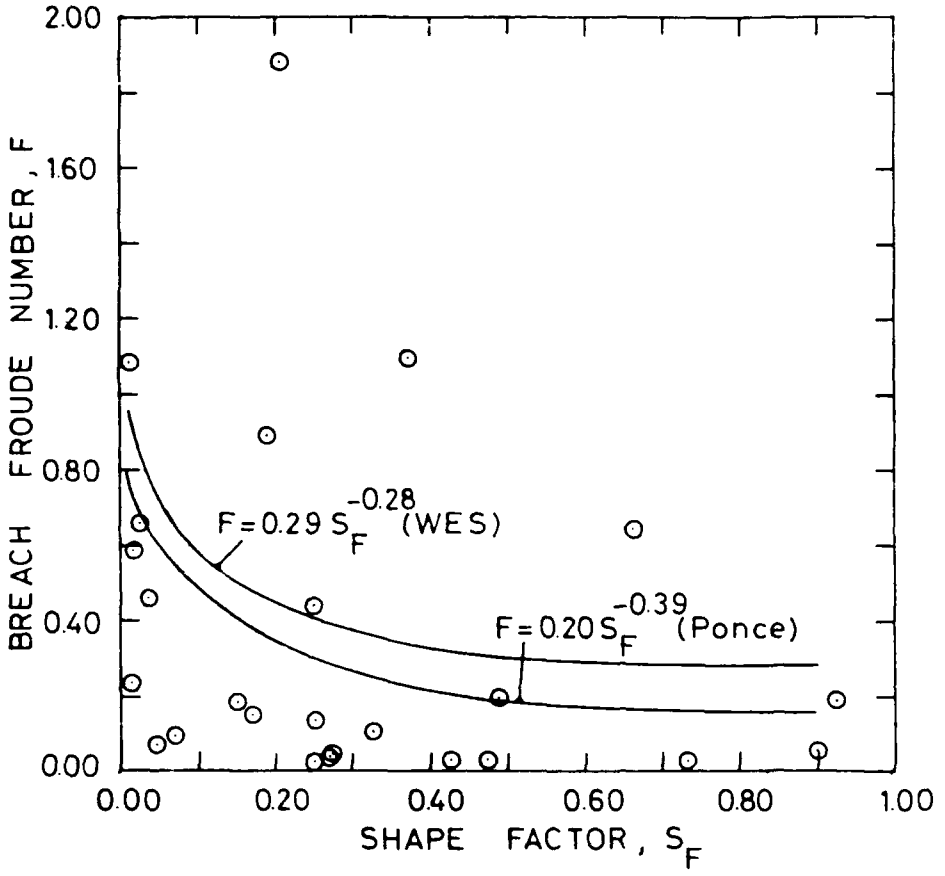

Figure 1. Breach Froude number versus shape factor (after Ponce 1982)

which is comparable to the equation reported by the US Army Corps of Engineers (1961),

$$F = 0.29S_F^{-0.28} \tag{6}$$

31. Another interesting compilation of breach characteristics data was presented by MacDonald and Langridge-Monopolis (1984), who analyzed 42 cases and suggested an empirical methodology for predicting the shape, size, and failure time for an earth-fill dam. Their methodology is based on Figures 2-4. In Figures 2 and 3, they make use of a "breach formation factor," which is defined as the product of the discharged volume of water and the difference in elevation between peak reservoir water surface and breach base. By estimating the breach formation factor, they obtain breach volume from Figure 2. Having the volume of breach, they use Figure 4 for prediction of

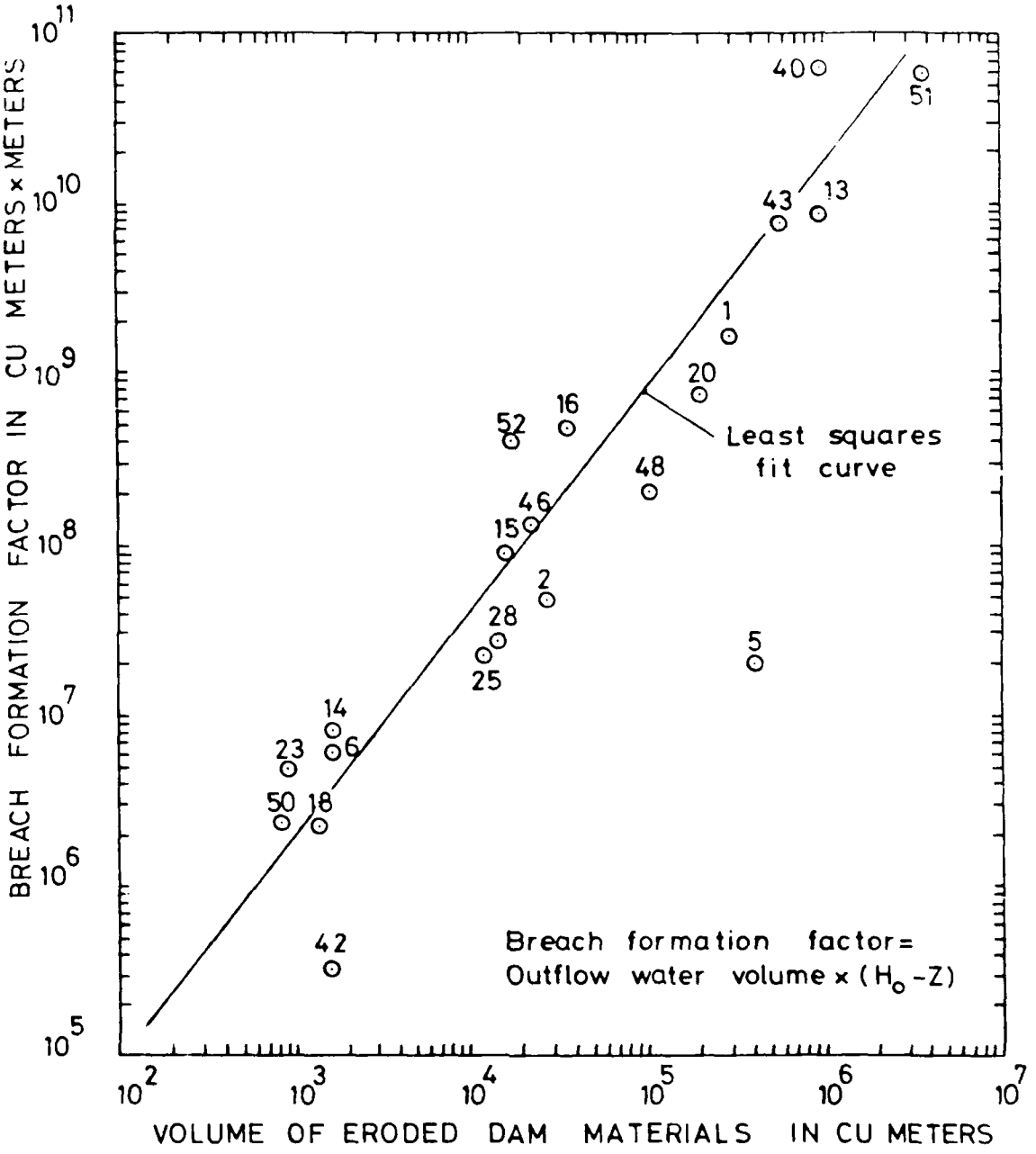

Figure 2. Outflow characteristics versus breach size (reference numbers are identified in Table 2) (after MacDonald and Langridge-Monopolis 1984)

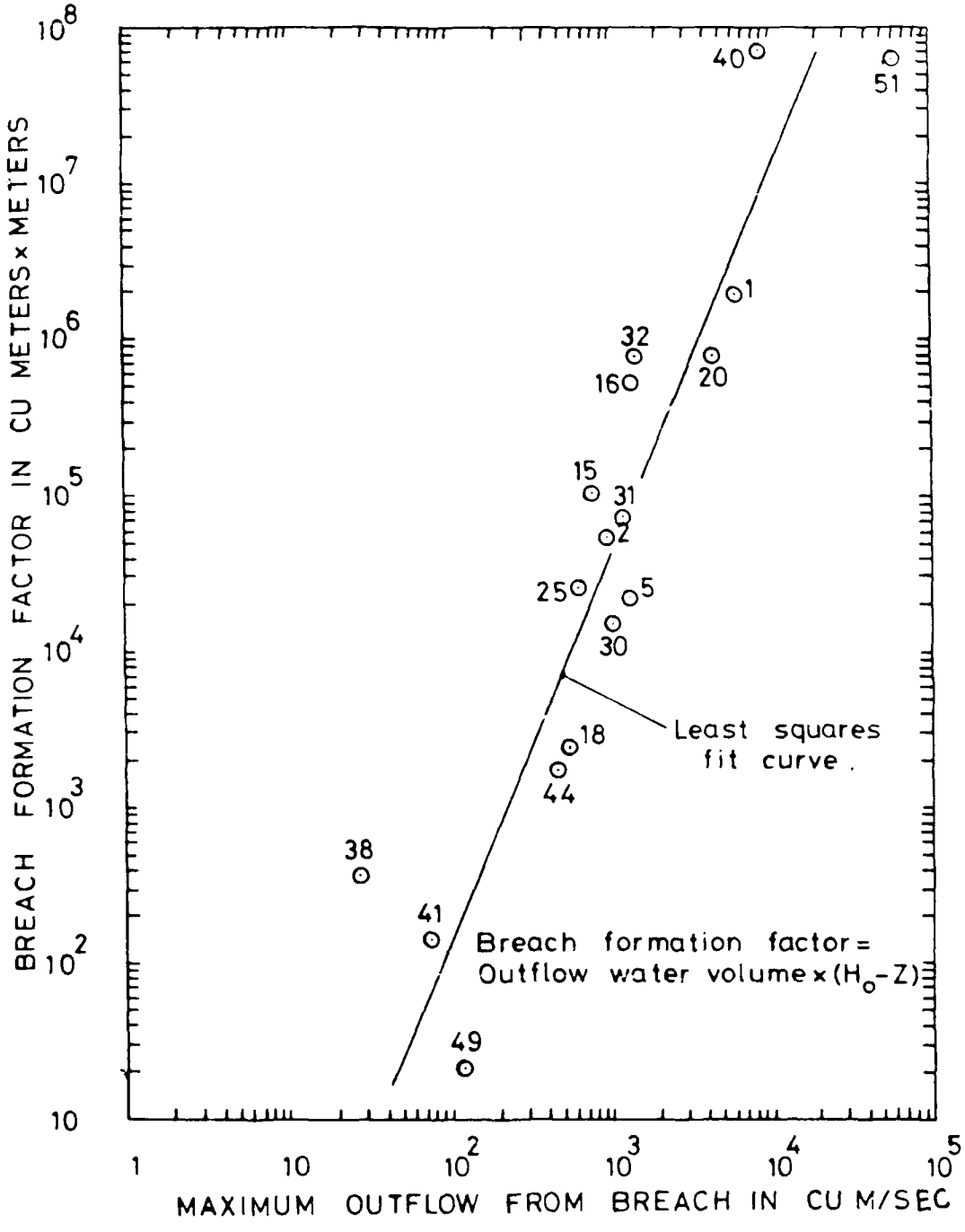

Figure 3. Outflow characteristics versus peak breach outflow (reference numbers are identified in Table 2) (after MacDonald and Langridge-Monopolis 1984)

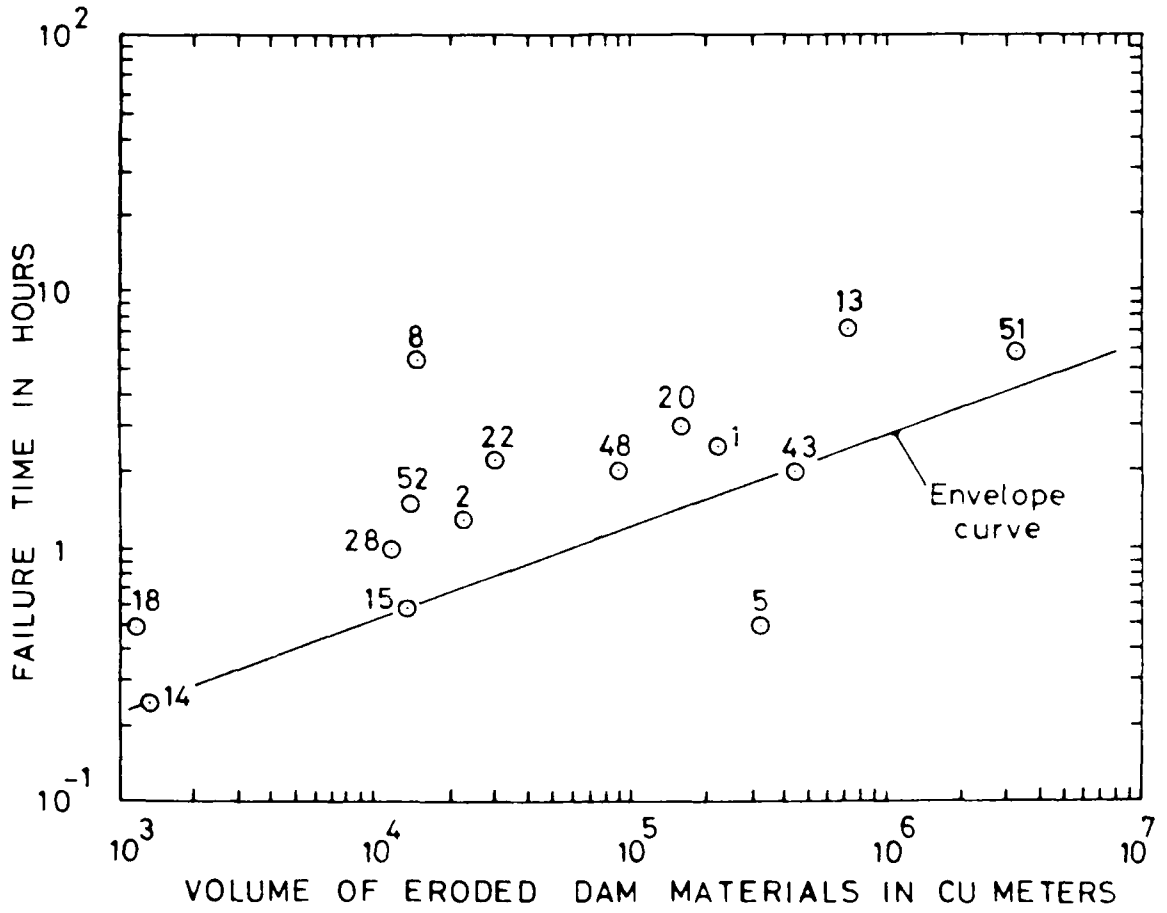

Figure 4. Breach failure time versus volume (reference numbers are identified in Table 2) (after MacDonald and Langridge-Monopolis 1984)

failure time. The same authors suggested a triangular breach shape with 2V:1H side slopes, which turns into a trapezoidal shape after the breach reaches the base of the dam. Houston (1984) reanalyzed the previous data, proposing a trapezoidal breach with 1V:1H side slopes and base width equal to the depth of the breach.

32. Further analysis of breach characteristics is given in Figures 5 and 6 where the breach top (B), bottom (b), and average widths are plotted versus the height of dam and the depth of breach, respectively. Using least squares curve fitting approximation, the following relations were obtained:

$$B = 4.45Z_o \quad (7)$$

$$b = 2.04Z_o \quad (8)$$

$$b = 2.66d \quad (9)$$

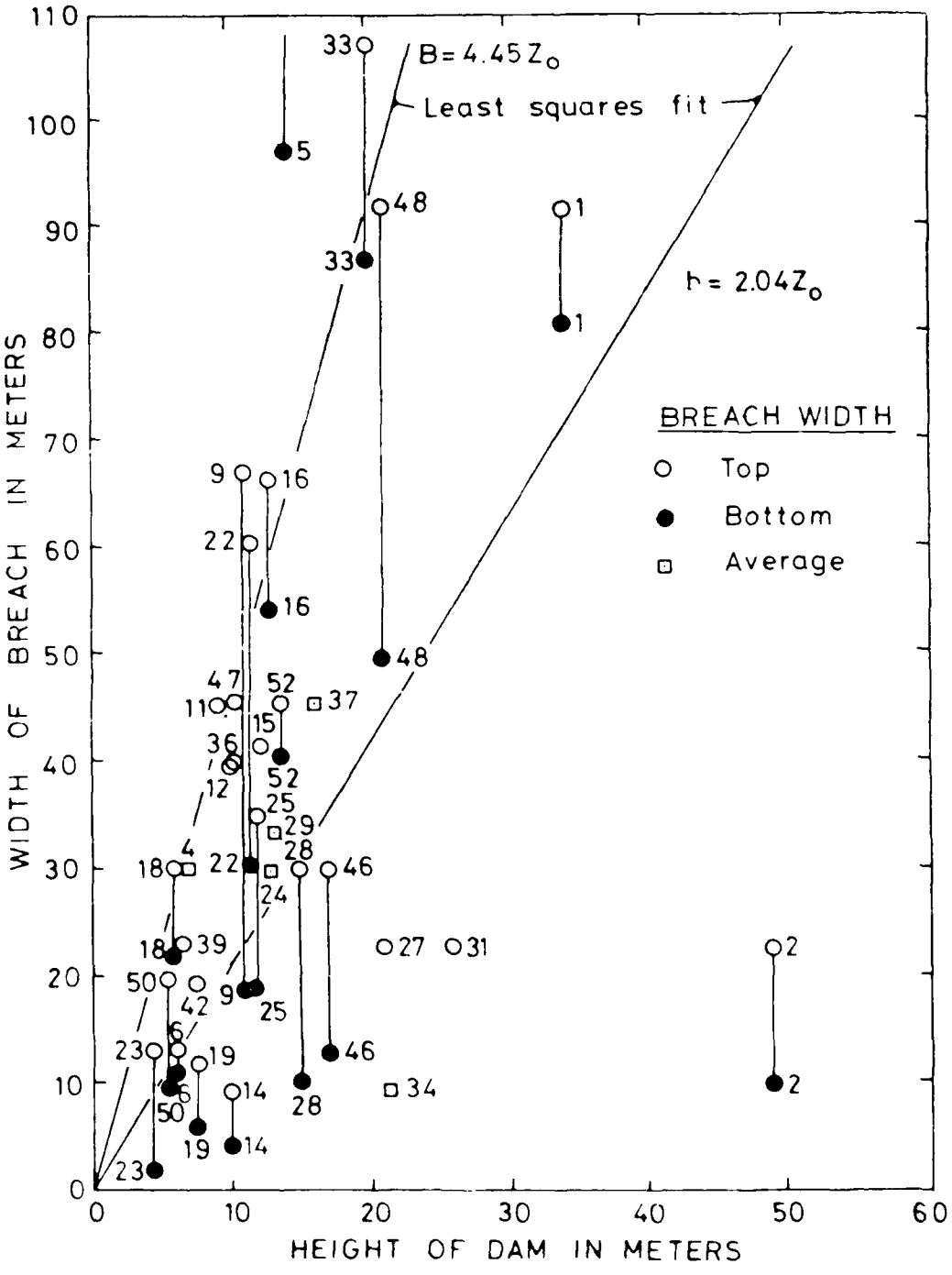

Figure 5. Breach width versus height of dam (reference numbers are identified in Table 2)

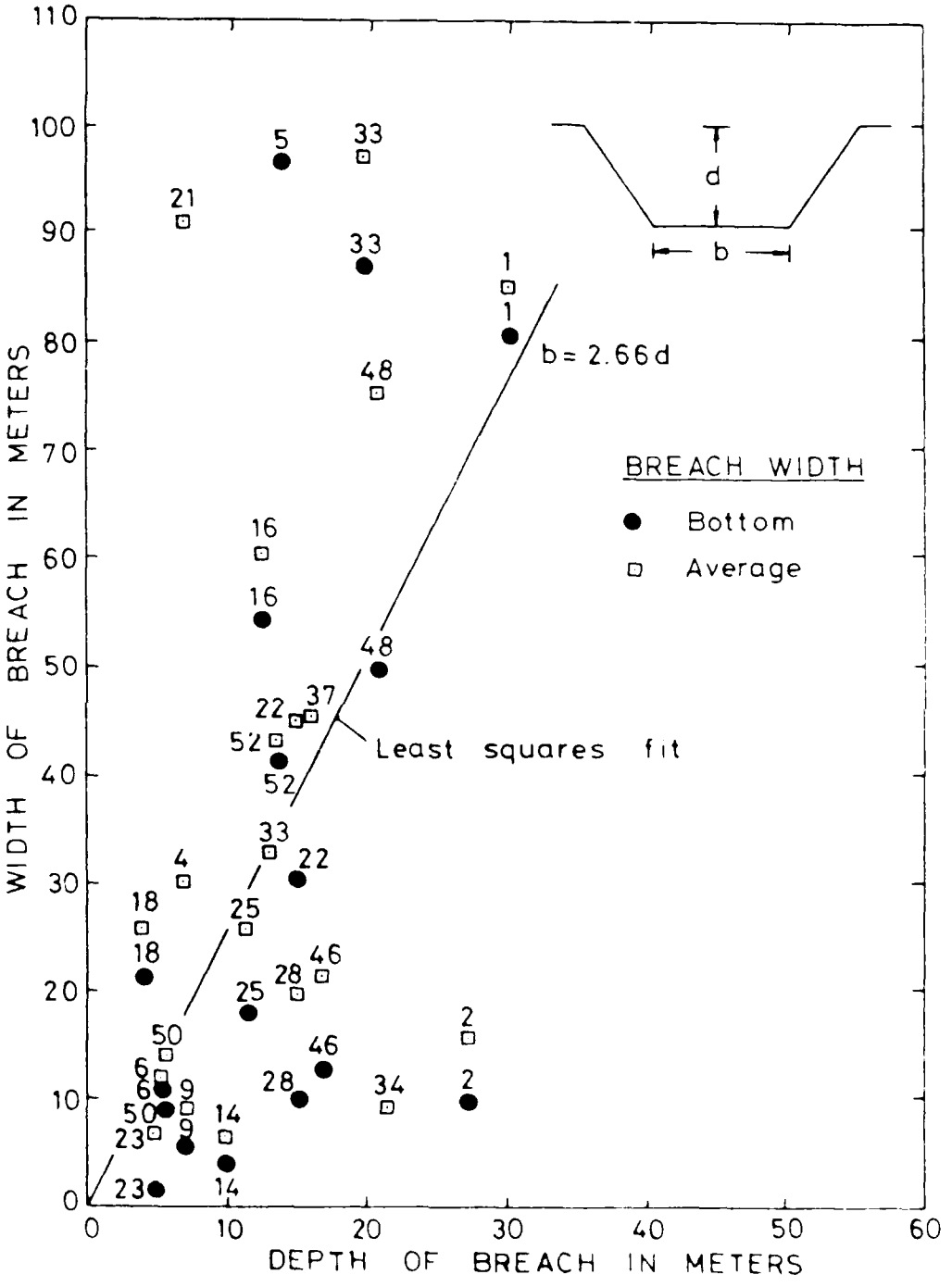

Figure 6. Breach width versus depth of breach (reference numbers are identified in Table 2)

The constant coefficient in Equation 8 is less than the one in Equation 9 because breach depth d is sometimes less than the dam height Z_c, which means partial failure occurred. Indeed, in 9 of 39 documented dam cases, the failure was partial.

33. Based on the data of Table 2, the probability of exceedance of dam failure time is plotted in Figure 7. In the same figure, the probability of exceedance of the initial hydraulic head for an overtopping failure event is also plotted using data from Singh and Snorrason (1982). Thus, with a 50-percent probability, failure time will be about 1.10 hr, while initial head will be approxiately 0.4 m.

34. Although these results provide valuable information about the order of magnitude of breach characteristics when applied, they should be used with caution and judgment. The scattering of the data points and lack of

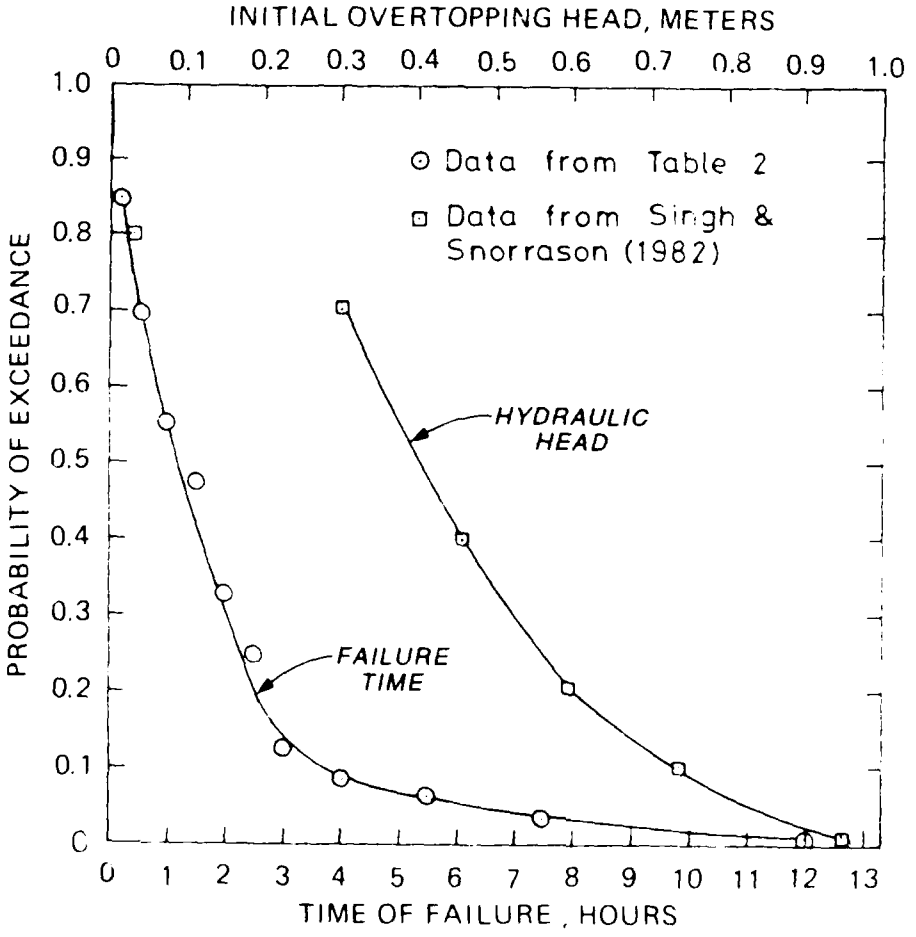

Figure 7. Probability of exceedance of initial overtopping hydraulic head and failure time

theoretical explanation restrict the applicability of those empirical relations and indicate the need for a more thorough and detailed analysis of breaching mechanisms.

Mathematical Modeling of Flood Routing

St. Venant system of equations

35. Propagation of a flood wave through the receiving channel and floodplain can be successfully described by means of unsteady, incompressible, free-surface hydrodynamic equations. More specifically, they compose the so-called St. Venant system of equations expressed as

$$\frac{\partial A}{\partial t} + \frac{\partial Q}{\partial x} = q_o \quad \text{(Continuity)} \tag{10}$$

$$\frac{\partial Q}{\partial t} + \frac{\partial}{\partial x}\left(\frac{Q^2}{A}\right) + gA\,\frac{\partial y}{\partial x} + gA\left(S_f - S_o\right) = 0 \quad \text{(Momentum)} \tag{11}$$

where

A = wetted cross section

t and x = time and distance coordinates, respectively

Q = water discharge

q_o = lateral inflow

y = water depth

S_f = energy loss gradient

S_o = slope of the channel

To determine the energy gradient, either Chezy's or Manning's friction relation can be applied. For completeness of the problem, both the initial and boundary conditions must be provided.

36. The St. Venant system of equations is a nonlinear partial differential system of the hyperbolic type for which no general analytical solution is known. Solution of that system can be obtained only by means of three main numerical techniques: the characteristics, the finite differences, and the finite elements. Each method is described in the following paragraphs.

37. Characteristics technique. The main feature of this method is the transformation of the original partial differential system of two equations

into an ordinary differential system of four equations. This is possible because the system is hyperbolic. The characteristics can be defined as propagation paths of a geometric or physical disturbance. For a channel of constant width and zero lateral inflow, Equations 10 and 11 can be written as

$$\frac{\partial y}{dt} + u \frac{\partial y}{\partial x} + y \frac{\partial u}{\partial x} = 0 \tag{12}$$

$$\frac{\partial u}{\partial t} + u \frac{\partial u}{\partial x} + g \frac{\partial y}{\partial x} + g(S_f - S_o) = 0 \tag{13}$$

Combining Equations 12 and 13 and the total differentials (du,dy) yields

$$\begin{bmatrix} 1 & u & 0 & y \\ 0 & g & 1 & u \\ dt & dx & 0 & 0 \\ 0 & 0 & dt & dt \end{bmatrix} \begin{bmatrix} \frac{\partial y}{dt} \\ \frac{dy}{\partial x} \\ \frac{\partial u}{\partial t} \\ \frac{\partial y}{\partial x} \end{bmatrix} = \begin{bmatrix} 0 \\ g\ (S_o - S_f) \\ dy \\ du \end{bmatrix} \tag{14}$$

Equation 14 has a defined solution if and only if (Abbott 1966):

$$\left(\frac{dx}{dt}\right)^+ = u + \sqrt{gy} = u + c_o = C^+ \tag{15}$$

$$\left(\frac{dx}{dt}\right)^- = u - \sqrt{gy} = u + c_o = C^- \tag{16}$$

$$\left(\frac{dJ}{dt}\right)^+ = \frac{d(u + 2c_o)}{dt} = g(S_o - S_f) \tag{17}$$

$$\left(\frac{dJ}{dt}\right)^- = \frac{d(u + 2c_o)}{dt} = g(S_o - S_f) \tag{18}$$

where

$C^{\pm}$ = wave characteristics

$J^{\pm}$ = Riemann's quasi-invariants

c_o = wave celerity

38. Thus, the system of Equations 12 and 13 has been transformed into the system of Equations 15-18. The new system can be solved graphically (Schonfeld 1951), semigraphically (Chow 1959), or numerically. The numerical solution is based on the finite-difference techniques. The solution can be obtained either on a characteristics grid (Figure 8) in explicit form (Faure and Nahas 1961) or implicit form (Amein 1966), or on a fixed grid (Figure 9) in explicit form (Stoker 1957) or implicit form (Mozayeny and Song 1969).

39. Finite-difference technique. The main feature of finite-difference techniques is approximation of the derivatives in the governing equations by truncated Taylor Series so that the solution is obtained on nodal points of a rectangular x-t fixed-grid system. The solution proceeds from time step j to time step $j+1$. If the computation advances by solving a single equation, the numerical scheme is explicit. If the computation requires the solution of a system of equations, the scheme is implicit. Explicit schemes were suggested by Isaacson, Stoker, and Troesch (1958), by Courant, Freidrichs, and Lewy (1967), by Lax and Wendroff (1960, 1964), and by Dronkers (1964). Implicit schemes were given by Preissman, Vasilier, and Abbott (Mahmood and Yevjevich 1975) and by Dronkers (1969).

40. Finite-element technique. In this method the solution domain is subdivided into a number of subdomains, the finite elements, and for each element the unknowns $\chi^{(e)}$ are approximated in discrete form as

$$\chi^{(e)} = \sum_{i}^{m} N_i \chi_i \tag{19}$$

where

N_i = shape functions

χ_i = value of the unknowns on the nodal points

m = number of nodes of each element

Substitution of the approximate solutions (Equation 19) into the governing equations produces an error that is minimized either by means of variational calculus or by the more general method of weighted residuals (Finlayson 1972).

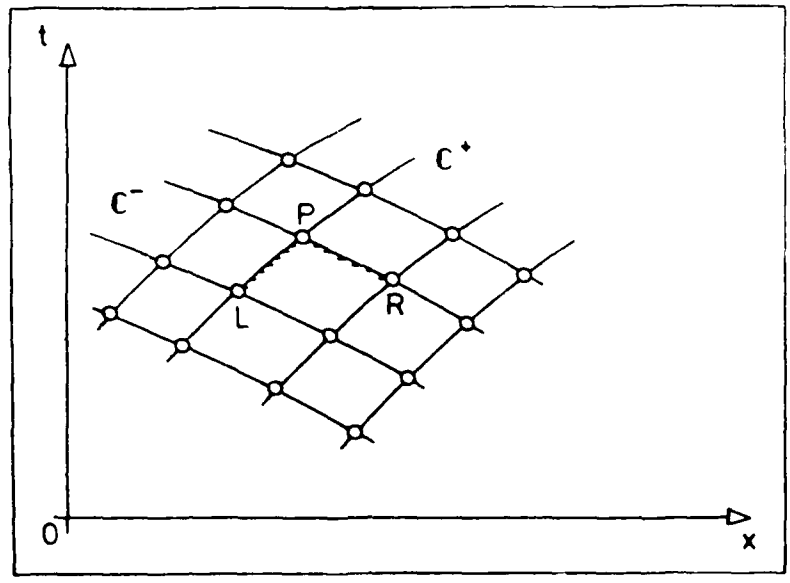

Figure 8. Two-dimensional characteristics grid (L = left, P = point of determination, R = right)

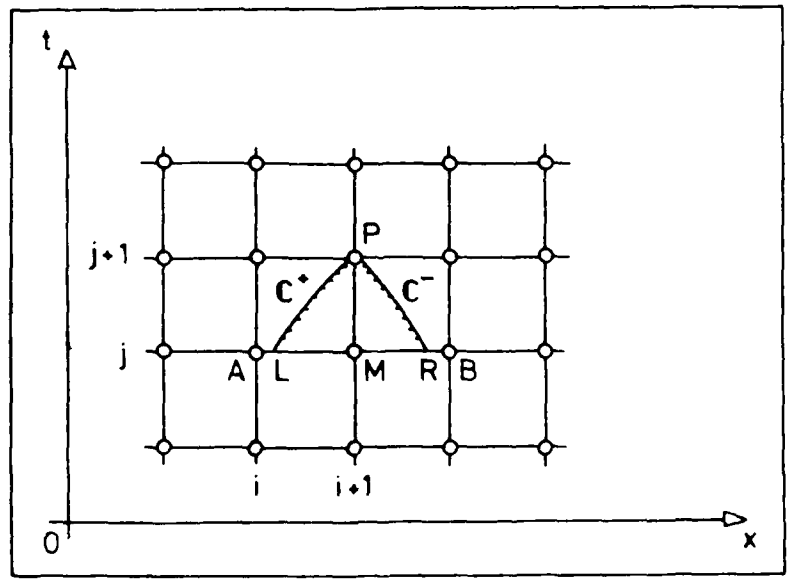

Figure 9. Characteristics on a rectangular fixed grid (A and B = arbitrary grid points, M = midpoint, j = discrete time, i = discrete longitudinal space)

In that way, a local algebraic equation is derived for each element. After assemblage of all local equations into a global system, solution is obtained by solving the system and determining the values of variables at each nodal point (Zienkiewicz 1971). Depending on the form of shaping functions, the numerical method can be either a hybrid finite element-finite difference scheme or a pure finite-element scheme. More specifically, if $N_i = N_i(x)$, then the finite element discretization is done only for the space coordinates, while the solution marches in time by a finite-differences algorithm (Taylor and Davis 1973). If $N_i = N_i(x,t)$, then the solution is based entirely on finite-element technique (Scarlatos 1982).

Simplified approaches

41. Depending on the physical conditions, the St. Venant system of equations can be reduced to a simpler form by neglecting one or more of the terms in the momentum equation (Equation 11 or 13). A visualization of various approximations can be given as follows:

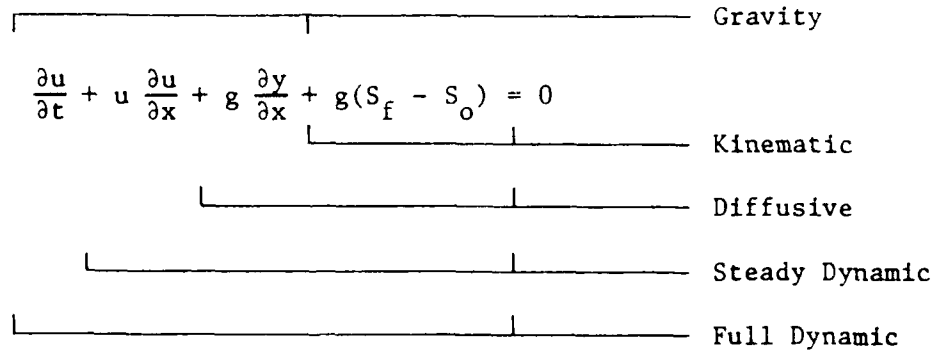

42. The advantage of these approximations is primarily the simplification of computational requirements. However, the physical problem itself dictates which one of the approximate forms is more appropriate. It has been proven that the kinematic wave model is a very useful technique for flood routing. An extensive treatment of kinematic wave modeling was given by Sherman and Singh (1978, 1982). Another approach to flood routing is the Muskingum method, where the dynamic equation is replaced by an empirical relation between water storage and inflow-outflow discharges (Singh and McCann 1980).

Classification and comparison of models

43. The St. Venant system written in the form of Equations 10 and 11 neglects the effects of wind stresses, atmospheric pressure differences, and the Coriolis Force. Knowledge of initial and boundary conditions is also required. Experience with the full dynamic model has shown that it can yield

results of sufficient accuracy, but the solution is sensitive and sometimes leads to computational instabilities. On the other hand, simplified models show a more stable solution behavior, and they produce some kind of results under all circumstances. In many cases, however, these results are very inaccurate and of no practical use. Precise delineation of conditions under which simplified models can be successfully applied has not yet been achieved. The problem of defining the best model is very complicated due to the large number of variables involved. Additional confusion is introduced by the special features of the numerical solution technique itself. When local and convective acceleration is negligible, the diffusive model can be applied. Furthermore, if pressure variation is small in comparison to gravity and friction effects, the kinematic wave approach is suggested.

PART III: GRADUAL DAM-BREAK EVOLUTION AND FLOOD PREDICTION

Dam-Break Evolution

44. Simulation of the total earth-fill dam-breach erosion process is a combination of hydrologic elements, hydrodynamics, sediment transport mechanics, and geotechnical aspects. The real-life problem is unsteady, nonhomogeneous, nonlinear, and three-dimensional, which is not theoretically well understood. Mathematical modeling of the phenomenon requires idealization of the real-life situation so that the leading physical processes can be described by a set of governing equations. Assumptions on which the governing equations are based, the ability to determine certain parameters involved, and accuracy of the solution algorithm control the validity of the model. For practicality, there is always a trade-off involving complexity, accuracy, and efficiency of the model.

45. Earth-fill dam-breach erosion is understood intuitively as a two-phase water-soil interacting system. Water from the reservoir flows through the breached section of the dam, causing enlargement of the breach either by erosion or sloughing. The process continues until the reservoir is emptied or the dam resists further erosion. In the following sections, each component and process of the reservoir-dam system will be presented. Assumptions and simplifications will be discussed and explained through physical reasoning.

Reservoir water mass balance

46. The volume of water stored within the reservoir $\forall$ is a function of the reservoir geometry. Theoretically, this volume can be estimated as

$$\forall = \int_0^H A_s(H)\,dH \tag{20}$$

where

H = reservoir water level measured from a reference datum

A_s = surface water area within the reservoir

Equation 20 assumes a horizontal water surface within the reservoir, neglecting any possible surface profile, which is for practical purposes correct under equilibrium conditions. When the dam is breached, water from the equilibrium stage within the reservoir starts to accelerate and converge toward

the breach, while at the same time there is a continuous depletion of the water volume $\forall$. This phenomenon is essentially dynamic and is controlled by both the mass continuity and momentum balance equations. Due to comparatively small velocities within the reservoir and the locality of the dynamic effects, the rate of water volume depletion can be described by a single mass continuity equation as

$$\frac{d\forall}{dt} = I_o - Q_b - Q_o - Q_{sp} \tag{21}$$

where

I_o = inflow

Q_b = breach outflow discharge

Q_o = outflow over the crest of the dam

Q_{sp} = outflow through the spillway and powerhouse outlet

The time derivative of the water volume can be written as

$$\frac{d\forall}{dt} = \frac{dV}{dH}\frac{dH}{dt} = A_s(H)\frac{dH}{dt} \tag{22}$$

where V is the reservoir water storage capacity. Combining Equation 21 and 22 yields

$$A_s(H)\frac{dH}{dt} = I_o - Q_b - Q_o - Q_{sp} \tag{23}$$

47. Inflow discharge I_o includes all water sources such as riverine water, watershed runoff, direct precipitation, and ground-water flow into the reservoir. The combined effect is given in the form of a hydrograph through statistical evaluation of existing data. The more extensive and accurate the data set, the more reliable the inflow hydrograph. In case of limited data, an inflow hydrograph should be assumed that corresponds as well as possible to the expected conditions.

48. Another specified variable is the outflow Q_{sp} . Indeed, the spillway capacity is given as a function of the water elevation H , while the powerhouse discharge is also a predetermined function of water elevation and time. Knowledge of both of these quantities is essential for efficient operation and management of the dam, so they are always accurately specified.

49. Before construction of a dam, the upstream valley that will serve as the artificial lake is mapped in detail to determine the storage capacity of the reservoir. Therefore, the relation $A_s = A_s(H)$ is a known function. In most cases, however, instead of the $A_s = A_s(H)$ relation, an equivalent relation of $\forall = \forall(H)$ is provided so that the $A_s(H)$ function can be obtained directly as the tangent at any point of the $\forall$-H curve.

50. Referring to Equation 23, it is obvious that the only unspecified quantities are the outflow discharges through the breach and over the crest of the dam. If those quantities could be expressed in terms of only the water elevation H , then Equation 23 would be an ordinary differential equation that can be solved easily. However, as it will be shown in the next section, breach outflow Q_b contains another unknown variable, the breach bottom elevation Z , so that Equation 23 cannot be solved directly. A schematic presentation of the geometric and physical quantities of dam-break problems is given as Figure 10.

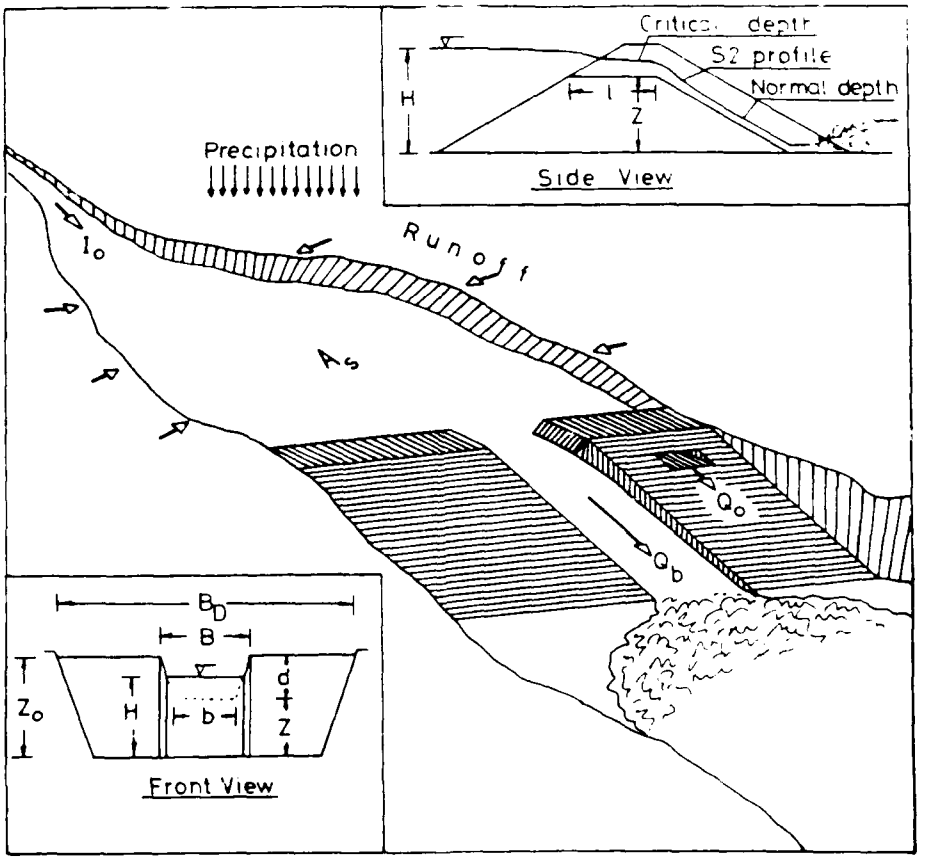

Figure 10. Geometric and physical characteristics of earth-dam failure

Hydraulics of flow through
the breach and over the crest

51. Flow through the breach and over the crest of the dam resembles flow over a broad-crested weir. Since there is no information for unsteady broad-crested weir flow, steady-state expressions for the flow will be used in this study. This is justified by the fact that, in the vicinity of the breach, local accelerations are much smaller than convective accelerations as the particles start moving from rest toward the breach. Therefore, quasi-steady conditions will describe the phenomenon fairly well, and both outflows through the breach and over the crest of the dam will be taken as

$$Q_b = [C_1^* b + C_2^* (H - Z) \tan \theta](H - Z)^{3/2} \tag{24}$$

$$Q_o = C_1^* (B_D - B)(H - Z_o)^{3/2} \tag{25}$$

where

C_1^* and C_2^* = dimensional coefficients

b = bottom width of the breach

Z = bottom elevation of the breach

θ = angle between vertical and the breach side

B_D = top width of the dam (crest length)

B = top width of the breach

Equation 24 corresponds to a trapezoidal-shaped breach, while Equation 25 corresponds to a rectangular-shaped weir. For $b = 0$, Equation 24 describes a triangular breach, and for $\theta = 0$, a rectangular one.

52. In the case of a rectangular weir, the theoretical value for C_1^* can be easily derived from critical flow conditions over the crest as

$$Q_b = g\left(\frac{A_b^3}{b}\right)^{1/2} = \left[g\,\frac{(by_c)^3}{b}\right]^{1/2} = \left[gb^2\left(\frac{2}{3}h\right)^3\right]^{1/2} = 1.7b(H - Z)^{3/2} \tag{26}$$

where

A_b = wetted cross section of the breach

y_c = critical depth

Therefore, in the metric unit system, $C_1^* = 1.7$. The theoretical value for the C_2^* coefficient in the same unit system is 1.35. In practice, those values should be reduced due to correction for velocity of approach (Brater 1959).

53. Further reduction of the values of coefficients C_1^* and C_2^* might be necessary when tailwater effects are present, i.e., when flow is submerged (Figure 11). In that case, these coefficients are modified from the equation

$$C_{1,2}^{*m} = C_{1,2}^{*}\left[1.0 - 27.8\left(\frac{y_o - Z}{H - Z} - 0.67\right)^2\right] \tag{27}$$

where

$C_{1,2}^{*m}$ = modified $C_{1,2}^{*}$ coefficient

$C_{1,2}^{*} = C_1^*$ or C_2^*

y_o = water depth at the tailwater section

Equation 27 is an empirical relation and implies that if the ratio of depth of submergence over hydraulic head is less than 0.67, the tailwater effects are negligible.

54. The water depth y_o is computed from Chezy's equation

$$Q = C_h(R_h S_o)^{1/2} A \tag{28}$$

or Manning's equation

$$Q = \frac{1}{n} R_h^{2/3} S_o^{1/2} A \tag{29}$$

where

C_h = Chezy's coefficient of friction

R_h = hydraulic radius at the tailwater cross section

n = Manning's coefficient of friction

Equations 28 and 29 are transcendental equations with respect to y_o and require a trial-and-error procedure for their solution.

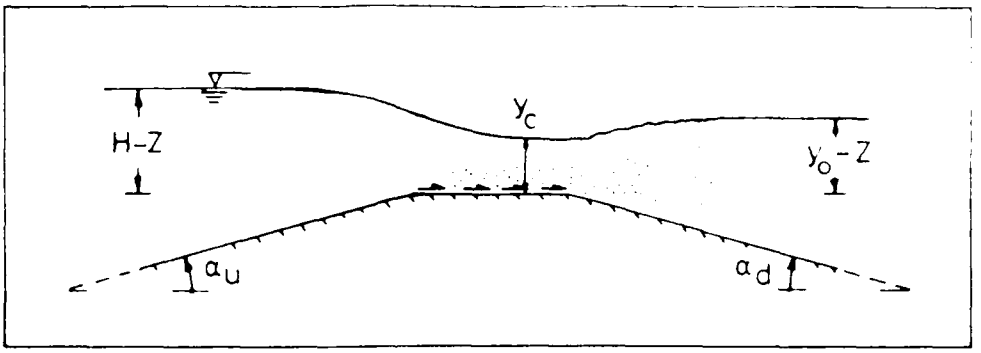

Figure 11. Submerged flow conditions

55. Combining Equations 23, 24, and 25, the reservoir water volume depletion equation reads

$$A_s(H)\frac{dH}{dt} = I_o(t) - [C_1^* b + C_2^*(H - Z)\tan\theta](H - Z)^{3/2}$$

$$- C_1^*(B_D - B)(H - Z_o)^{3/2} - Q_{sp}(H,t) \qquad (30)$$

Equation 30 is a nonlinear ordinary differential equation with two unknowns: water elevation H and breach bottom elevation Z. Those two unknowns are interdependent through the processes of outflow discharge and breach erosion. For completeness of the solution, an equation that describes dam-erosion characteristics should be derived.

Flow through breach on
the downstream face of dam

56. The main erosive force is water flowing at high velocities over the downstream face of the dam. Although the flow is unsteady, it can be approximated by quasi-steady-state conditions by the same reasoning used for the flow over the crest. According to experimental data of Pugh and Gray (1984), the flow over the whole top section of the breach can be assumed as being critical (Figure 12). Therefore, the water flow over the downstream face of the dam will be supercritical, reaching normal flow conditions after passing through an S2 profile (Figure 10).

57. When local accelerations are neglected, the momentum equation (Equation 13) can be written as

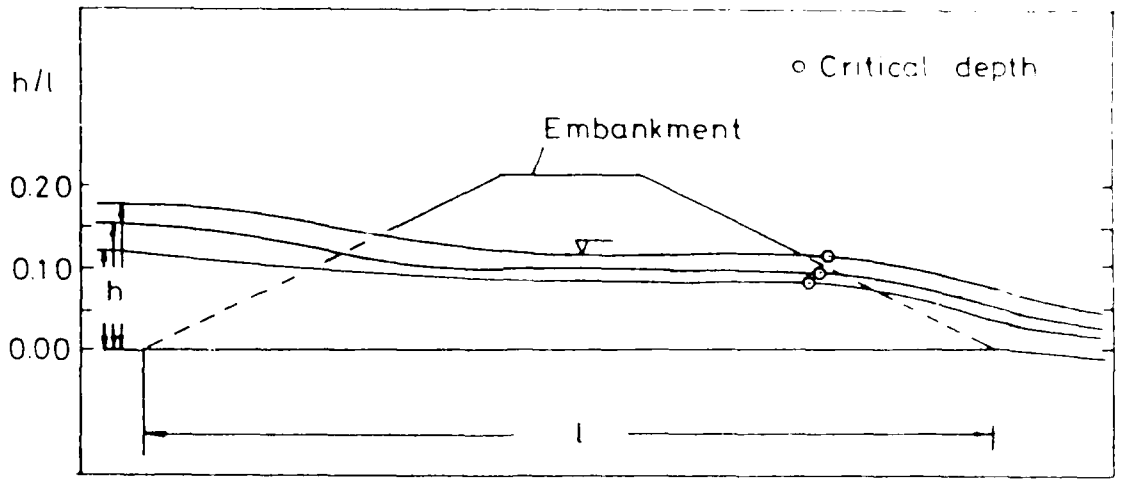

Figure 12. Flow over the crest breach section (after Pugh and Gray 1984)

$$\frac{d}{dx}\left(\frac{Q_b^2}{2gA_b^2}\right) + \frac{dy}{dx} + \left(S_f - S_o\right) = 0 \qquad (31)$$

Making use of Chezy's friction equation for S_f and after some mathematical manipulations, Equation 31 yields

$$\frac{dy}{dx}\left(1 - \frac{Q_b^2 B}{gA_b^3}\right) = S_o - \frac{Q_b^2}{C_h^2 A_b^2 R_h}$$

For steep slopes, Equation 31 should be corrected as

$$\frac{dy}{dx} = \frac{S_o - \dfrac{Q_b^2}{C_h^2 A_b^2 R_h}}{\cos \alpha_b - \dfrac{Q_b^2 B}{gA_b^3}} = F(y) \qquad (32)$$

where α_b is the angle of the downstream face of dam with the horizontal. Integration of Equation 32 requires an iterative technique. Since flow is

supercritical, the integration starts from the upstream boundary, i.e., the critical depth.

Erosion processes and sediment transport

58. After development of an initial breach on the dam, the hydrodynamic forces continue to enlarge the breach by eroding the soil material. Mechanics of sediment transport is a scientific discipline that has been developed in a semiempirical form mostly for the case of alluvial rivers. Because of a lack of information on sediment erosion under extremely dynamic conditions, such as those occurring during an earth-fill dam failure, sediment discharge will be estimated by a conventional method, the Einstein-Brown bed-load formula (Brown 1950). Although this method has been successfully applied for prediction of sediment transport in alluvial streams, its application to dam-erosion dynamics requires extrapolation beyond the range for which experimental data exist. The Einstein-Brown formula was chosen since it has been more widely tested than any other method (Simons and Senturk 1976). Besides, this method does not depend on a threshold value of shear stress for initiation of erosion, which cannot be determined easily.

59. Einstein-Brown bed-load formula. The basic idea of the Einstein-Brown theory is that initiation and cessation of sediment motion depend on the probability that relates instantaneous hydrodynamic lift forces to the submerged weight of a particle. Their final results are presented in the dimensionless expression

$$\Phi = {}^{c}\left(\frac{1}{\Psi}\right) \tag{33}$$

where

Φ = sediment transport rate function

Ψ = inverse of Shield's dimensionless shear stress

Explicitly, the quantities Φ and Ψ are given as

$$\Phi = \frac{q_{bw}}{\gamma_s K_E \sqrt{g\left(\frac{\gamma_s}{\gamma} - 1\right) D_s^3}} \tag{34}$$

and

$$\frac{1}{\Psi} = \frac{\tau}{\left(\gamma_2 - \gamma\right) D_s} \tag{35}$$

where

q_{bw} = bed-load discharge, weight per unit width

γ_s = specific weight of soil

K_E = constant

$$= \sqrt{\frac{2}{3} + \frac{36\nu^2}{gD_s^3\left(\frac{\gamma_s}{\gamma} - 1\right)}} - \sqrt{\frac{36\nu^2}{gD_s^3\left(\frac{\gamma_s}{\gamma} - 1\right)}} \tag{36}$$

γ = specific weight of water

D_s = representative size of bed sediment

τ = bed shear stress

γ_2 = specific weight of submerged soil

ν = kinematic viscosity of the water

Usually, D_s is taken as the median size D_{50}, while bed shear stress is estimated as

$$\tau = \gamma R_h S_f = \gamma \frac{u^2}{C_h^2} \tag{37}$$

60. The functional relationship of Equation 33 was determined using experimental data. A plot of the results is given as Figure 13. As shown in this figure, when $1/\Psi > 0.09$, Equation 33 becomes

$$\Phi = 40\left(\frac{1}{\Psi}\right)^3 \tag{38}$$

At this point, it should be mentioned that due to high shear stresses experienced in the dam-erosion problem, the value of $1/\Psi$ will be much higher than the limiting number of 2 given in Figure 13. Therefore, in that case, an extrapolation will be necessary.

61. Breach bottom erosion rate. Once the bed-load discharge q_{bw} has been estimated, the rate of erosion of the bottom of the breach can be directly calculated. Indeed, scouring ΔZ of the breach during time interval Δt can be given as

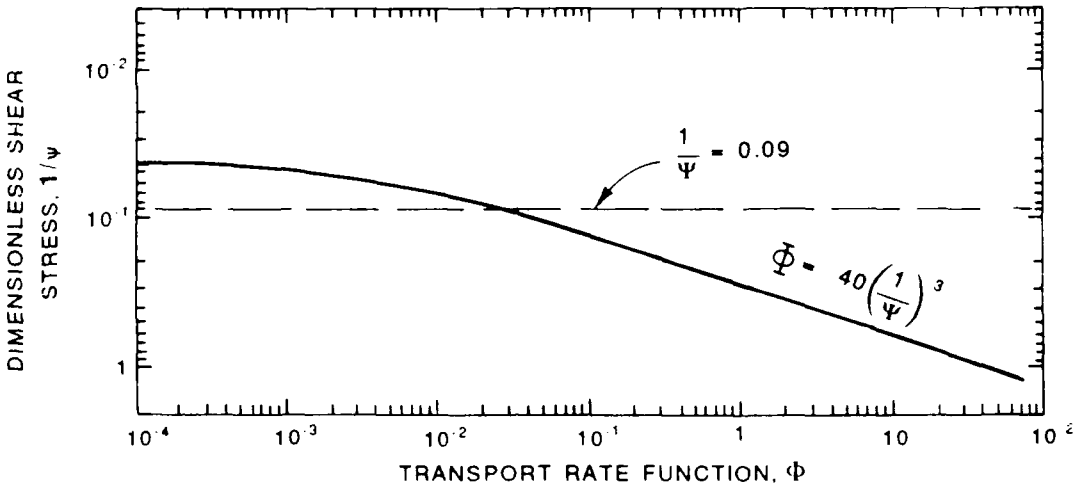

Figure 13. Transport rate function versus dimensionless shear stress

$$\Delta Z = \frac{q_{bw} \Delta t}{\gamma_s (1 - p) \ell} \tag{39}$$

where p is the soil porosity.

62. Since bed-load discharge depends on hydrodynamic conditions and those conditions change from critical to supercritical flow, erosion processes must be considered separately for the breach at the crest and the downstream face of dam.

Geotechnical considerations of breach slope stability

63. During the erosion processes of an earth-fill dam, the situation arises where breach slopes become unstable. This happens when the hydrodynamic forces associated with seepage are greater than the soil friction and cohesion. The problem can be successfully analyzed by the contour method (Chugaev 1964), in which the shearing surface is assumed, for simplicity, as a single plane passing through the toe of the slope. A schematic representation of the problem is given as Figure 14. The initial water table is the horizontal line 3-4. Due to breaching and depletion of the reservoir water, the water surface is drawn down to line 2-5, which will create a horizontal seepage force that along with gravity forces might cause failure of the slope. The main advantage of the contour method is that it requires knowledge of the

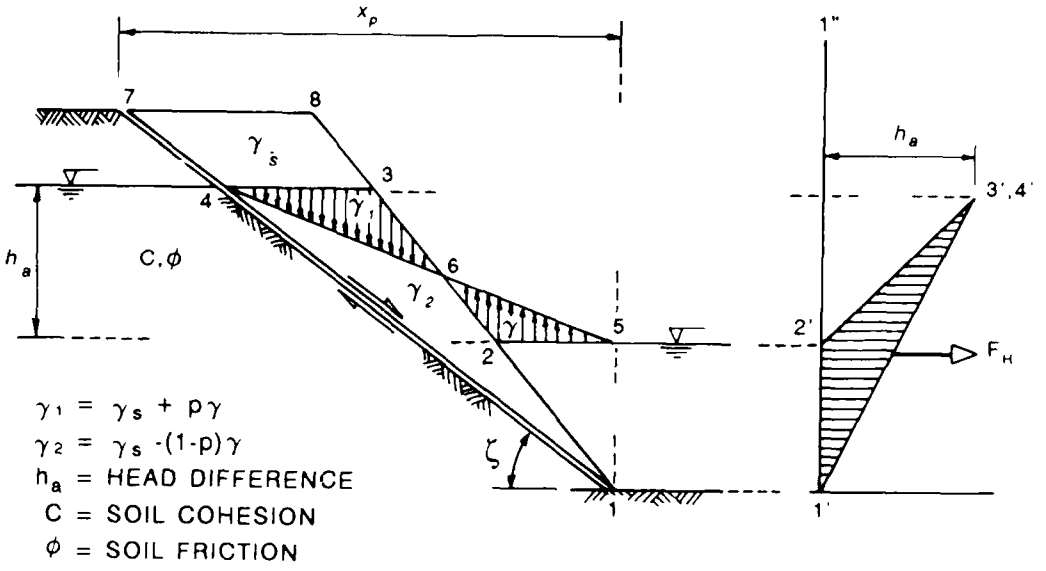

Figure 14. Characteristics of slope instability

head distribution only along the boundaries of the sliding wedge and not throughout the entire wedge.

64. In the contour method, the total seepage force acting on the wedge is obtained directly from the hydraulic head distribution. Let 1-7-8 be the sliding wedge. The piezometric line of the upper part of the wedge is represented by line 4-3-6-2-5, while the piezometric line for the shearing surface is given by straight line 4-6-5. Projecting the hydraulic heads on 1'-1" axis, the horizontal component F_H of the total seepage force is proportional to the area of triangle 1'-2'-3'.

65. For estimation of the weight of the wedge, the nonuniform presence of water within the sliding wedge should be considered. Indeed, the total weight of the wedge can be estimated by calculating the weight of the saturated soil as well as the buoyancy effects as follows. Section 3-4-7-8 is composed of dry soil (γ_s). In section 2-6-5, negative pressure is assumed, so that the specific weight is that of pure water but with a minus sign ($-\gamma$). Soil is saturated in section 3-6-4, so the specific weight is

$$\gamma_1 = \gamma_s + p\gamma \tag{40}$$

where γ_1 is the specific weight of saturated soil. Finally, the soil section 1-4-6 is submerged, with specific weight γ_2 given as

$$\gamma_2 = \gamma_s - (1 - p)\gamma \tag{41}$$

The total weight of sliding wedge, G, is the sum of the four separate parts, and for a wedge of unit width it yields

$$G = \gamma_s A_{(3\text{-}4\text{-}7\text{-}8)} - \gamma A_{(2\text{-}6\text{-}5)} + \gamma_1 A_{(3\text{-}6\text{-}4)} + \gamma_2 A_{(1\text{-}4\text{-}6)} \tag{42}$$

where $A_{(\ )}$ is the area of each individual section.

66. Stability or failure of the breach sides depends upon the balance of forces acting on the wedge. Those forces are the weight of the wedge, the seepage forces, the internal friction, and the cohesion. At the stage of equilibrium, the force balance equation yields (Chugaev 1964)

$$F_H + G \tan (\zeta - \phi) = Cx_p[1 + \tan \zeta \tan (\zeta - \phi)] \tag{43}$$

where

ζ = angle between the shearing plane and the horizontal

C = cohesion

x_p = horizontal projection of the shearing plane

Failure of the slope occurs when the right-hand side of Equation 43 is greater than the left-hand side.

Flood Routing by the Muskingum-Cunge Method

67. Once the outflow hydrograph from the breach is known, the flash flood can be routed through the downstream receiving channel. One well-established technique for flood routing is the Muskingum-Cunge method (Ponce and Yevjevich 1978). This method is based on a linear relation between inflow I, outflow $\emptyset$, and reach storage S, given the form

$$S = K[\alpha I + (1 - \alpha)\emptyset] \tag{44}$$

where

K = dimensional coefficient

α = weighting factor

Equation 44 is coupled with the volume continuity equation written as

$$\frac{dS}{dt} = I - \emptyset \tag{45}$$

In Equations 44 and 45, the function I is known either from the flash-flood hydrograph or from the computations of the adjacent upstream reach.

68. In contrast with the original Muskingum method where both K and α are constant parameters, in the Muskingum-Cunge method, K and α vary according to the expressions

$$K = \frac{\Delta x}{c_o} \tag{46}$$

and

$$\alpha = \frac{1}{2}\left(1 - \frac{q}{S_o c_o \Delta x}\right) \tag{47}$$

where

Δx = length of a channel reach

c_o = wave celerity

q = discharge of unit width

It has been proven that application of this routing technique can give results comparable in accuracy to the application of the diffusive model (Ponce and Yevjevich 1978).

Numerical Solutions of the Governing Equations

69. Once the governing equations have been defined, the next step is to determine their solution algorithm. Unfortunately, most of the equations cannot be solved analytically, so a numerical solution is required. In this section, emphasis will be restricted to certain independent solution techniques and not the overall dam-break problem.

Solution of the water-profile equation

70. For the solution of the water-profile relation (Equation 32), the numerical technique suggested by Prasad (1970) will be used. Let the flow profile be described by $y = f(x)$. Applying the trapezoidal rule of integration,

$$y_{i+1} = y_i + \frac{\left.\frac{dy}{dx}\right|_{i+1} + \left.\frac{dy}{dx}\right|_{i}}{2} \Delta x \tag{48}$$

where the subscript i refers to the distance along the channel and it increases downstream.

71. Based on Equations 32 and 48, the two unknowns y and dy/dx can be computed as follows:

Step 1. Estimate $(dy/dx)|_i$ from Equation 32, either from initial data or previous calculation.

Step 2. Set $(dy/dx)|_{i+1} = (dy/dx)|_i$ as a first approximation.

Step 3. Obtain an approximate value for y_{i+1} from Equation 48.

Step 4. Compute a new value for $(dy/dx)|_{i+1}$ from Equation 32 using the y_{i+1} obtained in step 3.

Step 5. If the new value of $(dy/dx)|_{i+1}$ is not very close to the value previously assumed or computed, then repeat steps 3-5. Otherwise, proceed to the next integration step and repeat the whole procedure.

The method is fast and accurate and can be programmed very easily.

Solution of the Muskingum-Cunge equation

72. Combining Equations 44-47 and setting them in finite-difference form, after some manipulations, results in the following equation:

$$\emptyset^{j+1} = C_1 I^j + C_2 I^{j+1} + C_3 \emptyset^j \tag{49}$$

where the upper index j refers to the time step and C_1, C_2, C_3 are numerical coefficients. The space-time discretization of the Muskingum-Cunge method is shown in Figure 15. From this figure it is evident that the outflow of a specific section is inflow for the downstream adjacent section.

73. The coefficients C_1, C_2, and C_3 can be evaluated, respectively, from the following relations:

$$C_1 = \frac{1 + C_4 - C_5}{1 + C_4 + C_5} \tag{50}$$

$$C_2 = \frac{-1 + C_4 + C_5}{1 + C_4 + C_5} \tag{51}$$

$$C_3 = \frac{1 - C_4 + C_5}{1 + C_4 + C_5} \tag{52}$$

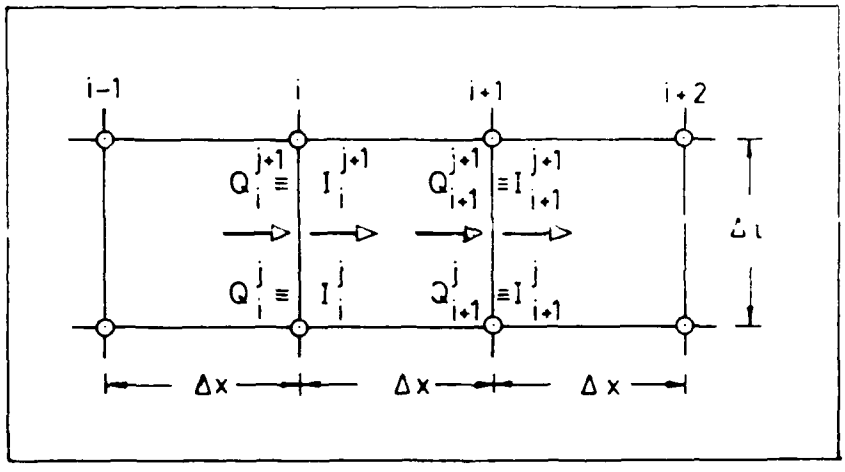

Figure 15. Space-time discretization for the Muskingum-Cunge method

in which C_4 and C_5 are defined as

$$C_4 = c_o\left(\frac{\Delta t}{\Delta x}\right) \tag{53}$$

and

$$C_5 = \frac{q/S_o}{c_o \Delta x} \tag{54}$$

The time step Δt is usually taken as constant. Both C_4 and C_5 have physical significance, being a ratio of celerities and diffusivities, respectively.

74. For the estimation of these coefficients, it is necessary to determine the wave celerity c_o and the unit width discharge q for each computational cell. The values of c_o and q are defined as

$$c_o = \left(\frac{dQ}{dA}\right)x \tag{55}$$

and

$$q = \frac{Q}{T} \tag{56}$$

where T is the top width of the channel wetted cross section. To compute coefficients C_4 and C_5, both c_o and q are obtained directly as a three-point average of their values at points (i,j), (i,j+1), and (i+1.j). This method has been proven sufficiently accurate in the simulation of flood flows (Ponce and Yevjevich 1978).

Newton-Raphson iteration algorithm

75. In many cases, especially when dealing with trapezoidal cross sections, the situation arises when the roots of an implicit algebraic function $y = f(x)$ should be determined. The most commonly used technique for that purpose is the Newton-Raphson iteration algorithm, given as follows:

$$x_{i+1} = x_i - \frac{f(x_i)}{f'(x_i)} \tag{57}$$

where i is the iteration index and $f'(x)$ is the first derivative. The method is very efficient and converges rapidly.

Fixed-point iteration algorithm

76. In certain cases, it is very convenient to use a more simplistic iteration algorithm such as the fixed-point scheme instead of the Newton-Raphson technique. A graphical description of that scheme is presented as Figure 16.

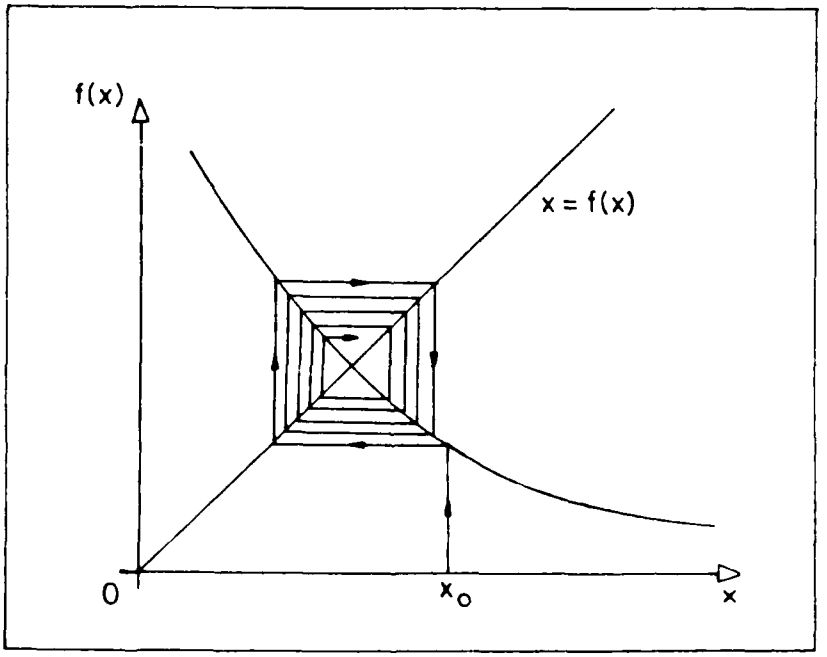

Figure 16. Fixed-point iteration algorithm

PART IV: COMPUTER MODEL FOR BREACH EROSION OF EARTH-FILL DAMS

77. The Breach Erosion of Earth-Fill Dams (BEED) computer model is a mathematical model developed for predicting the hydrograph of a flash flood due to gradual dam failure. The structure of the model is based on the quantitative and qualitative physical principles described in Parts II and III. The solution procedures and algorithms of the model are relatively simple and can be used in both microcomputers and mainframe computer systems.

Physical Description of BEED

78. Before presenting a quantitative description of the BEED model, it is important to examine the conceptual framework of the model and to discuss its physical reasoning and consistency as well as its applicability and limitations.

79. The model will be developed for a homogeneous dam with different but uniform slopes for the upstream and downstream faces. Physical and geometric characteristics of the dam and its surroundings should be specified. The model neglects the triggering mechanism of failure and can simulate the phenomenon only when a small breach has been developed at the crest of the dam. The size, shape, and location of this initial breach should be provided as initial conditions. Unfortunately, the selection of such conditions is based entirely on engineering judgment and not on quantitative information. For convenience, a rectangular initial breach shape with specified depth-over-width ratio can be assumed.

80. Once the initial breach has occurred, water from the reservoir starts flowing through the breach, causing enlargement of the breach and erosion of the downstream face of the dam. The erosion is restricted to a channel of the same top width as the breach at the crest of the dam. However, the erosion processes occurring on the crest and on the downstream face are considered separately because the water velocities are much higher down the face of the dam than they are over the crest; consequently, the downstream face erodes much faster.

81. The enlargement of the top breach follows a similar pattern except in the case where sloughing due to slope instability occurs. At this point, it

should be emphasized that the model incorporates only rectangular- or trapezoidal-shaped breaches.

82. Sloughing effects are considered only for the crest breach; the shape of the eroded channel on the downstream face is adjusted within the model to that of the crest. If the normal flow conditions at the downstream face require considerable distance to be developed, the slope should be subdivided into a number of reaches so that the erosion in each can be estimated separately. This will result in a steeper downstream slope. In most cases, however, normal flow conditions are established in a very short distance so that the effect of the S2 water profile can be neglected and the erosion of the downstream face can be assumed as being uniform.

83. When the flow conditions are submerged (i.e., when tailwater effects are present), the assumption is made that erosion occurs only on the top breach and not on the downstream face while breach outflow discharge is reduced.

84. Another characteristic feature of the program is that when the upstream and downstream slopes of the dam meet at a single point S , a sudden predetermined mass erosion is considered so that a new top horizontal breach channel of length ℓ_s is established. The upstream face slope of the dam remains unaltered during the failure processes. The program continues the simulation until either the reservoir is emptied of water or the dam resists any further erosion.

Solution Algorithm of BEED

85. The BEED model is designed to estimate dam-breach erosion processes to predict outflow discharge and to route it through the receiving channel. Because of the implicit form of the governing equations, the solution algorithm is iterative. However, practical experience indicates that convergence is achieved after few iterations.

86. The first step in the BEED model is definition of the geometric and physical features of the system. These are given separately for the dam, the reservoir, and the downstream channel. At the same time, all preliminary computations are executed, while initial conditions are specified.

87. More specifically, dam dimensions are provided along with soil characteristics such as specific weight, particle diameter size, cohesion,

internal friction angle, and surface roughness. Functional relationships for the spillway, powerhouse outlets, and the reservoir capacity are also specified. Description of the downstream receiving channel is given through definition of shape, size, and roughness of a certain number of reaches, which may be subdivided into smaller segments by linear interpolation techniques. Finally, the size and shape of the initial breach as well as the initial hydraulic head are specified a priori. Having all the required information available, the model proceeds by estimating reservoir water level, breach bottom elevation, and outflow discharge, which is subsequently routed downstream.

88. The main variables of the problem are reservoir water level H and breach bottom elevation Z. However, the breach outflow discharge Q_b is used as an additional variable during the iteration processes. For the solution, Equation 23 is discretized as

$$A_{s_{i+1}}\left(\frac{H_{i+1} - H_i}{\Delta t}\right) = \frac{1}{2}\left(I_{o_{i+1}} + I_{o_i} - Q_{b_{i+1}} - Q_{b_i} - Q_{o_{i+1}} - Q_{o_i} - Q_{sp_{i+1}} - Q_{sp_i}\right) \quad (58)$$

and then written as

$$H_{i+1} = H_i + \frac{\Delta t\left(I_{o_{i+1}} + I_{o_i} - Q_{b_{i+1}} - Q_{b_i} - Q_{o_{i+1}} - Q_{o_i} - Q_{sp_{i+1}} - Q_{sp_i}\right)}{ZA_{s_{i+1}}} \quad (59)$$

where i is referred to known time t and $i+1$ is referred to new time $t+\Delta t$. In Equation 59, the quantities H and Z are involved implicitly.

89. The computational steps for estimation of the variables are as follows:

Step 1. Set $\hat{H}_{i+1}$ and $\hat{Z}_{i+1}$ equal to values obtained from the previous time step or initial conditions ($\hat{}$ denotes uncorrected value).

Step 2. Compute outflow discharge $\bar{Q}_{i+1}$ from Equations 24 and 25 ($\bar{}$ denotes estimated value).

Step 3. Check for tailwater effects and, if needed, correct $\bar{Q}_{i+1}$, according to Equation 27.

Step 4. Compute sediment transport and rate of erosion from Equations 33, 34, 35, and 39. Then estimate $\tilde{Z}_{i+1}$ ($\sim$ denotes corrected value).

Step 5. If $|\tilde{Z}_{i+1} - \hat{Z}_{i+1}|$ is very small, proceed to the next step. Otherwise, set $\hat{Z}_{i+1} = \tilde{Z}_{i+1}$ and return to step 2.

Step 6. Compute $\tilde{H}_{i+1}$ from Equation 59.

Step 7. If $|\tilde{H}_{i+1} - \hat{H}_{i+1}|$ is not very small, proceed to the next step. If it is the first iteration, go to step 9 or return to step 2.

Step 8. Set $\hat{H}_{i+1} = \tilde{H}_{i+1}$, check for tailwater effects, and return to step 6.

Step 9. Check for slope stability using Equation 43.

Step 10. Adjust dam-breach dimensions.

Step 11. Compute total outflow discharge.

Step 12. If hydraulic head $h = H - Z$ is zero, proceed to the next step; otherwise, return to step 1.

Step 13. Estimate the Muskingum-Cunge coefficients from Equations 50-54.

Step 14. Route the flood according to Equation 49.

90. The solution algorithm of the BEED model is represented in flowchart form in Figure 17. The effects of nonuniform flow over the downstream face of the dam were neglected since normal flow conditions were attained in a very short distance due to high slopes.

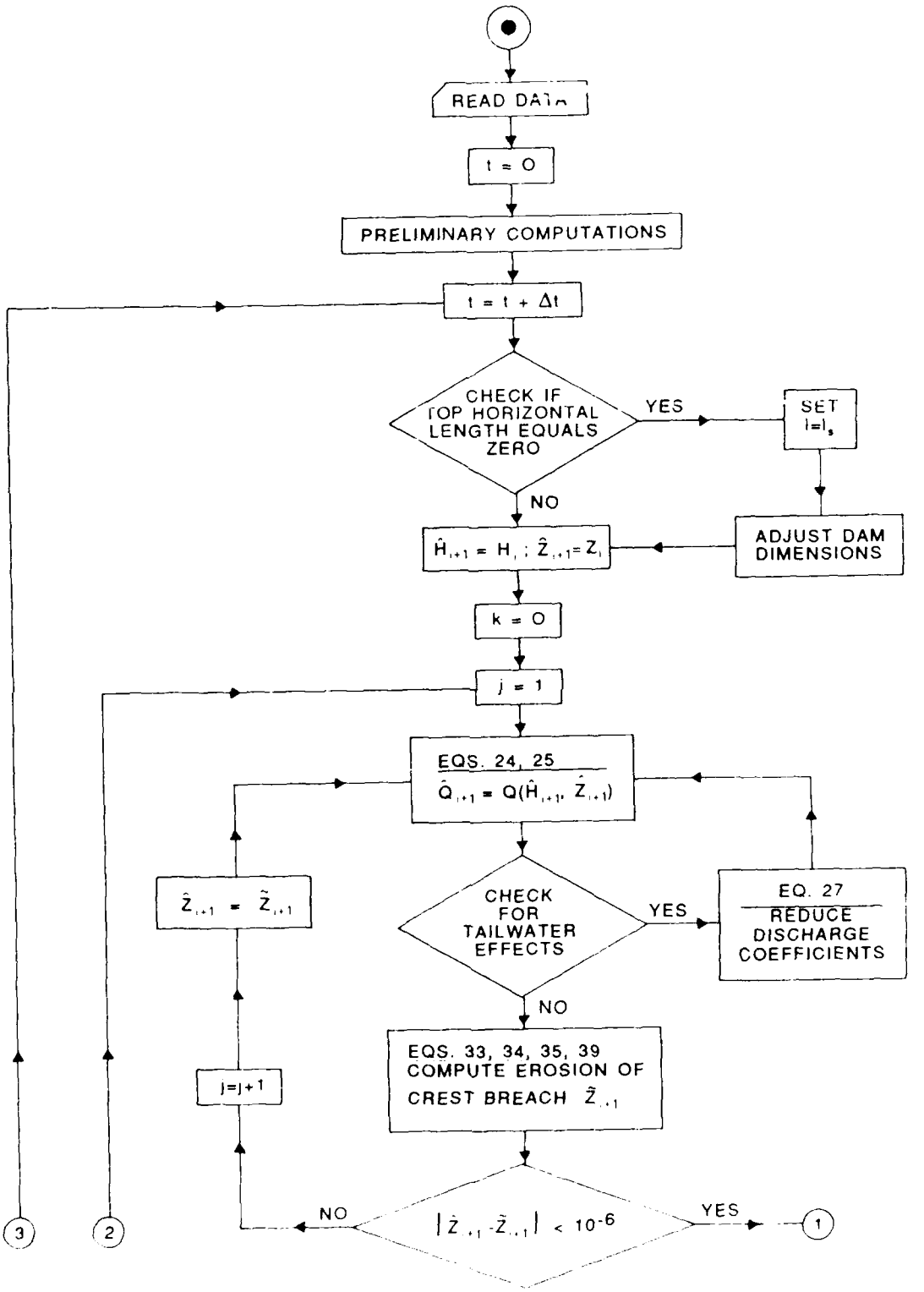

Figure 17. Flowchart of BEED computer model (Continued)

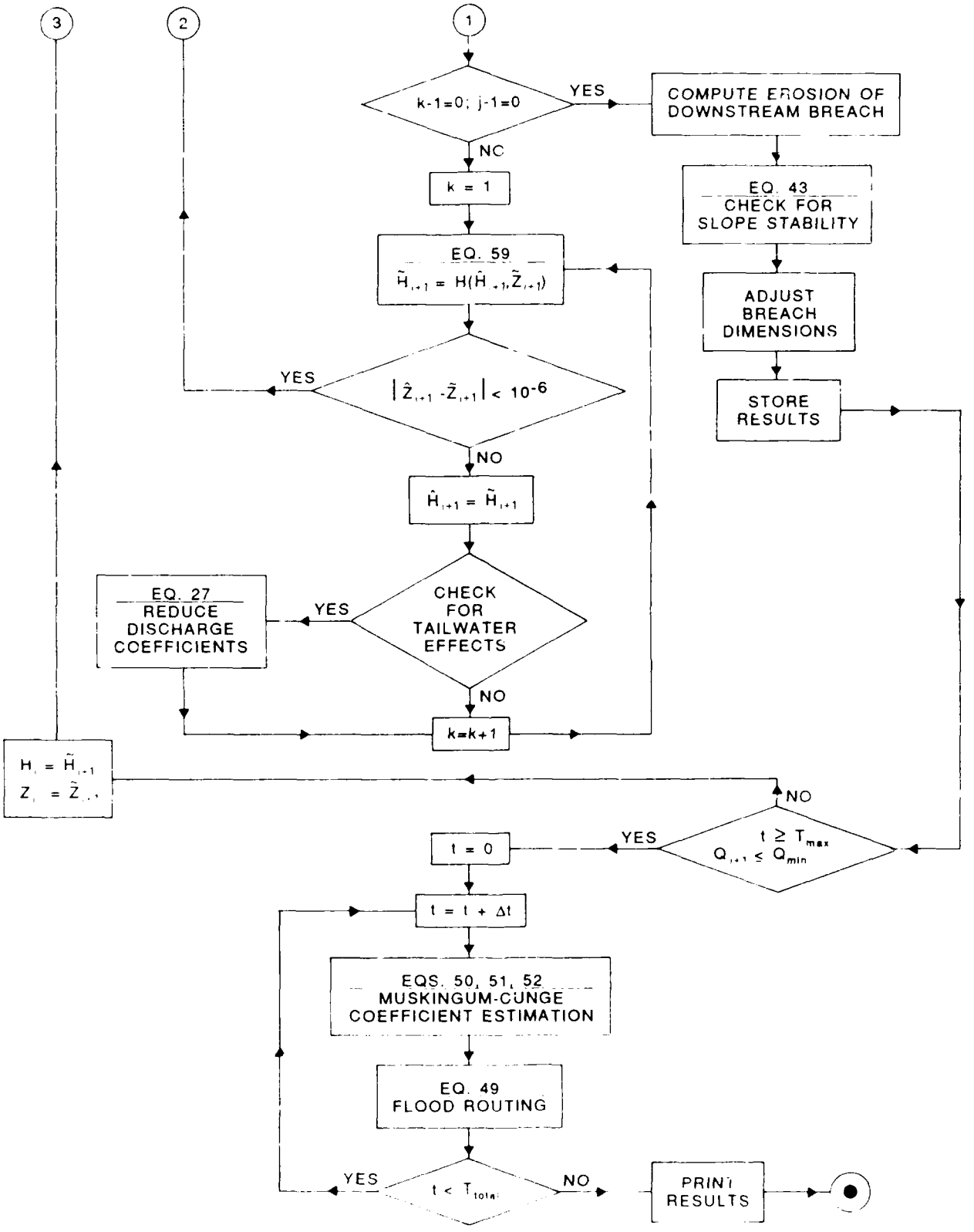

Figure 17. (Concluded)

PART V: ANALYTICAL SOLUTIONS OF GRADUAL DAM EROSION

91. A better insight of the physical processes and the significance of the controlling parameters of the gradual failure of a dam can be obtained through analytical expressions. Unfortunately, the governing equations are very complicated, so that a general analytical approach is not possible. The degree of complexity of the system can be drastically reduced by making proper simplifying assumptions and by lumping a number of physical parameters into a form of constant coefficients. In that case, closed-form solutions are feasible. The analysis in this section is based primarily on the principles presented in Part III.

92. Assuming that the inflow into the reservoir is of a much smaller order of magnitude than the breach outflow discharge and neglecting the spillway and powerhouse outflow, the mass continuity relation (Equation 23) becomes

$$A_s(H) \frac{dH}{dt} = -Q_b \tag{60}$$

Furthermore, if A_s is independent of H (i.e., prismatic reservoir) and the outflow is taken as

$$Q_b = uA_b \tag{61}$$

then Equation 60 yields

$$A_s \frac{dH}{dt} = -uA_b \tag{62}$$

where A_b can be rectangular, triangular, or trapezoidal. From Equations 24 and 25 it is evident that the water velocity at the breach can be estimated as

$$u = \alpha_1 (H - Z)^{\beta_1} \tag{63}$$

where α_1 and β_1 are proper coefficients. Combination of Equations 62 and 63 gives a single equation with two unknown quantities: the water depth H within the reservoir and the elevation of the bottom of the breach Z.

Therefore, an additional equation is required for the solution of the problem that should be obtained from the mechanics of sediment erosion.

93. It is known that the rate of erosion is a function of the bottom shear stresses or, equivalently, the square of the mean water velocity. Mathematically, this can be expressed as

$$\frac{dZ}{dt} = -\alpha_2 u^{\beta_2} \tag{64}$$

where α_2 and β_2 are proper coefficients. Depending on the value of the exponents β_1 and β_2, the system of Equations 62 and 64 can be linear or nonlinear. For completeness of the problem, the initial conditions

$$H = H_o \quad \text{and} \quad Z = Z_o \quad \text{at} \quad t = t_o \tag{65}$$

should be provided.

Rectangular Breach

94. For rectangular breach of constant width b, the cross section A_b is given as

$$A_b = b(H - Z) \tag{66}$$

This implies that the breach enlarges only in the vertical direction.

Linear case

95. If the rate of erosion is a linear function of the velocity ($\beta_2 = 1$), then the whole problem is linear. Combining Equations 62 and 66 yields

$$A_s \frac{dH}{dt} = -ub(H - Z) \tag{67}$$

Dividing Equation 67 by Equation 62 and rearranging,

$$\frac{dH}{dZ} = \frac{b}{\alpha_2 A_s} (H - Z) \tag{68}$$

and setting $h = H - Z$, then $dH/dZ = dh/dZ + 1$. Therefore,

$$\frac{dH}{dZ} = \frac{b}{\alpha_2 A_s} h - 1 \tag{69}$$

Separating the variables and integrating gives

$$\frac{\alpha_2 A_s}{b} \ln\left(\frac{bh}{\alpha_2 A_s} - 1\right) = Z + C_I \tag{70}$$

where C_I is an integration constant. From the initial conditions (Equation 65), C_I is estimated as

$$C_I = \frac{\alpha_2 A_s}{b} \ln\left[\frac{b(H_o - Z_o)}{\alpha_2 A_s} - 1\right] - Z_o \tag{71}$$

Substituting Equation 71 into Equation 70 gives (after some manipulations)

$$H = Z + \frac{\alpha_2 A_s}{b} + \left(H_o - Z_o - \frac{\alpha_2 A_s}{b}\right) \exp\left[-\frac{b}{\alpha_2 A_s}(Z_o - Z)\right] \tag{72}$$

Equation 72 prescribes the elevation of the breach bottom Z as a function of the water height H and breach characteristics.

96. It is desirable, however, to have Z as a direct function of time. Specifying coefficients α_1 and β_1 as $\alpha_1 = \sqrt{g}$ and $\beta_1 = 1/2$, Equation 64 becomes

$$\frac{dZ}{dt} = -\alpha_2 \sqrt{g(H - Z)} \tag{73}$$

Combining Equations 72 and 73 yields

$$\frac{dZ}{dt} = -\alpha_2 g \left\{\frac{\alpha_2 A_s}{b} + \left(H_o - Z_o - \frac{\alpha_2 A_s}{b}\right) \exp\left[-\frac{b}{\alpha_2 A_s}(Z_c - Z)\right]\right\}^{1/2} \tag{74}$$

By separating the variables, Equation 74 is written as

$$\frac{dZ}{\left[A_1 + A_2 \exp\left(-\frac{Z_o - Z}{A_1}\right)\right]^{1/2}} = -\alpha g \, dt \tag{75}$$

where A_1 and A_2 are given, respectively, as

$$A_1 = \frac{\alpha_2 A_s}{b} \tag{76}$$

$$A_2 = H_o - Z_o - \frac{\alpha_2 A_s}{b} \tag{77}$$

Referring to page 92 of Gradshteyn and Ruzik (1983), the solution of Equation 75 for $A_1 > 0$ is

$$A_1^{1/2} \ln \left\{ \frac{\left[A_1 + A_2 \exp\left(\frac{Z - Z_o}{A_1}\right)\right]^{1/2} - A_1^{1/2}}{\left[A_1 + A_2 \exp\left(\frac{Z - Z_o}{A_1}\right)\right]^{1/2} + A_1^{1/2}} \right\} = -\alpha g t + C_I \tag{78}$$

where

$$C_I = A_1^{1/2} \ln \left[\frac{\left(A_1 + A_2\right)^{1/2} - A_1^{1/2}}{\left(A_1 + A_2\right)^{1/2} + A_1^{1/2}} \right] \tag{79}$$

The final solution can be obtained from Equations 76-79. Indeed, after some algebraic calculations, $Z(t)$ is given as

$$Z(t) = Z_o + \frac{\alpha_2 A_s}{b} \ln \left(\frac{\alpha_2 A_s}{b(H_o - Z_o) - \alpha_2 A_s} \right) \left\{ -1 + \left(\sqrt{H_o - Z_o} + \sqrt{\frac{\alpha_2 A_s}{b}} \right) + \left(\sqrt{H_o - Z_o} - \sqrt{\frac{\alpha_2 A_s}{b}} \right) \exp\left(- \sqrt{\frac{g\alpha_2 b}{A}} \, t \right) \right\} \Bigg/ \left[\sqrt{H_o - Z_o} + \sqrt{\frac{\alpha_2 A_s}{b}} - \left(\sqrt{H_o - Z_o} - \sqrt{\frac{\alpha_2 A_s}{b}} \right) \exp\left(- \sqrt{\frac{g\alpha_2 b}{A_s}} \, t \right) \right]^2 \tag{80}$$

Equation 80 specifies the progression of breaching in time.

97. Commenting on the assumptions made for the derivation of Equation 80, the one that deviates mostly from reality is $\beta_2 = 1$. From experimental results, that exponent ranges from 4 to 6 (Laursen 1956). Numerically, this can be partially corrected by adjustment of the coefficient α_2 . Another critical point is the assumption of constant width b , which is very unlikely to occur in the case of a large dam.

Nonlinear case

98. In this case, $\beta_2 \neq 1$, i.e., erosion is a nonlinear function of the velocity. Dividing Equation 62 by Equation 64,

$$\frac{dH}{dZ} = \frac{A_b}{\alpha_2 A_s}\left(u^{1-\beta_2}\right) \tag{81}$$

Combining Equation 81 with Equations 63 and 66,

$$\frac{dH}{dZ} = \frac{b}{\alpha_2 A_s}\,\alpha_1^{1-\beta_2}(H - Z)^{1+\beta_1(1-\beta_2)} \tag{82}$$

Setting

$$A_3 = \frac{b\alpha_1^{1-\beta_2}}{\alpha_2 A_s} \tag{83}$$

and

$$A_4 = 1 + \beta_1(1 - \beta_2) \tag{84}$$

Equation 82 reduces to

$$\frac{dH}{dZ} = A_3(H - Z)^{A_4} \tag{85}$$

Equation 85 can be transformed to

$$A_3^{-(1/A_4)}\frac{dW}{dZ} + 1 = W^{A_4} \tag{86}$$

where $W = (H - Z)A_3^{1/A_4}$. Separation of the variables and integration of Equation 86 yields

$$\int \frac{dW}{1 - W^{A_4}} = -A_3^{1/A_4} Z + C_I \tag{87}$$

The left-hand side of Equation 87 is the Bakhmeteff function.

99. A closed-form solution is feasible if the coefficient A_4 is properly defined. Assuming $\beta_2 = 2$, $\alpha_1 = \sqrt{g}$, and $\beta_1 = 1/2$, then

$$A_1 = \frac{b}{\alpha_2 A_s g^{1/2}} \tag{88}$$

and

$$A_2 = \frac{1}{2} \tag{89}$$

so that Equation 87 becomes

$$\int \frac{dW}{1 - W^{1/2}} = -A_3^2 Z + C_I \tag{90}$$

By setting $W_1 = W^2$, Equation 90 can be easily integrated to give

$$W_1 = \ln \left(1 - W_1\right) = \left(\frac{A_3}{2}\right)^2 Z + C_I \tag{91}$$

or by inserting the transformations back,

$$\frac{b}{\alpha_2 A_s g^{1/2}} \sqrt{H - Z} + \ln \left(1 - \frac{b}{\alpha_2 A_s g^{1/2}} \sqrt{H - Z}\right) = \frac{1}{2g} \left(\frac{b}{\alpha_2 A_s}\right)^2 Z + C_I \tag{92}$$

From the initial conditions (Equation 65), the integration constant C_I can be estimated as

$$C_I = \frac{b}{\alpha_2 A_s g^{1/2}} \sqrt{H_o - Z_o} + \ln\left(1 - \frac{b}{\alpha_2 A_s g^{1/2}} \sqrt{H_o - Z_o}\right) - \frac{Z_o}{2g}\left(\frac{b}{\alpha_2 A_s}\right)^2 \tag{93}$$

Substitution of the integration constant into Equation 92 gives

$$\frac{b}{\alpha_2 A_s g^{1/2}}\left(\sqrt{H - Z} - \sqrt{H_o - Z_o}\right) + \ln\left[\frac{1 - \frac{b}{\alpha_2 A_s g^{1/2}} (H - Z)^{1/2}}{1 - \frac{b}{\alpha_2 A_s g^{1/2}} (H_o - Z_o)^{1/2}}\right] = \frac{1}{2g}\left(\frac{b}{\alpha_2 A_s}\right)^2 (Z - Z_o) \tag{94}$$

Equation 94 describes breach erosion in terms of the hydraulic head $H - Z$.

100. To establish the variable Z as an explicit function of time, an expression for the quantity $H - Z$ should be derived. For that purpose, Equation 64 is subtracted from Equation 62 while both Equations 63 and 66 are used,

$$\frac{d(H - Z)}{dt} = - \frac{b\alpha_1}{A_s} (H - Z)^{1+\beta_1} + \alpha_2 \alpha_1^{\beta_2} (H - Z)^{\beta_1 \beta_2} \tag{95}$$

Specifying the variables α_1, β_1, and β_2 as before,

$$\frac{d(H - Z)}{dt} = - \frac{b}{A_s} \sqrt{g}\ (H - Z)^{3/2} + \alpha_2 g (H - Z) \tag{96}$$

Separating the variables and setting

$$W_2 = \frac{b}{\alpha_2 A_2 g^{1/2}} \sqrt{H - Z}$$

then Equation 96 becomes

$$\frac{dW_2}{W_2(1 - W_2)} = \frac{g\alpha_2}{2} dt \tag{97}$$

or

$$\left(\frac{1}{W_2 - 1} - \frac{1}{W_2}\right) dW_2 = - \frac{g\alpha_2}{2} dt \tag{98}$$

Integration of Equation 98, determination of the integration constant, and substitution of the original variables provides

$$H - Z = \left\{ \frac{\alpha_2 A_s \sqrt{g(H_o - Z_o)}}{\left[\sqrt{H_o - Z_o} - \left(b\sqrt{H_o - Z_o} - \alpha_2 A_s \sqrt{g}\right) \exp\left(- \frac{\alpha_2 g}{2} t\right)\right]} \right\}^2 \tag{99}$$

Having the expression for the hydraulic head (Equation 99), the progression of the breaching can be directly estimated from Equation 94. The nonlinear case is an improvement of the linear one because it approximates the rate of erosion with a quadratic velocity function.

Triangular Breach

101. For triangular breach geometry, the cross-sectional area A_b is given as

$$A_b = s(H - Z)^2 \tag{100}$$

where s is the side slope (1V:sH). The assumption of constant side slope implies that the breach will enlarge in a similarity pattern.

Linear case

102. Again, for the linear case, $\beta_2 = 1$. Combining Equations 62 and 100 and dividing by Equation 64 yields

$$\frac{dH}{dZ} = \frac{s}{\alpha_2 A_2} (H - Z)^2 \tag{101}$$

Equation 101 can be rewritten as

$$\frac{d(H - Z)}{dZ} + 1 = \frac{s}{\alpha_2 A_s} (H - Z)^2 \tag{102}$$

Setting $h = H - Z$ in Equation 100, separating the variables, and using partial fractions gives

$$\frac{dh}{1 - \left(\frac{s}{\alpha_2 A_s}\right)^{1/2} h} + \frac{dh}{1 + \left(\frac{s}{\alpha_2 A_s}\right)^{1/2} h} = -2\, dZ \tag{103}$$

After integration, Equation 103 reads

$$\ln \left[\frac{1 + \left(\frac{s}{\alpha_2 A_s}\right)^{1/2} h}{1 - \left(\frac{s}{\alpha_2 A_s}\right)^{1/2} h} \right] = -2 \left(\frac{s}{\alpha_2 A_s}\right)^{1/2} Z + C_I \tag{104}$$

Estimating the integration constant C_I from the initial conditions and substituting back to Equation 104 gives (after some algebraic manipulations),

$$\left(\frac{s}{\alpha_2 A_s}\right)^{1/2} (H - Z) \tag{105}$$

$$= \left\{ \frac{-1 + \left(\frac{s}{\alpha_2 A_s}\right)^{1/2} (H_o - Z_o) + \left[1 + \left(\frac{s}{\alpha_2 A_s}\right)^{1/2} (H_o - Z_o)\right] \exp\left[2\left(\frac{s}{\alpha_2 A_s}\right)^{1/2} (Z_o - Z)\right]}{1 - \left(\frac{s}{\alpha_2 A_s}\right)^{1/2} (H_o - Z_o) + \left[1 + \left(\frac{s}{\alpha_2 A_s}\right)^{1/2} (H_o - Z_o)\right] \exp\left[2\left(\frac{s}{\alpha_2 A_s}\right)^{1/2} (Z_o - Z)\right]} \right\}$$

103. Equation 105 describes the changes of hydraulic head in terms of breach bottom elevation Z. Therefore, the function $Z = Z(t)$ must be determined. Equations 62, 63, and 64 can be combined to give

$$\frac{dH}{dt} - \frac{dZ}{dt} = -\frac{s}{A_s} g^{1/2}(H - Z)^{2.5} + \alpha_2 g^{1/2}(H - Z)^{1/2} \tag{106}$$

Setting $h = H - Z$ and separating the variables in Equation 106 gives

$$\frac{dh}{h^{1/2}\left(\frac{s}{\alpha_2 A_s} h^2 - 1\right)} = -\alpha_2 g^{1/2}\, dt \tag{107}$$

Referring to page 72 of Gradshteyn and Ryzhik (1983), the integral of Equation 107 is

$$\frac{\ln \frac{A_5^{1/4} - h^{1/2}}{A_5^{1/4} + h^{1/2}} - 2 \tan^{-1} \frac{h^{1/2}}{A_5^{1/4}}}{2 \frac{s}{\alpha_2 A_s} A_5^{3/4}} = -\alpha_2 g^{1/2} t + C_I \tag{108}$$

where A_5 is given as

$$A_5 = \frac{\alpha_2 A_s}{s} \tag{109}$$

By determining the integration constant C_I, Equation 108 yields

$$\ln \frac{\left(\frac{\alpha_2 A_s}{s}\right)^{1/4} - (H - Z)^{1/2}}{\left(\frac{\alpha_2 A_s}{s}\right)^{1/4} + (H - Z)^{1/2}} - 2 \tan^{-1} \frac{(H - Z)^{1/2}}{\left(\frac{\alpha_2 A_s}{s}\right)^{1/4}} = -2 \frac{\alpha_2^{3/4} s^{1/4}}{A_s^{1/4}} g^{1/2} t$$

$$+ \ln \frac{\left(\frac{\alpha_2 A_s}{s}\right)^{1/4} - (H_o - Z_o)^{1/2}}{\left(\frac{\alpha_2 A_s}{s}\right)^{1/4} + (H_o + Z_o)^{1/2}} - 2 \tan^{-1} \frac{(H_o - Z_o)^{1/2}}{\left(\frac{\alpha_2 A_s}{s}\right)^{1/2}} \tag{110}$$

Equations 105 and 109 can be combined to determine the erosion rate of breach bottom or the depletion of reservoir water.

Nonlinear case

104. For the nonlinear case, the erosion exponent will be taken as $\beta_2 = 2$, and the discharge exponent as $\beta_1 = 1/2$. Then, dividing Equation 62 by Equation 64,

$$\frac{dH}{dZ} = \frac{s}{\alpha_2 A_s g^{1/2}} (H - Z)^{1.5} \tag{111}$$

Setting $h = H - Z$ and separating the variables in Equation 111 gives

$$\frac{dh}{-1 + \frac{s}{\alpha_2 A_s g^{1/2}} h^{3/2}} = dZ \tag{112}$$

Equation 112 can be easily transformed to

$$\frac{W\, dW}{1 - W^3} = - \frac{A_b^{2/3}}{2} dZ \tag{113}$$

where

$$W = A_b^{1/3} h^{1/2}$$

and

$$A_b = \frac{s}{\alpha_2 A_s g^{1/2}} \tag{114}$$

Referring to page 64 of Gradshteyn and Ryzhik (1983), Equation 113 is integrated as

$$-\frac{1}{6}\ln\left[\frac{(1-W)^2}{1+W+W^2}\right]-\frac{1}{3^{1/2}}\tan^{-1}\left(\frac{2W+1}{3^{1/2}}\right)=-\frac{A_b^{2/3}}{2}Z+C_I \tag{115}$$

or

$$-\frac{1}{6}\ln\left[\frac{\left(1-A_b^{1/3}h^{1/2}\right)^2}{1+A_b^{1/3}h^{1/2}+A_b^{2/3}h}\right]-\frac{1}{3^{1/2}}\tan^{-1}\left[\frac{2A_b^{1/3}h^{1/2}+1}{3^{1/2}}\right]$$

$$=-\frac{A_b^{2/3}}{2}Z+C_I \tag{116}$$

Determining the integration constant C_I from initial conditions, the hydraulic head is specified as a function of Z as

$$\ln\left[\frac{1+A_b^{1/3}h^{1/2}+A_b^{2/3}h}{\left(1-A_b^{1/3}h^{1/2}\right)^2}\right]-2\left(3^{1/2}\right)\tan^{-1}\left(\frac{2A_b^{1/3}h^{1/2}+1}{3^{1/2}}\right)$$

$$=3A_b^{2/3}(Z_c-Z)+\ln\left[\frac{1+A_b^{1/3}h_o^{1/2}+A_b^{2/3}h_o}{\left(1-A_b^{1/3}h^{1/2}\right)^2}\right]$$

$$-2\left(3^{1/2}\right)\tan^{-1}\left(\frac{2A_b^{1/3}h_o^{1/2}+1}{3^{1/2}}\right) \tag{117}$$

105. To determine the variable Z explicitly, another equation is required. For this purpose, Equation 62 is subtracted from Equation 61:

$$\frac{dH}{dt}-\frac{dZ}{dt}=-\frac{sg^{1/2}}{A_s}(H-Z)^{2.5}+\alpha_2 g(H-Z) \tag{118}$$

By separating the variables, Equation 118 can be written as

$$\frac{dh}{h(1 - A_s h^{3/2})} = \alpha_2 g \, dt \tag{119}$$

Setting $W = A_6^{1/3} h^{1/2}$, Equation 119 is transformed to

$$\frac{dW}{W(1 - W^3)} = \frac{\alpha_2 g}{2} dt \tag{120}$$

Referring to page 61 of Gradshteyn and Ryzhik (1983), integration of Equation 120 gives

$$\frac{1}{3} \ln \frac{W^3}{1 - W^3} = \frac{\alpha_2 g}{2} t + C_I \tag{121}$$

Inserting initial conditions and transforming into the original variable $h = H - Z$, Equation 121 becomes

$$H - Z = \frac{H_o - Z_o}{\left\{ \frac{s}{\alpha_2 A_s^{1/2}} \left(H_o - Z_o\right)^{3/2} + \left[1 - \left(\frac{s}{\alpha_2 A_s g^{1/2}} \right) H_o - Z_o \right]^{3/2} \exp\left(-\frac{3}{2} \alpha_2 g t \right) \right\}^{2/3}} \tag{122}$$

Equations 117 and 122 can be used to estimate the variables $H = H(t)$ and $Z = Z(t)$.

Trapezoidal Breach

106. For trapezoidal breach, the cross-sectional area is defined as

$$A_b = b(H - Z) + s(H - Z)^2 \tag{123}$$

where b is the bottom width. During computations, the bottom width is assumed as constant.

Linear case

107. Dividing Equation 62 by Equation 64 and using Equation 123 yields

$$\frac{dH}{dZ} = \frac{1}{\alpha_2 A_s}\left[b(H - Z) + s(H - Z)^2\right] \tag{124}$$

Setting $h = H - Z$ and separating the variables, Equation 124 becomes

$$\frac{dh}{-\alpha_2 A_s + bh + sh^2} = \frac{1}{\alpha_2 A_s}\, dZ \tag{125}$$

Referring to page 68 of Gradshteyn and Ryzhik (1983), the integral of Equation 125 is

$$\frac{1}{b^2 + 4\alpha_2 s A^{1/2}} \ln \frac{(b^2 + 4\alpha_2 s A_s)^{1/2} - (b + 2sh)}{(b^2 + 4\alpha_2 s A_s)^{1/2} + (b + 2sh)} = \frac{1}{\alpha_2 A_s} Z + C_I \tag{126}$$

Defining the integration constant and inserting in Equation 126 results, after some algebraic manipulations, in the following:

$$\begin{aligned} 2s(H - Z) = \Bigg\{ & \left[\left(b^2 + 4\alpha_2 s A_s\right)^{1/2} - b\right]\left[\left(b^2 + 4\alpha_2 s A_s\right)^{1/2} + b + 2s(H_o - Z_o)\right] \\ & - \left[\left(b^2 + 4\alpha_2 s A_s\right)^{1/2} - b - 2s(H_o - Z_o)\right] \\ & \cdot \left[\left(b^2 + 4\alpha_2 s A_s\right)^{1/2} + b\right] \exp\left[\left(b^2 + 4\alpha_2 s A_s\right)^{1/2}\left(Z - Z_o/\alpha_2 A_s\right)\right] \Bigg\} \Bigg/ \\ & \Bigg\{ \left(b^2 + 4\alpha_2 s A_s\right)^{1/2} + b + 2s(H_o - Z_o) + \left[\left(b^2 + 4\alpha_2 s A_s\right)^{1/2} \right. \\ & \left. - b - 2s\left(H_o - Z_o\right)\right] \exp\left[\left(b^2 + 4\alpha_2 s A_s\right)\left(Z - Z_o/\alpha_2 A_s\right)\right] \Bigg\} \end{aligned} \tag{127}$$

108. The second equation required for determination of variables H and Z can be obtained again by subtracting Equation 64 from Equation 62.

$$\frac{dH}{dt} - \frac{dZ}{dt} = -\frac{1}{A_s}\left[g(H - Z)\right]^{1/2}\left[b(H - Z) + s(H - Z)^2\right] + \alpha_2\left[(H - Z)\right]^{1/2} \tag{128}$$

Writing Equation 128 in terms of the hydraulic head and separating the variables yields

$$\frac{dh}{h^{1/2}(-\alpha_2 A_s + bh + sh^2)} = -\frac{g^{1/2}}{A_s}\,dt \tag{129}$$

By setting $W = h^{1/2}$, Equation 129 transforms to

$$\frac{dW}{(-\alpha_2 A_s + bW^2 + sW^4)} = -\frac{g^{1/2}}{2A_s}\,dt \tag{130}$$

Referring to page 67 of Gradshteyn and Ryzhik (1983), integration of Equation 130 gives

$$\frac{s\left(\int \frac{dW}{A_7 + sW^2} - \int \frac{dW}{A_8 + sW^2}\right)}{\left(b^2 + 4\alpha_2 sA_s\right)^{1/2}} = -\frac{g^{1/2}}{2A_s}\,t + C_I \tag{131}$$

where

$$A_7 = \frac{b}{2} - \frac{1}{2}\left(b^2 + 4\alpha_2 sA_s\right)^{1/2} \tag{132}$$

and

$$A_8 = \frac{b}{2} + \frac{1}{2}\left(b^2 + 4\alpha_2 sA_s\right)^{1/2} \tag{133}$$

109. Equation 131 can be further simplified as

$$\frac{s}{(A_8 - A_7)}\left[\frac{1}{2i\left(A_7 s\right)^{1/2}} \ln \frac{A_7 + iW\left(A_7 s\right)^{1/2}}{A_7 - iW\left(A_7 s\right)^{1/2}} - \frac{1}{\left(A_8 s\right)^{1/2}} \tan^{-1} W\left(\frac{s}{A_8}\right)^{1/2}\right] = -\frac{g^{1/2}}{2A_s} t + C_I \qquad (134)$$

where i is the imaginary number. Transforming back to h and inserting the value of C_I according to initial conditions, after some algebraic calculations, results in

$$\ln \left(\frac{b}{2} - \frac{1}{2}\left(b^2 + 4\alpha_2 s A_s\right)^{1/2} + i\left\{ s(H - Z)\left[\frac{b}{2} - \frac{1}{2}\left(b^2 + 4\alpha_2 s A_s\right)^{1/2}\right]\right\}^{1/2} \Big/ \right.$$

$$\left. \frac{b}{2} - \frac{1}{2}\left(b^2 + 4\alpha_2 s A_s\right)^{1/2} - i\left\{ s(H - Z)\left[\frac{b}{2} - \frac{1}{2}\left(b^2 + 4\alpha_2 s A_s\right)^{1/2}\right]\right\}^{1/2} \right)$$

$$- 2i\left\{\left[\frac{b}{2} - \frac{1}{2}\left(b^2 + 4\alpha_2 s A_s\right)^{1/2}\right]^{1/2} \Big/ \left[\frac{b}{2} + \frac{1}{2}\left(b^2 + 4\alpha_2 s A_s\right)^{1/2}\right]^{1/2}\right\}$$

$$\tan^{-1}\left\{ s(H - Z) \Big/ \left[\frac{b}{2} + \frac{1}{2}\left(b^2 + 4\alpha_2 s A_s\right)^{1/2}\right]\right\}^{1/2}$$

$$= -it\frac{\sqrt{g}}{s}\left[\frac{b}{2} - \frac{1}{2}\left(b^2 + 4\alpha_2 s A_s\right)^{1/2}\right]\left(b^2 + 4\alpha_2 s A_s\right)^{1/2}$$

$$+ \ln \left(\frac{b}{2} - \frac{1}{2}\left(b^2 + 4\alpha_2 s A_s\right)^{1/2} + i\left\{ s(H_o - Z_o)\left[\frac{b}{2} - \frac{1}{2}\left(b^2 + 4\alpha_2 s A_s\right)^{1/2}\right]\right\}^{1/2} \Big/ \right.$$

$$\left. \frac{b}{2} - \frac{1}{2}\left(b^2 + 4\alpha_2 s A_s\right)^{1/2} - i\left\{ s(H_o - Z_o)\left[\frac{b}{2} - \frac{1}{2}\left(b^2 + 4\alpha_2 s A_s\right)^{1/2}\right]\right\}^{1/2} \right)$$

$$- 2i\left\{\left[\frac{b}{2} - \frac{1}{2}\left(b^2 + 4\alpha_2 s A_s\right)^{1/2}\right]^{1/2} \Big/ \left[\frac{b}{2} + \frac{1}{2}\left(b^2 + 4\alpha_2 s A_s\right)^{1/2}\right]^{1/2}\right\}$$

$$\tan^{-1}\left\{ s(H_o - Z_o) \Big/ \left[\frac{b}{2} + \frac{1}{2}\left(b^2 + 4\alpha_2 s A_s\right)^{1/2}\right]\right\}^{1/2} \qquad (135a)$$

110. If we let $b_o = \frac{b}{2} - \frac{1}{2}(b^2 + 4\alpha_2 sA_s)^{1/2}$, and $b_1 = \frac{b}{2} + \frac{1}{2}(b^2 + 4\alpha_2 sA_s)^{1/2}$, Equation 135 can be simply put as

$$\ln\left\{\frac{b_o + i\left[s(H - Z)b_o\right]^{1/2}}{b_o - i\left[s(H - Z)b_o\right]^{1/2}}\right\} - 2i\frac{(b_o)^{1/2}}{(b_1)^{1/2}}\tan^{-1}\left[\frac{s(H - Z)}{b_1}\right]^{1/2}$$

$$= -it\frac{\sqrt{g}}{s}(b_o)(b^2 + 4\alpha sA_s)^{1/2} + \ln\left\{\frac{b_o + i\left[s(H_o - Z_o)b_o\right]^{1/2}}{b_o - i\left[s(H_o - Z_o)b_o\right]^{1/2}}\right\}$$

$$- 2i\frac{(b_o)^{1/2}}{(b_1)^{1/2}}\tan^{-1}\left[\frac{s(H_o - Z_o)}{b_1}\right]^{1/2} \qquad (135b)$$

The system of Equations 127 and 135 determines the two unknown variables H and Z.

Nonlinear case

111. The nonlinear case of trapezoidal breach cannot be solved analytically even for simple specialized coefficients.

PART VI: APPLICATION AND RESULTS

112. The performance of the BEED model was tested for two historical dam-failure cases: the man-made earth-fill Teton Dam in Idaho, USA, and the Huaccoto natural dam on a tributary of the Mantaro River in Peru. The input parameters for both cases were taken from existing data.

Simulation of Teton Dam Failure

113. Teton Dam, a 93-m-high earth-fill structure, experienced failure on 5 June 1976. On 3 June 1976, leakage was detected at the toe of the dam. By early morning on 5 June a large leak caused by piping occurred 40 m below the crest near the right abutment, and by noon of that day the crest of the dam was breached. The water in the reservoir was almost at full capacity (3.1×10^3 m^3), and the total mass of water was released in approximately 4 hr, producing a maximum outflow discharge of 6.6×10^4 m^3/sec. At peak flow, the breach was estimated as trapezoidal with 150-m top width and slopes 1V:0.5H. This failure event caused $70 million in property damage and loss of six human lives.

114. The dam had a 915-m-long crest and was composed of mixtures of clay, silt, sand, and rock fragments obtained from excavations and borrow areas of the Teton River canyon area. The geometric characteristics of the dam are given in Figure 18. The reservoir capacity and the spillway and powerhouse-outlet discharge curves are defined in Figure 19. Figure 20 shows a map of the flooded area, which extended approximately 103 km downstream to near the Shelley gaging station on the Snake River. The geometric and physical characteristics of various sections of the flooded area are defined in Table 3 (Ray and Kjelstrom 1978).

Model calibration

115. The BEED model simulation was started after an initial trapezoidal breach with sides 1V:0.25H developed at the crest of the dam. The slopes of the dam were taken as 1V:3.08H and 1V:2.55H for the upstream and downstream faces, respectively. The initial hydraulic head was taken equal to 1 m of water flowing from the trapezoidal breach, where the ratio of bottom width to water depth was 0.5. The median soil particle diameter was taken as 3 mm, the

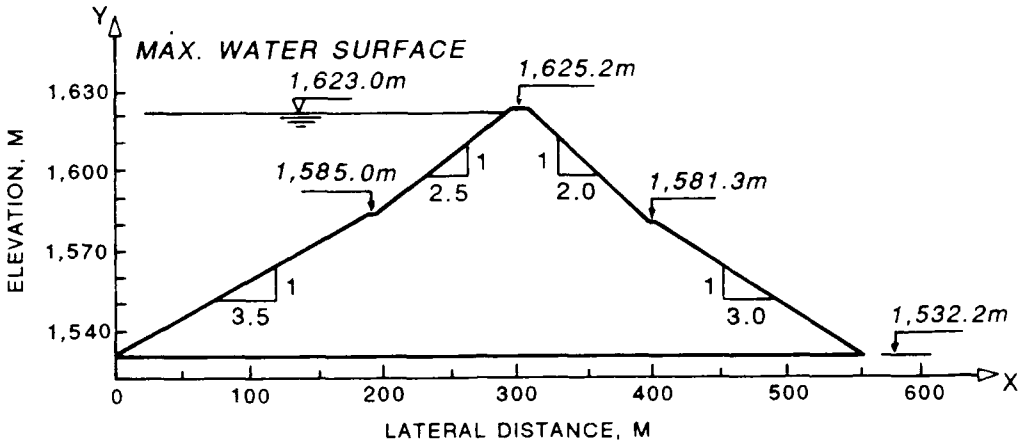

Figure 18. Geometric characteristics of Teton Dam

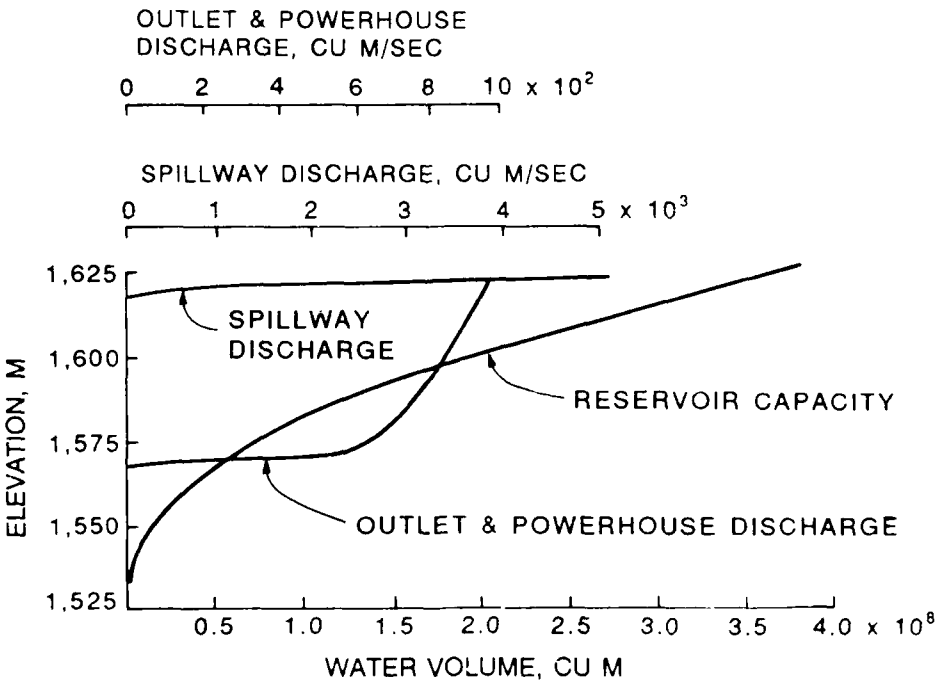

Figure 19. Operational characteristics of Teton Dam

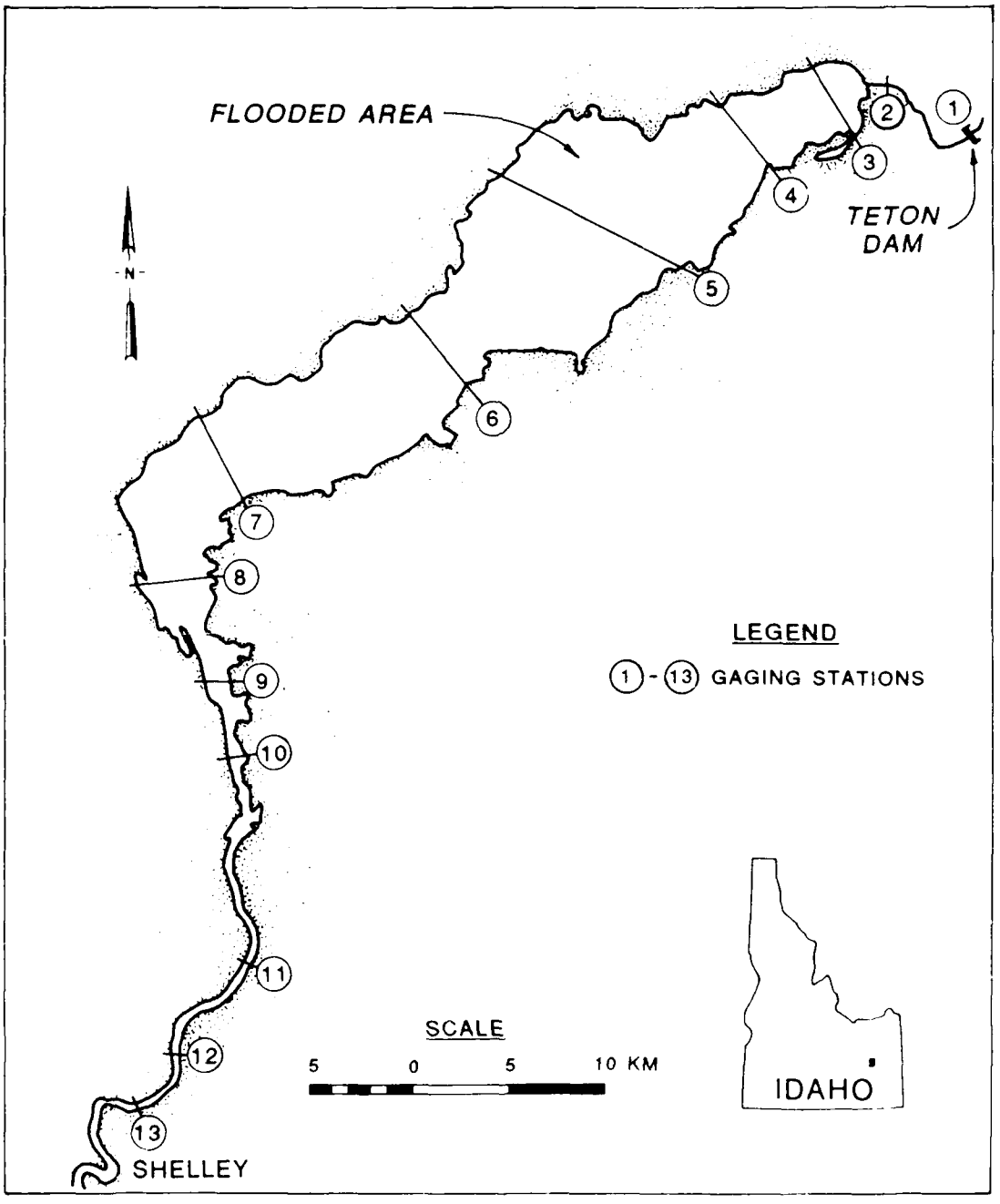

Figure 20. Downstream floodplain of Teton Dam

Table 3

Geometric and Physical Characteristics of Cross Sections of the Flooded Area Between Teton Dam and Shelley Gage on the Snake River

Station Number*	Distance from Teton Dam km	Width m	Slope %	Manning's Coefficient of Friction
1	0	300	0.0025	0.032
2	7.24	470	0.0018	0.035
3	10.46	4,400	0.0012	0.032
4	14.80	4,600	0.0027	0.030
5	26.39	10,200	0.0042	0.037
6	36.36	5,200	0.00032	0.042
7	52.45	5,200	0.00076	0.040
8	62.59	3,900	0.0014	0.037
9	71.76	1,300	0.0014	0.035
10	75.95	260	0.0014	0.033
11	90.75	140	0.0014	0.040
12	97.83	200	0.0014	0.035
13	103.30	170	0.0014	0.036

Source: Ray and Kjelstrom 1978. Station locations are shown in Figure 20.

porosity as 0.2, and the specific weight of soil as 2.5 tons (2.3 metric tons)/m^3. Other soil characteristics were assumed as follows: cohesion strength 49,000 N/m^2; angle of internal friction, 40 deg; and Chezy's coefficient of roughness, 50 $m^{1/2}$/sec (Ray and Kjelstrom 1978). The relation for the Einstein-Brown bed-load transport function for values of $1/\Psi$ higher than 2 was taken as

$$\Phi = 139.3\left(\frac{1}{\Psi}\right)^{1.2} \tag{136}$$

The coefficient and the exponent in Equation 136 were obtained by trial and error, since there are no laboratory or field data in that range of high shear

stresses. All data required for flood routing were taken from Table 3. The assumed inflow hydrograph $I_o = I_o(t)$ is shown in the following tabulation.

Time hr	Discharge m^3/sec
0	28.32
0.5	84.96
1	158.59
2	212.40
3	192.58
4	130.27
6	67.97
8	42.48
10	28.32
27.5	28.32

Simulation results

116. The computed outflow (Figure 21) indicates that the timing, shape, and magnitude of the estimated outflow hydrograph compare quite well with the observed values. The higher peak outflow, total volume, and delayed falling limb of the simulated hydrograph may be attributed to the fact that the program continued the simulation until erosion reached the bottom of the dam, while in reality, the breach bottom terminal elevation was about 14 m above ground level. At peak outflow discharge, the simulated breach was trapezoidal, with a top width of 161 m and side slopes of 1V:0.675H. This breach is very similar to the field data breach reported as having a 152.4-m top width and side slopes of 1V:0.5H. After the peak flow, however, the model estimated a total width of 295 m, much higher than a recorded width of approximately 200 m.

117. Routing of the predicted outflow discharge produced a hydrograph for station 13 near Shelley that was sharper and much higher than the one recorded (Figure 22). The discrepancy can be attributed to the fact that the BEED model used the values of slope and friction that were given for the flood channel, and not its adjacent floodplain, which presumably had less slope and higher friction. Another possible reason for the inaccuracy is the steepness of the breach outflow discharge, which acted like a shock wave. Improvement can be obtained either by using a more accurate routing approach, such as the

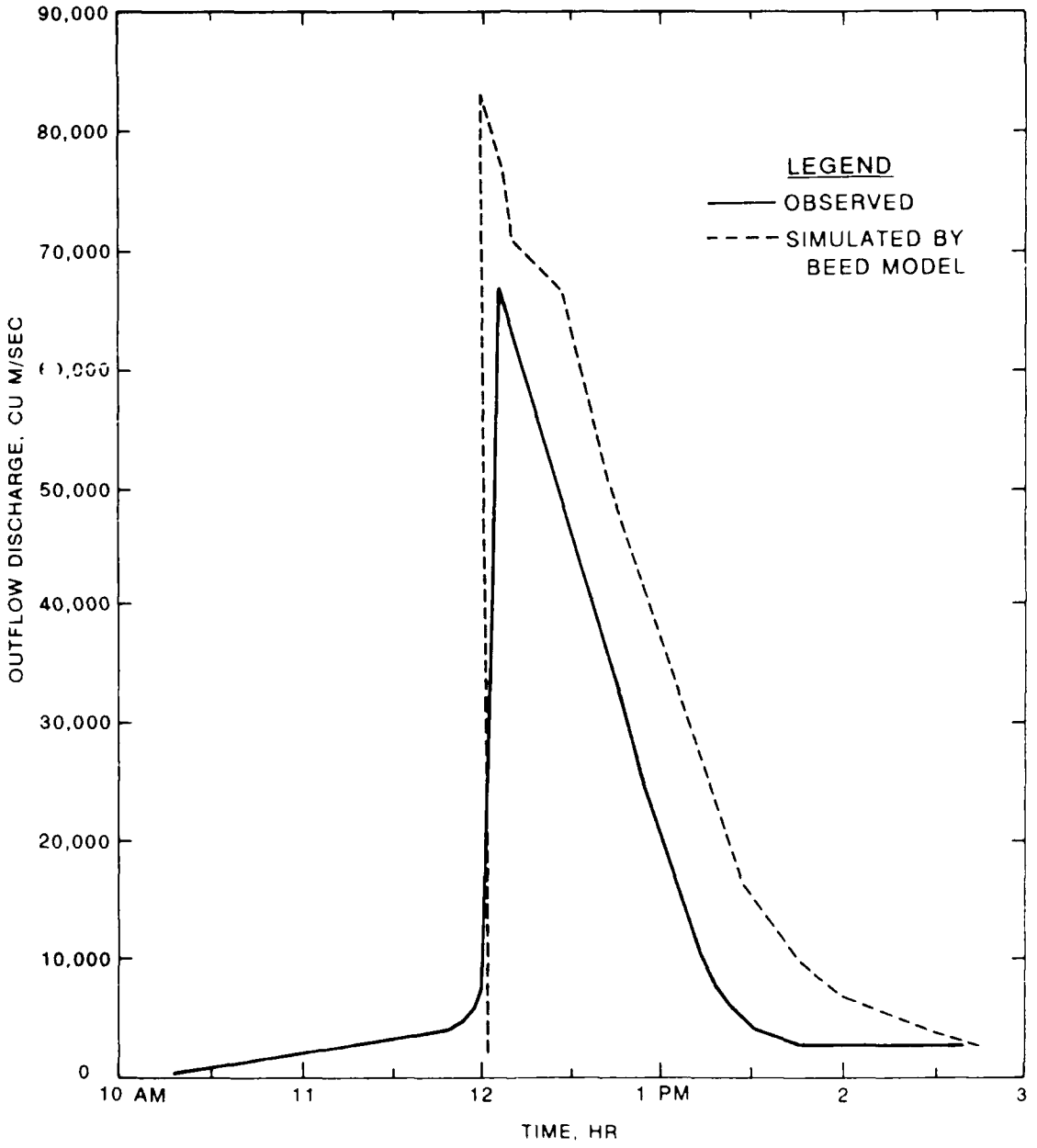

Figure 21. Outflow discharge resulting from failure of Teton Dam

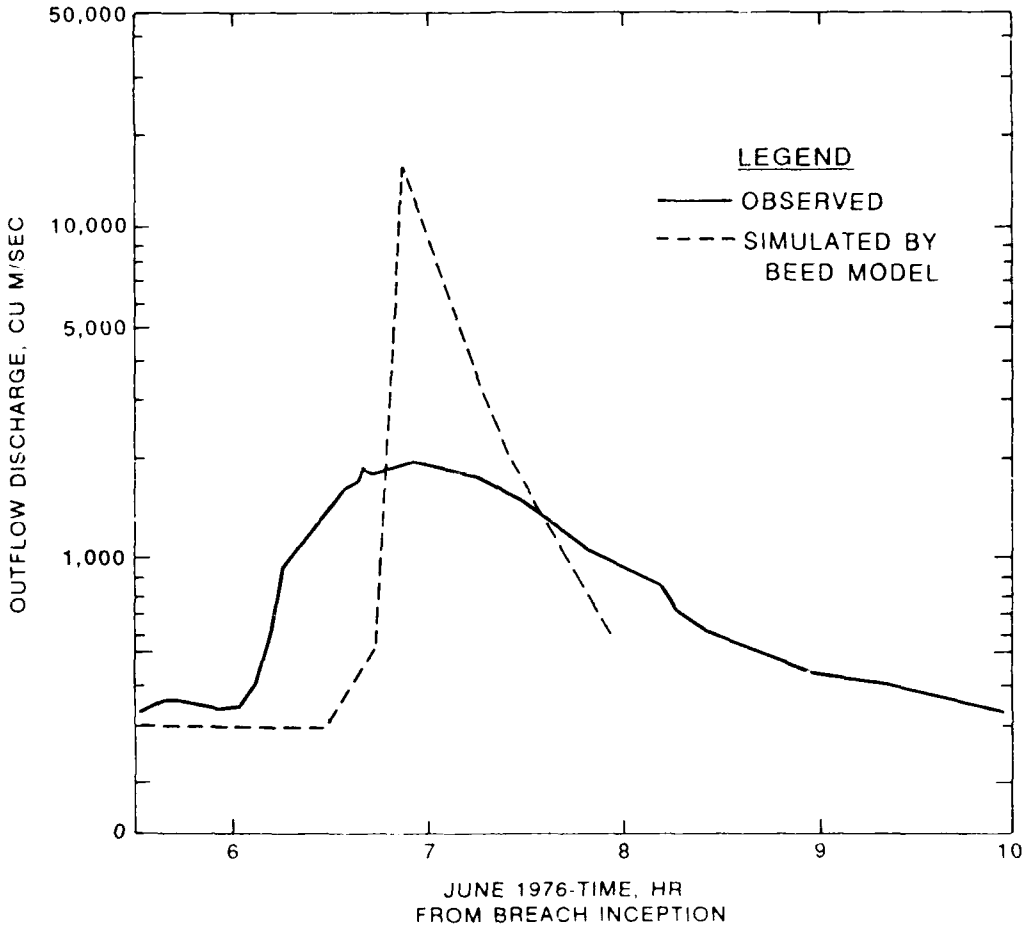

Figure 22. Outflow discharge hydrograph at Shelley station

St. Venant system of equations, or extending the Muskingum method to incorporate two-dimensional flow behavior.

118. To evaluate the dependence of the system on the various physical parameters, a sensitivity analysis was conducted by changing the input parameters within certain ranges. The basic characteristics were as follows:

C_h = 50 $m^{1/2}$/sec	ϕ = 40 deg
D_{50} = 3 mm	p = 0.2
C = 49,000 N/m	tan θ = 0.25

The relative difference in discharge (RDD) is defined as

$$RDD = \frac{Q_x - Q_b}{\frac{1}{2}\left(Q_x + Q_b\right)} \times 100 \qquad (137)$$

where Q_x is the computed outflow discharge and Q_b is the basic outflow discharge and both were computed as presented in Table 4.

119. Table 4 offers evidence that the peak outflow discharge is insensitive to most physical parameters except the angle of internal friction. The time of occurrence of peak discharge increases with increasing Chezy's coefficient of friction. The opposite is true for the median particle diameter, cohesion, internal friction, and porosity. The side slope of breach at the time of peak discharge is larger for low values of cohesion, internal friction, and/or porosity. In general, within a certain degree of accuracy, the model can be considered as insensitive to variation of those physical parameters.

120. Special attention should be given to the determination of the ratio between breach bottom width and hydraulic head and to the expression for the Einstein-Brown formula. Unfortunately, the data are insufficient to define these characteristics accurately, and a trial-and-error procedure is required.

Simulation of Failure of Huaccoto Dam

121. On April 25, 1974, a landslide that occurred in Cochacay Creek, a tributary of the Mantaro River in Peru, created the Huaccoto natural dam. The landslide material consisted mostly of silty sand and clay with D_{50} of about 11 mm, but there was also material in size up to 1 m. The embankment was 170 m in height, and its lateral base length was 3,803 m. The geometric characteristics of Huaccoto Dam are represented in Figure 23. The dam created an artificial lake with a maximum capacity of 8.87×10^8 m^3. The reservoir capacity curve is given as Figure 24.

122. Huaccoto Dam failed from overtopping. During the period 6-8 June 1974, the overtopping flow created a channel along the downstream face of the dam and, in the next 6 to 10 hr, a rapid increase in erosion resulted in

Table 4

Results of Sensitivity Analysis for Teton Dam

Parameter	Value				
Chezy's coefficient of friction, $m^{1/2}/sec$	30	40	50	60	70
RDD	5.10	1.00	0	3.60	3.09
Time of peak outflow discharge, hr	0.74	1.00	1.26	1.49	1.73
Breach side slopes at peak discharge, IV:sH	0.675	0.675	0.675	0.675	0.675
Median particle diameter, mm	1	3	5		
RDD	1.39	0	-1.17		
Time of peak outflow discharge, hr	1.94	1.26	1.15		
Breach side slopes at peak discharge	0.675	0.675	0.675		
Cohesion in N/m^2	30,000	40,000	49,000		
RDD	0.48	5.55	0		
Time of peak outflow discharge, hr	1.42	1.26	1.26		
Breach side slopes at peak discharge	0.811	0.675	0.675		
Soil internal friction angle, deg	30	40			
RDD	18.99	0			
Time of peak outflow discharge, hr	1.42	1.26			
Breach side slopes at peak discharge	0.811	0.675			
Porosity	0.2	0.3	0.5		
RDD	0	0.33	-5.18		
Time of peak outflow discharge, hr	1.26	1.04	0.73		
Breach side slopes at peak discharge	0.675	0.675	0.550		

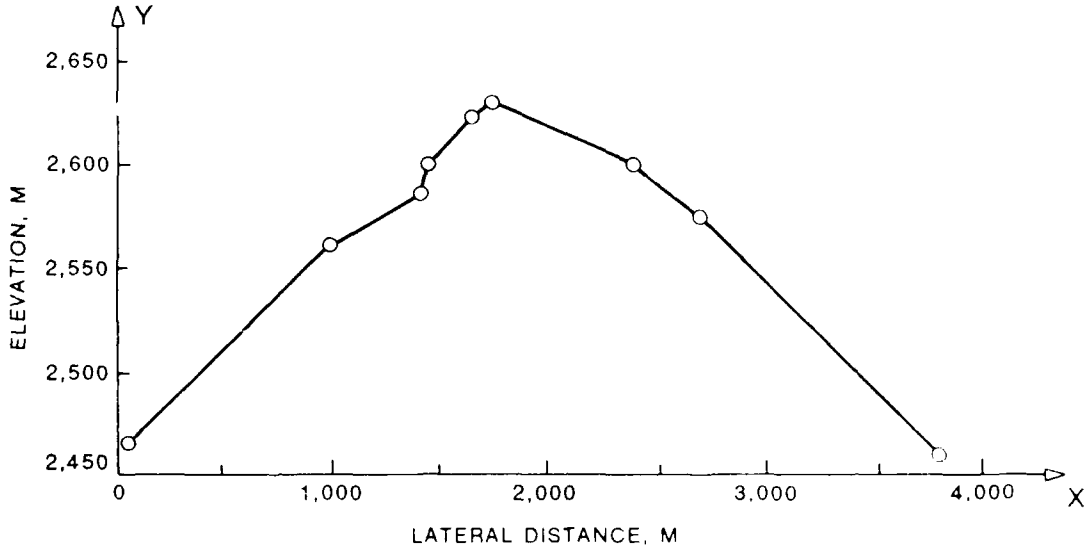

Figure 23. Geometric characteristics of Huaccoto Dam

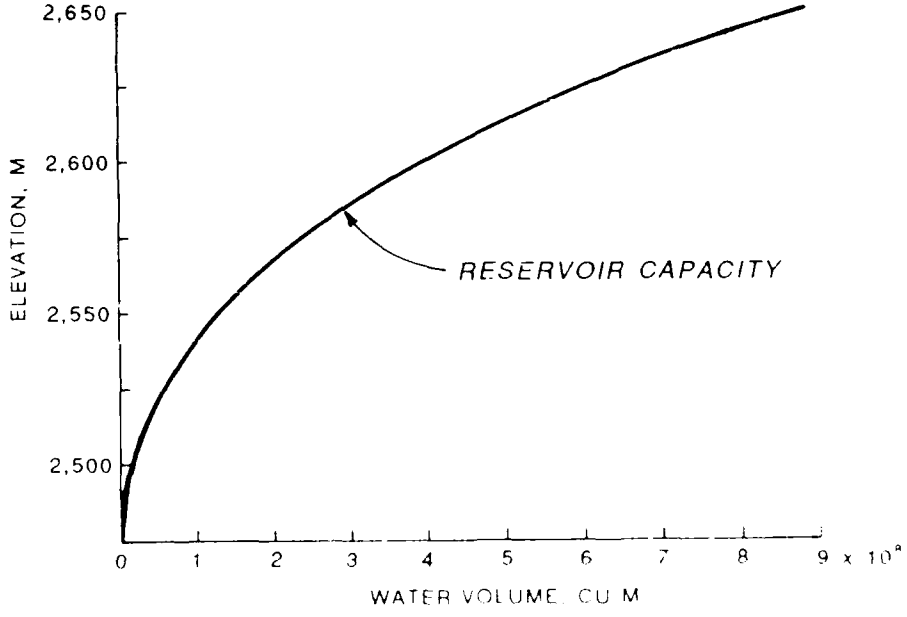

Figure 24. Reservoir capacity of Huaccoto Dam

a final trapezoidal breach of 107-m depth, 200- to 230-m top width, and side slopes of about 1V:1H. The peak outflow discharge was reported to be from 1.0 $\times 10^4$ to 1.80 $\times 10^4$ m^3/sec.

Model calibration

123. The BEED model started the simulation after an initial trapezoidal breach with sides 1V:0.25H developed at the crest of the dam. The slopes of the dam were taken as 1V:1?.56H and 1V:12.49H for upstream and downstream faces, respectively. The initial hydraulic head was taken equal to 1 m of water. The ratio of bottom width over hydraulic head was 0.4. The median particle size was taken as 15 mm, the porosity as 0.4, and the specific weight of soil as 2.5 tons (2.3 metric tons)/m^3. Other soil characteristics were assumed as follows: cohesion strength, 40,000 N/m^2; angle of internal friction, 40 deg; and Chezy's coefficient of friction, 50 $m^{1/2}$/sec (Ponce 1982, Fread 1984). The Einstein-Brown bed-load function for values of 1/? higher than 2 was taken as constant and equal to 360. The inflow hydrograph was considered to be very small and thus was neglected.

Simulation results

124. The computed outflow presented in Figure 25 shows that the shape, timing, and magnitude of the computer hydrograph resembled fairly well the one observed. Here it should be noted that higher simulated discharge in this case does not constitute inaccuracy for the model because there are conflicting reports of the actual peak discharge ranging from 10,000 to 18,000 m^3/sec with a more likely value of 13,500 m^3/sec. At the time of peak outflow discharge, the breach had a top width of 167 m and side slopes of 1V:1.378H. Those results are very close to field reports that give a top breach width of 198 m and side slopes of 1V:1H. The terminal breach obtained by the simulation was 89 m deep and had a bottom width of 14.61 m. The side slopes were 1V:1.67H, indicating that mass failures of the breach side slopes occurred following peak discharge.

125. During calibration of the BEED model for the Buccheto Dam, it was noted that the bed-load function used for Teton Dam (Equation 136) was not applicable, as it was giving very high erosion rates and subsequently high outflow discharges. The effects of the various selected functions on the magnitude and timing of outflow discharge are presented in the following tabulation.

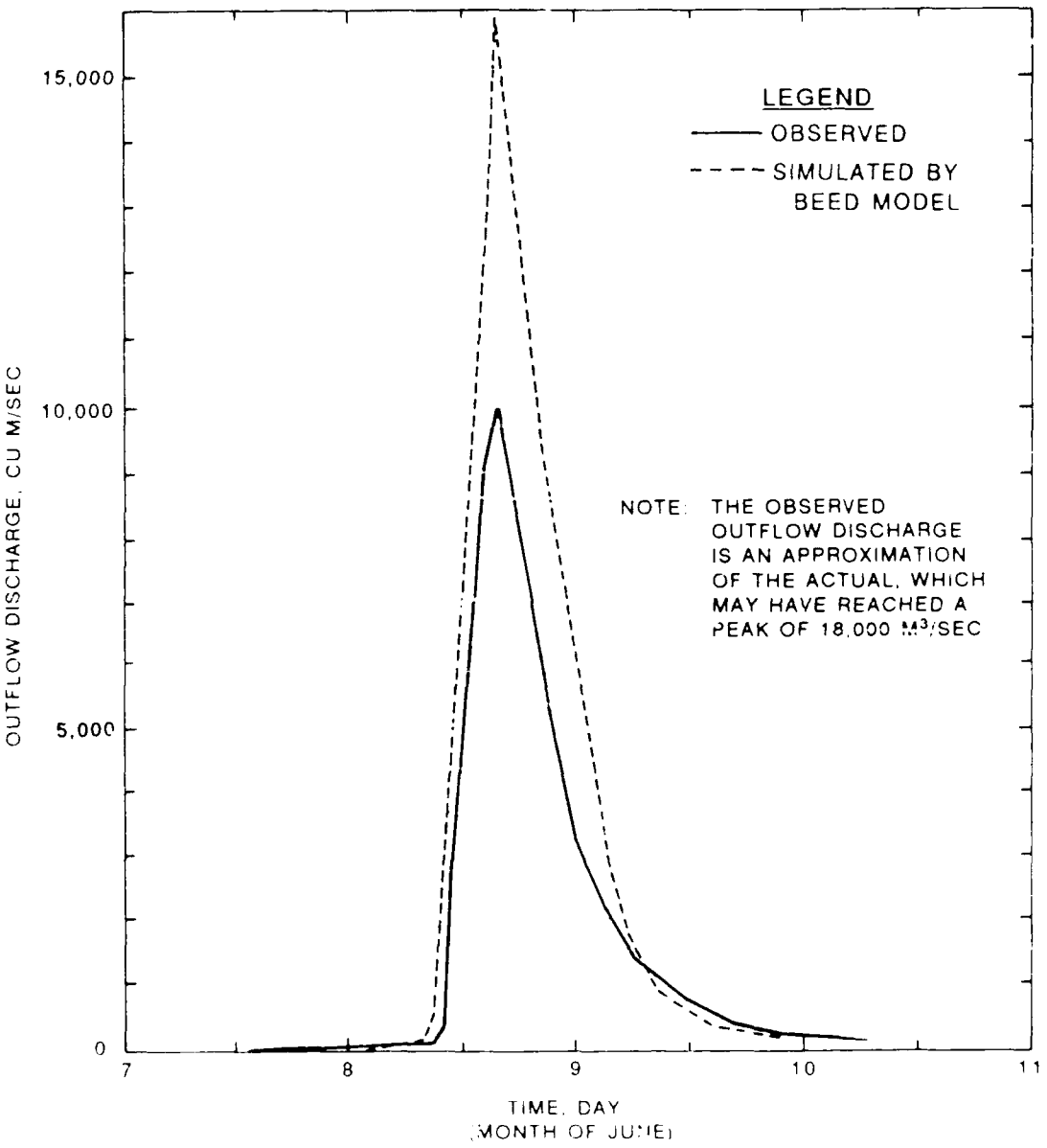

Figure 25. Outflow discharge resulting from failure of Buccoto Dam

Function	α	154.55	160.00	171.48	211.12	226.27	320.00
$\Phi = f\left(\frac{1}{\Psi}\right) = \alpha\left(\frac{1}{\Psi}\right)^{B}$	B	1.05	1.00	0.9	0.6	0.5	0
Peak outflow discharge, m^3/sec		81,000	78,015	73,077	68,021	54,861	16,700
Time of peak outflow discharge, hr		19.34	19.56	19.99	21.85	22.80	27.30

The sensitivity of the model to the bed-load discharge formula is an indication of the need for basic research on erosion processes under high shear stresses.

Analytical results

126. The uncertainty associated with the lumped erosivity coefficient α_2 in the analytical solutions and the assumption of a constant water surface A_s make the calibration of those solutions very difficult. Comparing these solutions with the governing equations of the BEED model, it is evident that the coefficient α_2 is a function of surface roughness, cohesion, angle of internal friction, porosity, specific gravity, and water viscosity.

127. To investigate the behavior of analytical solutions, a limited number of tests were conducted for the nonlinear case of the rectangular breach. For these tests, a hypothetical dam of the following characteristics was assumed: initial height of dam, 1 m; initial breach bottom elevation, 0.90 m; breach width, 0.2 m; water surface area, 1,000 m^2; and erosivity coefficient equal to 0.001 and 0.01 for the first and second cases, respectively. In the first case, after 100 sec the breach bottom elevation was 0.975 m and the hydraulic head was 0.026 m. In the second case, after 48 sec, the dam had eroded completely and the hydraulic head receded by a maximum of 0.87 m.

128. Changing the water surface area from 1,000 to 100 m, setting the breach width equal to 0.1 m, assuming an initial breach bottom elevation of 0.95 m, and trying the same problem for $\alpha_2 = 0.1$ and 0.01, complete erosion was achieved in 8 min in the first case, while it took 67 min in the second case. The peak hydraulic head was 0.89 m for $\alpha_2 = 0.1$ and 0.81 for $\alpha_2 = 0.01$.

129. Those few results stress the fact that, before attempting to use the analytical solutions, both the erosivity coefficient α_2 and the water surface area should be properly calibrated and defined. An interesting result from the analytical solutions is that peak outflow discharge is obtained at the time the breach reached its terminal depth. This is in agreement with results from the BEED model.

PART VII: CONCLUSIONS AND RECOMMENDATIONS

130. The conclusions obtained from this study can be summarized as follows:

a. With consideration of both surface erosion and sloughing of the breach sides due to instability, the BEED model satisfactorily simulates the processes of gradual erosion of earth-fill dams.

b. The accuracy of the BEED model is comparable to the accuracy of other existing models, but the physical basis of the governing processes is improved.

c. The model is not very sensitive to the variations of the roughness coefficient, the median particle diameter porosity, and soil cohesion. For changes within reasonable ranges of values, the model produced a relative error in peak outflow discharge of less than 5 percent.

d. The internal angle of friction of the soil is important for estimation of peak outflow discharge.

e. Low values of porosity, internal friction, and/or porosity result in a wider terminal breach.

f. The ratio of bottom breach width over hydraulic head performed well for values of 0.5 and 0.4 for Teton Dam and Huaccoto Dam, respectively. However, there is no evidence that the same values can be applicable for other cases.

g. The Einstein-Brown formula for values of the dimensionless shear stress ($1/\Psi$) greater than 2 is difficult to estimate a priori, and a trial-and-error process is required. The results are sensitive to the selection of this function.

h. The peak outflow discharge is obtained when the breach reaches its terminal bottom elevation.

i. Sloughing of breach sides may occur even after the occurrence of peak outflow discharge.

j. The routing part of the BEED model overestimates the discharge hydrograph at downstream stations. This may be attributed to the fact that the breach outflow hydrograph is very steep and acts like a shock wave. Also, two-dimensional effects of flow over the floodplain might contribute to the discrepancies.

131. Based on the experience gained from this study, the following recommendations for further study are given.

a. Extension of the BEED model to include options of other sediment transport theories, such as Schoklitsch, Meyer-Peter and Mueller, and the Bagnold power method.

b. Application of the BEED model to as many historical cases as possible for estimation of the range of physical parameters, and determination of the optimum technique for sediment transport processes.

c. Calibration of the analytical solutions according to data obtained from simulation of the BEED model.

d. Extension of the routing part of the BEED model to incorporate two-dimensional flow along the floodplain.

e. Extension of the BEED model by coupling flood routing with sediment routing along the downstream channel.

REFERENCES

Abbott, M. B. 1966. An Introduction to the Method of Characteristics, American Elsevier, New York.

Amein, M. 1966. "Streamflow Routing on Computer by Characteristics," Water Resources Research, Vol 2, No. 1, pp 123-130.

Brater, E. 1959. "Hydraulics," Civil Engineering Handbook, L. C. Urquhart, ed., McGraw-Hill, New York, Section 4.

Brown, C. B. 1950. Engineering Hydraulics, H. Rouse, ed., John Wiley and Sons, New York.

Brown, R. J., and Rogers, D. C. 1977. "A Simulation of the Hydraulic Events During and Following the Teton Dam Failure," Proceedings of Dam-Break Flood Routing Model Workshop, Bethesda, MD, October 18-20, pp 131-163.

_____. 1981. "User Manual for Program BRDAM," Engineering and Research Center, Bureau of Reclamation, Denver, CO.

Chow, V. T. 1959. Open Channel Hydraulics, International Student Edition, McGraw-Hill, New York.

Chugaev, R. R. 1964. "Stability Analysis of Earth Slopes," Israel Program for Scientific Translations, Jerusalem.

Courant, R., Friedrichs, K. O., and Lewy, H. 1967 (Mar). "On the Partial Difference Equations of Mathematical Physics," IBM Journal, pp 215-234.

Cristofano, E. A. 1965. "Method of Computing Rate of Failure of Earth Fill Dams," Bureau of Reclamation, Denver, CO.

Dronkers, J. J. 1964. Tidal Computations in Rivers and Coastal Waters, North-Holland Publishing Company, Amsterdam.

_____. 1969. "Tidal Computations for Rivers, Coastal Areas and Seas," Journal of the Hydraulics Division, ASCE, Vol 95, No. HY1, Proc. Paper 6341, pp 29-77.

Faure, J., and Nahas, N. 1961. "Etude Numerique et Experimentale d'Intumescences a Forte Courbure du Front," La Houille Blanche, No. 5, pp 576-587.

Finlayson, B. A. 1972. The Method of Weighted Residuals and Variational Principles, Academic Press, New York.

Fread, D. L. 1977. "The Development and Testing of a Dam-Break Flood Forecasting Model," Proceedings of Dam-Break Flood Routing Model Workshop, Bethesda, MD, October 18-20, pp 164-197.

_____. 1978. "NWS Operational Dynamic Wave Model, Verification of Mathematical and Physical Models in Hydraulic Engineering," Proceedings of the 26th Annual ASCE Hydraulics Division Specialty Conference, College Park, MD, pp 455-464.

_____. 1980. "Capabilities of NWS Model to Forecast Flash Floods Caused by Dam Failures," Proceedings of Second Conference on Flash Floods, American Meteorological Society, Boston, MA, March 18-20, pp 171-178.

_____. 1981. "Some Limitations of Dam-Breach Flood Routing Models," ASCE Fall Convention, October 20-30, St. Louis, MO.

Fread, D. L. 1984. "A Breach Erosion Model for Earthen Dams," National Weather Service Report, NOAA, Silver Spring, MD.

Gradshteyn, I. S., and Ryzhik, I. M. 1983. Table of Integrals, Series and Products, Academic Press, New York.

Gruner, E. 1967. "The Mechanism of Dam Failure," Neuvieme Congres des Grands Barrages, CIGB, Q. 34, R. 12, Istanbul, pp 197-206.

Harris, G. W., and Wagner, D. A. 1967. "Outflow from Breached Earth Dams," B.S. thesis, University of Utah, Salt Lake City, UT.

Houston, M. 1984. "Breaching Characteristics of Dam Failures, Discussion," Journal of Hydraulic Engineering, ASCE, Vol 110, No. 11, pp 1125-1129.

Isaacson, E., Stoker, J. J., and Troesch, A. 1958. "Numerical Solution of Flow Problems in Rivers," Journal of the Hydraulics Division, ASCE, Vol 84, Proceedings Paper 1810.

Jansen, R. B. 1980. Dam and Public Safety, Water and Power Resources Service, US Government Printing Office, Denver, CO.

Laursen, E. M. 1956. "The Application of Sediment Transport Mechanics to Stable Channel Design," Journal of the Hydraulics Division, ASCE, Vol 82, No. HY4.

Lax, P. D., and Wendroff, B. 1960. "Systems of Conservation Laws," Communications on Pure and Applied Mathematics, Vol 13, pp 217-237.

_____. 1964. "Difference Schemes with High Order of Accuracy for Hyperbolic Equations," Communications on Pure and Applied Mathematics, Vol 17, p 381.

Lou, W. C. 1981. "Mathematical Modeling of Earth Dam Breaches," Ph.D. dissertation, Colorado State University, Fort Collins, CO.

MacDonald, T. C., and Langridge-Monopolis, J. 1984. "Breaching Characteristics of Dam Failures," Journal of Hydraulic Engineering, ASCE, Vol 110, No. 5, pp 567-586.

Mahmood, K., and Yevjevich, V., eds. 1975. Unsteady Flow in Open Channels, 2 vols, Water Resources Publications, Fort Collins, CO.

Mozayeny, B., and Song, C. S. 1969. "Propagation of Flood Waves in Open Channels," Journal of the Hydraulics Division, ASCE, Vol 95, No. HY3, Proceedings Paper 6561, pp 877-892.

Ponce, V. M. 1982. "Documented Cases of Earth Dam Breaches," San Diego State University Series No. 82149, San Diego, CA.

Ponce, V. M., and Tsivoglou, A. J. 1981. "Modeling Gradual Dam Breaches," Journal of the Hydraulics Division, ASCE, Vol 107, No. HY7, Proceedings Paper 16372, pp 829-838.

Ponce, V. M., and Yevjevich, V. 1978. "Muskingum-Cunge Method with Variable Parameters," Journal of the Hydraulics Division, ASCE, Vol 104, No. HY12, pp 1663-1667.

Prasad, R. 1970. "Numerical Method of Computing Flow Profiles," Journal of Hydraulics Division, ASCE, Vol 96, No. HY1, pp 75-85.

Pugh, C. A., and Gray, F. W., Jr. 1984. "Fuse Plug Embankments in Auxiliary Spillways - Developing Design Guidelines and Parameters," Bureau of Reclamation Report, Denver, CO.

Ray, H. A., and Kjelstrom, L. C. 1978. "The Flood in Southeastern Idaho from the Teton Dam Failure of June 5, 1976," Open File Report 77-765, US Geological Survey, Reston, VA.

Scarlatos, P. D. 1982. "A Pure Finite Element Method for the Saint Venant Equations," Coastal Engineering, Amsterdam, Vol 6, pp 27-45.

Schonfeld, J. C. 1951. "Propagation of Tides and Similar Waves," Ph.D. thesis, Technische Hogeschool te Delft, The Netherlands.

Sherman, B., and Singh, V. P. 1978. "A Kinematic Model for Surface Irrigation," Water Resources Research, Vol 14, No. 2, pp 357-364.

_____. 1982. "A Kinematic Model for Surface Irrigation: An Extension," Water Resources Research, Vol 18, No. 3, pp 659-667.

Simons, D. B., and Senturk, F. 1976. Sediment Transport Technology, Water Resources Publications, Fort Collins, CO.

Singh, V. P., and McCann, R. C. 1980. "A Study of the Muskingum Method of Flood Routing," Report MSSU-EIRS-CE-80-2, Mississippi State University, Mississippi State, MS.

Singh, K. P., and Snorrason, A. 1982. "Sensitivity of Outflow Peaks and Flood Stages to the Selection of Dam Breach Parameters and Simulation Models," State Water Survey Division Report 289, Surface Water Section, University of Illinois, Urbana, IL.

Stoker, J. J. 1957. Water Waves, Interscience Publisher, New York.

Taylor, C., and Davis, J. 1973. "Finite Element Numerical Modeling of Flow and Dispersion in Estuaries, International Association for Hydraulic Research, Proceedings Paper C39.

US Army Corps of Engineers. 1961. "Floods Resulting from Suddenly Breached Dams; Report 2, Conditions of Minimum Resistance; Hydraulic Model Investigation," Miscellaneous Paper 2-374, US Army Engineer Waterways Experiment Station, Vicksburg, MS.

_____. 1975. "National Program of Inspection of Dams," Washington, DC.

Zienkiewicz, O. C. 1971. The Finite Element Method in Engineering Science, McGraw-Hill, London, England.

APPENDIX A: USER'S MANUAL FOR BEED-I MODEL

1. The BEED model has two versions: BEED-I is written in FORTRAN 77 language and is intended for use in mainframe computer facilities, while BEED-II is written in ZBASIC and is suitable for Zenith Z100 microcomputers. Both versions contain the same computational elements, and their objective is the same. However, version II may impose memory storage limitations, while its efficiency measured in CPU time is 30 to 60 times less than version I.

2. The program consists of the MAIN program and six subroutines:

   a. MAIN program includes the iterative algorithm for estimation of water surface level H2 and breach bottom elevation DZT1. It also contains computations of the discharge QTT at the various down stream channel cross sections during flood-routing processes.

   b. Subroutine COVOL computes changes in reservoir water volume capacity.

   c. Subroutine COQSOI estimates spillway outflow, powerhouse outlet outflow, and inflow discharge.

   d. Subroutine COQBV estimates bed-load sediment transport in volume per unit width and unit time, using the Einstein-Brown formula.

   e. Subroutine COY2YT calculates water depth at the tailwater section by using the Newton-Raphson or a fixed-point iteration algorithm.

   f. Subroutine COQB2 estimates reduced discharge coefficients for consideration of submerged flow conditions.

   g. Subroutine COATW calculates cross-sectional area and top width of flood channel computational segments.

Input Data

3. Input characteristics in both versions are the same. Of course, the FORMAT statements of BEED-I do not apply to BEED-II. For consistency, however, it is suggested that the same format structure be used for both versions. Input data are divided into groups. Each group contains certain variables, as described below.

   a. Group 1.

      (1) Physical characteristics and properties of dam.

      CH, DS, SP, P, NIU, PHI, COH - Format (4F8.4, F11.7, 2F10.2)

      CH: Chezy's coefficient of friction for the breach in $m^{1/2}/sec$

DS: representative value of dam material diameter (usually D_{50}) in meters

SR: relative specific weight of dam material (γ_s/γ)

P: soil porosity

NIV: kinematic viscosity of water in m^2/sec

PHI: angle of internal friction of dam material in degrees

COH: cohesion of dam material in N/m^2

(2) Geometric characteristics of dam.

LB, LT, LC, HTD, HB - Format (5F10.3)

LB: longitudinal length of the base of dam in meters

LT: horizontal projection of upstream slope of dam in meters

LC: longitudinal length of dam crest in meters

HTD: height of dam crest in meters

HB: elevation of dam bottom in meters

(3) Initial conditions of dam-breach computations.

H1T, Z1T, Z2MIN, DTB - Format (4F10.3)

H1T: initial water level in the reservoir in meters

Z1T: initial elevation of breach bottom in meters

Z2MIN: minimum permissible breach bottom elevation (usually Z2MIN = HB) in meters

DTB: basic time step for breach erosion computations in seconds

(4) Breach erosion characteristics.

L1MIN, SEC, EXPO, X, ZT - Format (5F10.3)

L1MIN: minimum longitudinal horizontal length of breach bottom at the top of dam in meters

SEC: coefficient of sediment transport function (i.e., $\Phi = \sec(1/\Psi)^{EXPO}$

EXPO: exponent of sediment transport function

X: initial ratio of breach bottom width to initial hydraulic head

ZT: initial side slope of breach section

(5) Choice of iterative algorithm.

NOF1 - Format (I2)

NOF1: If NOF1 = 0 , the Newton-Raphson algorithm is used for computation of normal depths.

If NOF1 = 1 , the fixed-point iteration is used for computation of normal depths.

b. Group 2.

(1) Computational time characteristics.

TSIM, DTR - Format (2F11.7)

TSIM: time of simulation in hours

DTR: time interval for flood routing in hours

(2) Computational distance characteristics.

DXMIN - Format (F10.3)

DXMIN: maximum permissible channel reach distance in meters

Note: If distance between two consecutive stations is greater than DXMIN, the program generates intermediate sections until that condition is satisfied.

(3) Flood channel geometric and physical characteristics.

BV(I), ZV(I), CHV(I), NMV(I), SV(I), DIST(I), PRT(I) -

Format (3F10,2, 2F10.5, F10.2, F4.1)

Note: This card is repeated until all sections are input. The last card may say 9999.0 for BV(I) and 0.0 for the rest. The first section is used for the tailwater-effects check immediately downstream of the dam.

BV(I): channel bottom width at section (I) in meters

ZV(I): channel side slope at section (I) in m/m (the channel is assumed symmetrical)

CHV(I): Chezy's coefficient of friction at section (I) in $m^{1/2}/sec$

NMV(I): Manning's coefficient of friction at section (I)

Note: Only one coefficient of friction can be specified. The other must be set equal to 0.0. All sections must have the same coefficient of friction.

SV(I): channel slope at section (I) in m/m

DIST(I): distance from dam to section (I) along the channel in meters

PRT(I): parameter to specify whether hydrograph at section (I) will be printed; if yes, PRT(I) = 1; if not, PRT(I) = 0.0

(4) Flood channel initial conditions.

QTTLS - Format (F10.2)

QTTLS: assumed initial discharge at the last section in m^3/sec

Note: Initial discharges at the rest of sections are defined by interpolation between initial total discharge from dam HYD(1) and QTTLS.

c. Group 3.

(1) Reservoir characteristics.

HVL(I), VOL(I) - Format (F10.2, F15.2)

HVL(I): reservoir water level associated with stored water volume in meters

VOL(I): volume of stored water when reservoir water level is HVL(I) in m^3

Note: Maximum number of data, including last card, is 20. Last card must say 9999.0 for HVL(I) and 010 for VOL(I). First card must correspond to dam bottom elevation.

(2) Spillway characteristics.

HSP(I), QSP(I) - Format (2F10.2)

HSP(I): water elevation associated with spillway outflow discharge in meters

QSP(I): spillway discharge at water elevation HSP(I) in m^3/sec

Note: Same comments as in (1).

(3) Powerhouse outlet characteristics.

HOV(I), QOV(I) - Format (2F10.2)

HOV(I): water elevation associated with outlet discharge in meters

QOV(I): outlet discharge at water elevation HOV(I) in m^3/sec

Note: Same comments as in (1).

(4) Inflow hydrograph characteristics.

TIF(I), INF(I) - Format (2F10.2)

TIF(I): time associated with inflow discharge in meters

INF(I): inflow discharge at time TIF(I) in m^3/sec

Note: Maximum number of data, including last card, is 20. Last card must say 9999.0 for TIF(I) and 0.0 for INF(I).

Output Data

4. Output data are outlined below.

a. Part A - Basic Data.

DTB: basic time step for breach erosion computation in seconds

DTR: time interval for flood routing in hours

SEC: sediment transport equation coefficient

EXPO: sediment transport equation exponent

CH: Chezy's friction coefficient for the dam in $m^{1/2}/sec$

DS: dam material particle diameter in meters

PHI: internal friction angle of dam material in degrees

COH: cohesive strength of dam material in N/m^2

ZT: initial side slope of breach section in m/m

X: initial ratio breach bottom width over initial hydraulic head

H1T: initial reservoir water elevation

Z1T: initial breach bottom elevation

DXMIN: maximum distance for routing sections

b. Part B - Breach Erosion Simulation.

TT: time in hours

QB2: breach outflow discharge in m^3/sec

H2(REL): ratio (H2-HB)/(H1T-HB)

Z2(REL): ratio (Z2-HB)/(Z1T-HB)

BRHT: breach section depth = HTD-Z2 in meters

B2: breach bottom width in meters

B2T: breach top width = B2 + 2.0 * ZT * BRHT in meters

c. Part C - Hydrograph at Damsite.

T: time in hours

QTT: total discharge = QB2 + QSP2 + QOT2 in m^3/sec

d. Part D - Flood Routing.

T: time in hours

1,2,3.: sections along the channel reach at which the hydrograph QTT (m^3/sec) is printed

TTTP: lag time of hydrograph at each section

APPENDIX B: LISTING OF BEED-I COMPUTER PROGRAM

```
ISN    1          REAL HVL(20),VCL(20),HSP(20),QSP(20),HCU(20),QCU(20),
                 1 TIF(20),INF(20),INF1,INF2,THYD(3000),HYD(3000),
                 2 QIN(3000),QTT(600,4),BV(600),ZV(600),CHV(600),
                 3 NMV(600),SV(600),DIST(600),PRT(600),
                 4 QTTPT(50),NIU,LR,LT,LC,K,L1,L2,LSS1,LSS2,LSS3,NCRV,
                 5 LHS,NMS,K1,NMV2,L1MIN,QMAXM(600),TTRAV(600),
                 6 TTTR(600),TTTP(50)
ISN    2           INTEGER SUBM,MPPST(50)
C
C*****************************************************************
C
C     P   R   O   G   R   A   M       B   E   E   D       I
C
C
C          - V E P S I O N    F O P T R A N   7 7 -
C
C*****************************************************************
C
C*****************************************************************
C
C               M   A   I   N       P   R   O   G   R   A   M
C
C*****************************************************************
C
C
C*****************************************
C         F   O   R   M   A   T   S
C*****************************************
C
ISN    3          10 FORMAT(4F8.4,F11.7,2F10.2)
ISN    4          15 FORMAT(5F10.3)
ISN    5          20 FORMAT(4F10.3)
ISN    6          25 FORMAT(5F10.3)
ISN    7          30 FORMAT(I2)
ISN    8          35 FORMAT(2F11.7)
ISN    9          37 FORMAT(F10.3)
ISN   10          40 FORMAT(3F10.2,2F10.5,F10.2,F4.1)
ISN   11          42 FORMAT(F10.2)
ISN   12          45 FORMAT(F10.2,F15.2)
ISN   13          50 FORMAT(2F10.2)
ISN   14         100 FORMAT('1',4X,'DTR (S)=',F10.3,5X,'DTR (H)=',F10.6)
ISN   15         105 FORMAT(5X,'SEC=',F7.3,5X,'EXPO=',F7.3,5X,'CH=',F7.3,
                    1 5X,'DS=',F8.5)
ISN   16         110 FORMAT(5X,'PHI=',F8.2,5X,'CCH=',F8.2,5X,'ZT=',F5.2,
                    1 5X,'X=',F5.2)
ISN   17         111 FORMAT(5X,'H1T=',F10.3,5X,'Z1T=',F10.3)
ISN   18         112 FORMAT(5X,'DXMIN=',F10.3)
ISN   19         113 FORMAT('0',4X,'BREACH EROSION SIMULATION')
ISN   20         115 FORMAT(1X)
ISN   21         120 FORMAT('0',3X,'TT (H)',3X,'QB2 (M3/S)',2X,'H2(REL)',
                    1 3X,'Z2(REL)',2X,'BPHT (M)',4X,'B2 (M)',3X,'B2T (M)')
ISN   22         130 FORMAT(1X,12F10.2)
```

```
ISN        23      145 FORMAT(1X,'ZT NEW=',F6.3)
ISN        24      150 FORMAT('1',1X,'HYDROGRAPH AT THE DAM SITE')
ISN        25      155 FORMAT('0',6(2X,'T (H)',2X,'QTT (M3/S)',2X))
ISN        26      165 FORMAT(6(3X,F5.2,F11.2,2X))
ISN        27      170 FORMAT('1',1X,'FLOOD ROUTING')
ISN        28      175 FORMAT('0',4X,'T (H)',15X,'QTT (M3/S) AT STATION K')
ISN        29      180 FORMAT('0',10X,10(I10,1X))
ISN        30      190 FORMAT(1X,F8.3,4X,10(F10.1,1X))
                C
                C ***************************************
                C          D A T A   P R O C E S S I N G
                C ***************************************
                C
ISN        31      465 READ(5,10)CH,DS,SF,P,NIU,PHI,COH
ISN        32          READ(5,15)LB,LT,LC,HTD,HP
ISN        33          READ(5,20)H1T,Z1T,Z2MIN,DTP
ISN        34          READ(5,25)L1MIN,SEC,EXPC,X,ZT
ISN        35          READ(5,30)NOFL
ISN        36          READ(5,35)TSIM,DTP
ISN        37          READ(5,37)DXMIN
                C
                C READ DATA FOR FLOOD ROUTING AND DEFINE
                C INTERMEDIATE SECTIONS
                C
ISN        38              J=1
ISN        39              READ(5,40)BV(J),ZV(J),CHV(J),NMV(J),SV(J),DIST(J),
                          1 PRT(J)
ISN        40      470 READ(5,40)BV2,ZV2,CHV2,NMV2,SV2,DIST2,PRT2
ISN        41          IF(BV2.EQ.9999.0)GO TO 460
ISN        42          IF(DIST2-DIST(J).GT.DXMIN)THEN
ISN        43            NINT=(DIST2-DIST(J))/DXMIN+1
ISN        44          ELSE
ISN        45            NINT=1
ISN        46          ENDIF
ISN        47          J1=J
ISN        48          JT=J+NINT-1
ISN        49          DO 1000 J=J1,JT
ISN        50              BV(J+1)=BV(J1)+(BV2-BV(J1))*(J+1-J1)/NINT
ISN        51              ZV(J+1)=ZV(J1)+(ZV2-ZV(J1))*(J+1-J1)/NINT
ISN        52              CHV(J+1)=CHV(J1)+(CHV2-CHV(J1))*(J+1-J1)/NINT
ISN        53              NMV(J+1)=NMV(J1)+(NMV2-NMV(J1))*(J+1-J1)/NINT
ISN        54              SV(J+1)=SV(J1)+(SV2-SV(J1))*(J+1-J1)/NINT
ISN        55              DIST(J+1)=DIST(J1)+(DIST2-DIST(J1))*(J+1-J1)/NINT
ISN        56              PRT(J+1)=0.0
ISN        57     1000 CONTINUE
ISN        58          PRT(JT+1)=PRT2
ISN        59          J=J1+NINT
ISN        60          GO TO 470
ISN        61      460 NS=J
                C
                C READ INITIAL DISCHARGE AT LAST SECTION
                C
ISN        62          READ(5,42)QTTLS
                C
                C READ VOLUME STORED BY THE RESERVOIR
                C
```

```
ISN        63          I=0
ISN        64        540 I=I+1
ISN        65            READ(5,45)HVL(I),VOL(I)
ISN        66            IF(HVL(I).NE.9999.0)GO TO 540
                  C
                  C READ SPILLWAY DISCHARGE
                  C
ISN        67          I=0
ISN        68        560 I=I+1
ISN        69            READ(5,50)HSP(I),QSP(I)
ISN        70            IF(HSP(I).NE.9999.0)GO TO 560
                  C
                  C READ OUTLET DISCHARGE
                  C
ISN        71          I=0
ISN        72        580 I=I+1
ISN        73            READ(5,50)HOU(I),QOU(I)
ISN        74            IF(HOU(I).NE.9999.0)GO TO 580
                  C
                  C READ INFLOW HYDROGRAPH TO THE RESERVOIR
                  C
ISN        75          I=0
ISN        76        600 I=I+1
ISN        77            READ(5,50)TIF(I),INF(I)
ISN        78            IF(TIF(I).NE.9999.0)GO TO 600
                  C
                  C PRINT HEADINGS
                  C
ISN        79            WRITE(6,100)DTB,DTR
ISN        80            WRITE(6,105)SEC,EXPO,CH,DS
ISN        81            WRITE(6,110)PHI,COH,ZT,X
ISN        82            WRITE(6,111)H1T,Z1T
ISN        83            WRITE(6,112)DXMIN
ISN        84            WRITE(6,113)
ISN        85            WRITE(6,115)
ISN        86            WRITE(6,120)
ISN        87            WRITE(6,115)
                  C
                  C ***************************************************************
                  C
                  C                  BREACH EROSION SIMULATION
                  C
                  C ***************************************************************
                  C
                  C ****************************************
                  C      I N I T I A L    V A L U E S
                  C ****************************************
                  C
                  C TT     = TIME
                  C DTB    = BASIC TIME INTERVAL
                  C DT     = VARIABLE TIME INTERVAL
                  C DZ1    = BREACH EROSION AT THE TOP OF THE DAM DURING DT
                  C DZ2    = BREACH EROSION AT THE DOWNSTREAM FACE DURING DT
                  C DZT1   = BREACH DEPTH AT THE TOP
                  C DZT2   = BREACH DEPTH AT THE DOWNSTREAM FACE
                  C H2     = RESERVOIR LEVEL
```

```
C Z2     = BREACH BOTTOM LEVEL
C AA     = UPSTREAM FACE ANGLE WITH THE HORIZONTAL
C BB     = DOWNSTREAM FACE ANGLE WITH THE HORIZONTAL
C K      = EINSTEIN-BROWN'S EQUATION COEFFICIENT
C A      = DUMMY VARIABLE USED TO COMPUTE B2
C B2     = BREACH BOTTOM WIDTH
C HYD(J)= OUTFLOW HYDROGRAPH
C NT     = NUMBER OF TIME STEPS USED FOR HYD(J)
C
ISN      88          TT=0.0
ISN      89          DZ1=0.0
ISN      90          DZ2=0.0
ISN      91          H2=H1T
ISN      92          Z2=Z1T
ISN      93          DZT1=HTD-Z2
ISN      94          DZT2=HTD-Z2
ISN      95          AA=ATAN((HTD-HB)/LT)
ISN      96          BB=ATAN((HTD-HB)/(LB-LT-LC))
ISN      97          K=36.0*NIU*NIU/(9.8*DS**3*(S?-1))
ISN      98          K=SQRT(2./3.+K)-SQRT(K)
C
C COMPUTE SPILLWAY,OUTLET & INFLOW DISCHARGES
C
ISN      99          CALL COQSOI(H2,QSP2,HSP,QSP,QOU2,HOU,QOU,TT,INF2,TIF,
                    1 INF)
ISN     100          QMAX=.0001
ISN     101          A=H2-Z2
ISN     102          B2=X*A
C
C COMPUTE QB2 AND CHECK FOR TAILWATER EFFECTS
C
ISN     103          B2S=BV(1)
ISN     104          ZS=ZV(1)
ISN     105          CHS=CHV(1)
ISN     106          NMS=NMV(1)
ISN     107          SS=SV(1)
ISN     108          CALL COQB2(H2,Z2,B2,ZT,NOF1,B2S,ZS,CHS,NMS,SS,QB2,
                    1 Z2MIN,SUBM,QOU2,QSP2,HB)
ISN     109          NT=3600*TSIM/DTB
ISN     110          QTT2=QSP2+QOU2+QB2
ISN     111          HYD(1)=QTT2
C
C ***************************************************
C       LOOP TO COMPUTE HYD(J) -BEGINNING
C ***************************************************
C
ISN     112          DO 1482 J=1,NT
C
C ***************************************
C       VALUES FROM LAST ITERATION
C ***************************************
C
C COMPUTE BREACH BOTTOM WIDTH
C
ISN     113     1035 IF(H2-Z2.GT.A)A=H2-Z2
ISN     115          B2=X*A
```

```
ISN    116          IF(QMAX.LT.QB2)QMAX=QB2
ISN    118          DT=DTB
ISN    119          H1=H2
ISN    120          Z1=Z2
ISN    121          DZT1=DZT1+DZ1
ISN    122          DZT2=DZT2+DZ2
ISN    123          CALL COVOL(H1,VOL1,HVL,VOL)
ISN    124          QB1=QB2
ISN    125          QTT1=QTT2
                C
                C IF QB2/QMAX.LE.0.005,DEFINE QB2 BY INTERPOLATION AND DO
                C NOT COMPUTE DZ1,DZ2.
                C
ISN    126          IF(QB1/QMAX.GT.0.005)GO TO 1055
ISN    127          QB2=.0005*QMAX+(QB1-.0005*QMAX)*(3600*TSIM-TT-DT)/
                   1  (3600*TSIM-TT)
ISN    128          H2=Z2+(QB2/(1.45*B2))**(2./3.)
                C
                C U1=WATER VELOCITY AT THE TOP OF THE DAM
                C
ISN    129          U1=QB2/((B2+ZT*(H2-Z2))*(H2-Z2))
ISN    130          GO TO 1280
ISN    131     1055 IF(DZT1.GE.HTD-Z2MIN)THEN
ISN    132            DZT1=HTD-Z2MIN
ISN    133            GO TO 1130
ISN    134          ENDIF
                C
                C L1=BREACH LENGTH AT THE TOP OF THE DAM
                C
ISN    135          L1=LC+DZT1*(1/TAN(AA)+1/TAN(BB))-DZT2/SIN(BB)
ISN    136          IF(L1.LT.0.0)THEN
ISN    137            L1=LIMIN
ISN    138            DZT1=(L1-LC+DZT2/SIN(BB))/(1/TAN(AA)+1/TAN(BB))
ISN    139          ENDIF
ISN    140          IF(DZT1.GE.HTD-Z2MIN)THEN
ISN    141            DZT1=HTD-Z2MIN
ISN    142            L1=0.0
ISN    143            DZT2=SIN(BB)*(LC+DZT1*(1/TAN(AA)+1/TAN(BB))-L1)
ISN    144          ENDIF
                C
                C L2=BREACH LENGTH AT THE DOWNSTREAM FACE
                C
ISN    145          L2=(HTD-HB-DZT1)/SIN(BB)
                C
                C ****************************************
                C      LOOP TO COMPUTE H2  -BEGINNING
                C ****************************************
                C
ISN    146     1130 H2T=H2
                C
                C ****************************************
                C      LOOP TO COMPUTE DZ1  -BEGINNING
                C ****************************************
                C
ISN    147     1140 DZ=DZ1
ISN    148          Z2=HTD-DZT1-DZ1
```

```
ISN    149          IF(Z2.LE.Z2MIN)THEN
ISN    150            Z2=Z2MIN
ISN    151            QBV1=0.0
ISN    152            DZ1=0.0
ISN    153            QBV2=0.0
ISN    154            DZ2=0.0
ISN    155            GO TO 3230
ISN    156          ENDIF
                C
                C COMPUTE QB2 AND CHECK FOR SUBMERGENCE
                C
ISN    157          B2S=BV(1)
ISN    158          ZS=ZV(1)
ISN    159          CHS=CHV(1)
ISN    160          NMS=NMV(1)
ISN    161          SS=SV(1)
ISN    162          CALL COQB2(H2,Z2,B2,ZT,NOF1,B2S,ZS,CHS,NMS,SS,QB2,
                   1 Z2MIN,SUBM,QOU2,QSP2,HB)
                C
                C ****************************************
                C      DETERMINATION OF DZ1
                C ****************************************
                C
ISN    163          U1=QB2/((B2+ZT*(H2-Z2))*(H2-Z2))
                C
                C COMPUTE SEDIMENT DISCHARGE (VOLUME BASIS)
                C
ISN    164          CALL COQBV(U1,SR,CH,DS,FSI1,SFC,EXPO,QBV1,K)
ISN    165          IF(Z2.NE.Z2MIN)GO TO 1190
ISN    166            QBV1=0.0
ISN    167            DZ1=0.0
ISN    168            GO TO 1210
ISN    169     1190 DZ1=QBV1*DT/(L1*(1-P))
ISN    170          IF(DZ1.LE.1.0)GO TO 1210
ISN    171          DT=DT/10
ISN    172          GO TO 1190
ISN    173     1210 IF(ABS(DZ1-DZ).GT.0.005)GO TO 1140
                C
                C ****************************************
                C      LOOP TO COMPUTE DZ1  -END
                C ****************************************
                C
                C ****************************************
                C      COMPUTATION OF H2
                C ****************************************
                C
ISN    174     3230 IF(ABS(H1-H2).LT.0.01)THEN
ISN    175            HSV=H1-2.0
ISN    176          ELSE
ISN    177            HSV=H2
ISN    178          ENDIF
                C
                C COMPUTE VOLUME STORED BY THE RESERVOIR
                C
ISN    179          CALL COVOL(HSV,VOL2,HVL,VOL)
                C
```

```
                C COMPUTE SPILLWAY,OUTLET & INFLOW DISCHARGES
                C
ISN       180         CALL COQSOI(H2,QSP2,HSP,QSP,QOU2,HOU,QOU,TT+DT,INF2,
                     1 TIF,INF)
                C
                C COMPUTE QB2 AND CHECK FOR TAILWATER EFFECTS
                C
ISN       181         B2S=BV(1)
ISN       182         ZS=ZV(1)
ISN       183         CHS=CHV(1)
ISN       184         NMS=NMV(1)
ISN       185         SS=SV(1)
ISN       186         CALL COQB2(H2,Z2,B2,ZT,NOF1,B2S,ZS,CHS,NMS,SS,QB2,
                     1 Z2MIN,SUBM,QOU2,QSP2,HB)
ISN       187         H2C=H1+DT*0.5*(INF1+INF2-QTT1-QSP2-QOU2-QB2)*(HSV-H1)
                     1 /(VOL2-VOL1)
ISN       188         IF(ABS(H2C-H2).LE.0.005)GO TO 1270
ISN       189         H2=H2C
ISN       190         GO TO 3230
ISN       191    1270 IF(ABS(H2-H2T).GT.0.01)GO TO 1130
                C
                C ****************************************
                C      LOOP TO COMPUTE H2  -END
                C ****************************************
                C
                C ****************************************
                C       DETERMINATION OF DZ2
                C ****************************************
                C
ISN       192         IF(SUBM.EQ.1)THEN
ISN       193            U2=0.0
ISN       194         ELSE
ISN       195            SD=(HTD-HB)/(LB-LT-LC)
ISN       196            ZD=ZT*DZT1/DZT2
                C
                C COMPUTE Y2 AND U2 ALONG THE DOWNSTREAM FACE OF THE DAM
                C
ISN       197            CALL COY2YT(NOF1,B2,ZD,CH,0.0,SD,QB2,Y2)
ISN       198            U2=QB2/((B2+ZD*Y2)*Y2)
ISN       199         ENDIF
                C
                C COMPUTE SEDIMENT DISCHARGE (VOLUME BASIS)
                C
ISN       200         CALL COQBV(U2,SR,CH,DS,FSI2,SEC,EXPO,QBV2,K)
ISN       201         IF(Z2.LE.Z2MIN)THEN
ISN       202           U2=0.0
ISN       203           QBV2=0.0
ISN       204           DZ2=0.0
ISN       205         ELSE
ISN       206           DZ2=QBV2*DT/(L2*(1-P))
ISN       207         ENDIF
                C
                C PRINT RESULTS
                C
ISN       208    1280 TT=TT+DT
ISN       209         QTT2=QSP2+QOU2+QB2
```

```
ISN    210          TTH=TT/3600
ISN    211          RH2=(H2-HB)/(H1T-HB)
ISN    212          RZ2=(Z2-HB)/(Z1T-HB)
ISN    213          BRHT=HTD-Z2
ISN    214          B2T=B2+2.0*ZT*BRHT
ISN    215          WRITE(6,130)TTH,QB2,RH2,RZ2,BRHT,B2,B2T
                C
                C ***************************************
                C      DETERMINATION OF LATERAL SLOPE
                C ***************************************
                C
ISN    216          IF(QB2/QMAX.LE.0.005)GO TO 1470
ISN    217          AP=ATAN(1/ZT)
ISN    218   1355  AP=AP-5/57.29578
ISN    219          IF(AP)1470,1360,1360
ISN    220   1360  LSS1=(HTD-Z2)*(1/TAN(AP)-ZT)
ISN    221          LSS2=(H1T-Z2)*(1/TAN(AP)-ZT)
ISN    222          LSS3=(H2-Z2)*ZT
ISN    223          H4=LSS2*(H1T-H2)*TAN(AP)/(H2-Z2+(H1T-H2)*(1-ZT*
                   1  TAN(AP)))
ISN    224          A1=0.5*(LSS1*(HTD-Z2)-LSS2*(H1T-Z2))
ISN    225          A2=0.5*LSS2*H4
ISN    226          A3=0.5*LSS2*(H1T-Z2)-A2
ISN    227          A4=0.5*LSS3*(H1T-H2-H4)
ISN    228          FG=9800*(SR*A1+(SR+P)*A2+(SR-(1-P))*A3-A4)
ISN    229          FH=4900*(H1T-H2)*(H2-Z2)
ISN    230          NORM=FG*COS(AP)-FH*SIN(AP)
ISN    231          IF(NORM.LE.0.0)NORM=0.0
ISN    233          LHS=FG*SIN(AP)+FH*COS(AP)
ISN    234          RHS=NORM*TAN(PHI/57.29578)+COH*(HTD-Z2)/SIN(AP)
ISN    235          IF(LHS.LE.RHS)GO TO 1355
ISN    236          ZT=1/TAN(AP)
ISN    237          WRITE(6,145)ZT
ISN    238   1470  IF(J*DTB.GT.TT)GO TO 1035
ISN    239          HYD(J+1)=QTT1+(J*DTB-TT+DT)*(QTT2-QTT1)/DT
ISN    240   1482  CONTINUE
                C
                C ***************************************************
                C      LOOP TO COMPUTE HYD(J)  -END
                C ***************************************************
                C
ISN    241          WRITE(6,150)
ISN    242          WRITE(6,155)
ISN    243          WRITE(6,115)
ISN    244          NTT=NT+1
ISN    245          DO 1504 J=1,NTT
ISN    246             THYD(J)=(J-1)*DTB/3600
ISN    247   1504  CONTINUE
ISN    248          WRITE(6,165)(THYD(J),HYD(J),J=1,NTT)
                C
                C ***************************************************
                C
                C                F L O O D   R O U T I N G
                C
                C ***************************************************
                C
```

```
                C  PRINT HEADINGS
                C
ISN        249      503 WRITE(6,170)
ISN        250          WRITE(6,175)
                C
                C*****************************************
                C       INITIAL CONDITIONS
                C*****************************************
                C
                C  HYDROGRAPH IN SECTION 1
                C
ISN        251          NR=TSIM/DTR
ISN        252          I=2
ISN        253          DO 1550 N=1,NR
ISN        254          I=I-1
ISN        255     1545 IF(I*DTB-N*3600*DTR.GE.-0.001)GO TO 1547
ISN        256          I=I+1
ISN        257          GO TO 1545
ISN        258     1547 QIN(N)=HYD(I)+(HYD(I+1)-HYD(I))*(N*3600*DTR-(I-1)
                       1 *DTB)/DTB
ISN        259     1550 CONTINUE
                C
                C  DEFINITION OF THE SECTIONS TO BE PRINTED
                C
ISN        260          M=1
ISN        261          DO 1650 J=1,NS
ISN        262              IF(PRT(J).EQ.0.0)GO TO 1650
ISN        263                MPRST(M)=PRT(J)
ISN        264                M=M+1
ISN        265     1650 CONTINUE
ISN        266          MT=M-1
ISN        267          WRITE(6,180)(MPRST(M),M=1,MT)
ISN        268          WRITE(6,115)
                C
                C  INITIAL DISCHARGE AT EVERY SECTION (LINEAR INTERPOLATION)
                C
ISN        269          DO 1680 J=1,NS
ISN        270             QTT(J,2)=QTTLS+(HYD(1)-QTTLS)*(NS-J)/(NS-1)
ISN        271             QTT(J+1,2)=QTTLS+(HYD(1)-QTTLS)*(NS-J-1)/(NS-1)
ISN        272             QMAXM(J)=0.001
ISN        273     1680 CONTINUE
                C
                C*****************************************
                C       LOOP THROUGH TSIM  -BEGINNING
                C*****************************************
                C
                C  ALPHA1=KINEMATIC WAVE APPROXIMATION COEFFICIENT AT
                C          SECTIONS (J,N) AND (J,N+1)
                C  ALPHA2=KINEMATIC WAVE APPROXIMATION COEFFICIENT AT
                C          SECTION (J+1,N)
                C  BETHA= KINEMATIC WAVE APPROXIMATION EXPONENT
                C  CA=FLOOD WAVE CELERITY AT SECTION (J,N)
                C  CB=FLOOD WAVE CELERITY AT SECTION (J,N+1)
                C  CC=FLOOD WAVE CELERITY AT SECTION (J+1,N)
                C
ISN        274          DO 1950 N=1,NR
```

```
ISN      275            QTT(1,3)=QIN(N)
ISN      276            NST=NS-1
                  C
                  C ****************************************
                  C       LOOP ALONG CHANNEL  -BEGINNING
                  C ****************************************
                  C
ISN      277            DO 1890 J=1,NST
ISN      278            IF(NMV(J).EQ.0.0)THEN
ISN      279              ALPHA1=CHV(J)*SQRT(SV(J))
ISN      280              ALPHA2=CHV(J+1)*SQRT(SV(J+1))
ISN      281              BETHA=1.5
ISN      282            ELSE
ISN      283              ALPHA1=SQRT(SV(J))/NMV(J)
ISN      284              ALPHA2=SQRT(SV(J+1))/NMV(J+1)
ISN      285              BETHA=5./3.
ISN      286            ENDIF
ISN      287            CA=BETHA*ALPHA1**(1.0/BETHA)*(QTT(J,2)/BV(J))
                       1   **((BETHA-1.0)/BETHA)
ISN      288            CB=BETHA*ALPHA1**(1.0/BETHA)*(QTT(J,3)/BV(J))
                       1   **((BETHA-1.0)/BETHA)
ISN      289            CC=BETHA*ALPHA2**(1.0/BETHA)*(QTT(J+1,2)/BV(J+1))
                       1   **((BETHA-1.0)/BETHA)
                  C
                  C COMPUTE FLOOD WAVE CELERITY AND UNIT WIDTH DISCHARGE
                  C
ISN      290            C=(CA+CB+CC)/3.0
ISN      291            QM=(QTT(J,2)/BV(J)+QTT(J,3)/BV(J)+QTT(J+1,2)/
                       1   BV(J+1))/3.0
                  C
                  C COMPUTE PARAMETERS FOR MUSKINGUM METHOD
                  C
ISN      292            IF(C.EQ.0.0)THEN
ISN      293              QTT(J+1,3)=QTT(J+1,2)
ISN      294            ELSE
ISN      295              K1=(DIST(J+1)-DIST(J))/C
ISN      296              X=0.5*(1.0-2*QM/((SV(J)+SV(J+1))*C*(DIST(J+1)
                       1     -DIST(J))))
ISN      297              IF(X.LT.0.0)X=0.0
                  C
                  C COMPUTE COEFFICIENTS
                  C
ISN      299              C4=3600*DTR/K1+2.0*(1-X)
ISN      300              C1=(3600*DTR/K1+2.0*X)/C4
ISN      301              C2=(3600*DTR/K1-2.0*X)/C4
ISN      302              C3=(2.0*(1-X)-3600)*DTR/K1)/C4
ISN      303              QTT(J+1,3)=C1*QTT(J,2)+C2*QTT(J,3)+C3*QTT(J+1,2)
ISN      304              IF(QMAXM(J+1).LT.QTT(J+1,3))QMAXM(J+1)=QTT(J+1,3)
ISN      306              IF(QTT(J+1,3).LT.0.0)THEN
ISN      307                PRINT*,'J=',J
ISN      308                PRINT*,'DIST(J)=',DIST(J)
ISN      309                PRINT*,'QTT(J+1,3)=',QTT(J+1,3)
ISN      310                PRINT*,'MODIFY SPACE AND/OR TIME INTERVALS'
ISN      311                STOP
ISN      312              ENDIF
ISN      313            ENDIF
```

```
ISN      314     1890 CONTINUE
C
C  ****************************************
C        LOOP ALONG CHANNEL  -END
C  ****************************************
C
C CTRAV=MEAN WAVE CELERITY
C TTRAV=ACCUMULATED TIME OF TRAVEL OF THE WAVE
C
ISN      315           TR=N*DTR
ISN      316           M=1
ISN      317           DO 1920 J=1,NS
ISN      318              IF(PRT(J).EQ.0.0)GO TO 1920
ISN      319                QTTPT(M)=QTT(J,3)
ISN      320                M=M+1
ISN      321     1920  CONTINUE
ISN      322           MT=M-1
ISN      323           WRITE(6,190)TR,(QTTPT(M),M=1,MT)
ISN      324           DO 1940 J=1,NS
ISN      325              QTT(J,1)=QTT(J,2)
ISN      326              QTT(J,2)=QTT(J,3)
ISN      327     1940  CONTINUE
ISN      328     1950  CONTINUE
ISN      329           TTTR(1)=0.0
ISN      330           DO 2100 J=1,NST
ISN      331              CTRAV=BETHA*(SQRT(SV(J))/NMV(J))**(1.0/BETHA)*
                1           (0.5*QMAXM(J)/BV(J))**((BETHA-1.0)/BETHA)
ISN      332              TTRAV(J+1)=(DIST(J+1)-DIST(J))/CTRAV
ISN      333              TTTR(J+1)=0.0
ISN      334     2100  CONTINUE
ISN      335           DO 2300 J=1,NST
ISN      336              DO 2400 I=1,J
ISN      337                 TTTR(J+1)=TTTR(J+1)+TTRAV(I+1)
ISN      338     2400        CONTINUE
ISN      339     2300  CONTINUE
ISN      340           PRINT*,'--- LAG TIMES ---'
ISN      341           M=1
ISN      342           DO 2500 J=1,NS
ISN      343              IF(PRT(J).EQ.0.0)GO TO 2500
ISN      344                TTTP(M)=TTTP(J)
ISN      345                M=M+1
ISN      346     2500  CONTINUE
ISN      347           MT=M-1
ISN      348           WRITE(6,190)TR,(TTTP(M) M=1,MT)
C
C  ****************************************
C       LOOP THROUGH TSIM  -END
C  ****************************************
C
ISN      349           STOP
C
C  ********************************************************************
C
C          E N D   O F   T H E   M A I N   P R O G R A M
C
C  ********************************************************************
```

```
ISN          1            SUBROUTINE COVOL(HSV,VL,HVL,VOL)
                     C
                     C ****************************************
                     C    DETERMINATION OF RESERVOIR VOLUME
                     C ****************************************
                     C
ISN          2            REAL HVL(20),VOL(20)
ISN          3            I=1
ISN          4            IF(HSV.LT.HVL(I))THEN
ISN          5               VL=0.0
ISN          6            ELSE
ISN          7     3050      IF(HSV.LE.HVL(I+1))GO TO 3060
ISN          8               I=I+1
ISN          9               GO TO 3050
ISN         10     3060      VL=VOL(I)+(VOL(I+1)-VOL(I))*(HSV-HVL(I))/(HVL(I+1)
                    1            -HVL(I))
ISN         11            ENDIF
ISN         12            RETURN
ISN         13            END
```

```
ISN        1          SUBROUTINE COQSOI(H2,QSPL,HSP,QSP,QOUT,HOU,QOU,TSI,
                     1INFL,TIF,INF)
                   C
                   C ***************************************
                   C  ESTIMATION OF SPILLWAY,OUTLET &
                   C        INFLOW DISCHARGES
                   C ***************************************
                   C
ISN        2          REAL HSP(20),QSP(20),HOU(20),QOU(20),TIF(20),INF(20),
                     1  INFL
                   C
                   C COMPUTE SPILLWAY DISCHARGE
                   C
ISN        3          I=1
ISN        4          IF(H2.LT.HSP(I))THEN
ISN        5            QSPL=0.0
ISN        6          ELSE
ISN        7   3090     IF(H2.LE.HSP(I+1))GO TO 3100
ISN        8            I=I+1
ISN        9            GO TO 3090
ISN       10   3100     QSPL=QSP(I)+(QSP(I+1)-QSP(I))*(H2-HSP(I))/(HSP(I+1)
                     1     -HSP(I))
ISN       11          ENDIF
                   C
                   C COMPUTE OUTLET DISCHARGE
                   C
ISN       12          I=1
ISN       13          IF(H2.LT.HOU(I))THEN
ISN       14            QOUT=0.0
ISN       15          ELSE
ISN       16   3130     IF(H2.LE.HOU(I+1))GO TO 3140
ISN       17            I=I+1
ISN       18            GO TO 3130
ISN       19   3140     QOUT=QOU(I)+(QOU(I+1)-QOU(I))*(H2-HOU(I))/(HOU(I+1)
                     1     -HOU(I))
ISN       20          ENDIF
                   C
                   C COMPUTE INFLOW DISCHARGE
                   C
ISN       21          I=1
ISN       22          IF(TSI.LT.TIF(I))THEN
ISN       23            INFL=INF(I)
ISN       24          ELSE
ISN       25   3170     IF(TSI.LE.TIF(I+1))GO TO 3180
ISN       26            I=I+1
ISN       27            GO TO 3170
ISN       28   3180     INFL=INF(I)+(INF(I+1)-INF(I))*(TSI-TIF(I))
                     1     /(TIF(I+1)-TIF(I))
ISN       29          ENDIF
ISN       30          RETURN
```

```
ISN        1            SUBROUTINE CQQBV(U,SP,CH,DS,FSI,SEC,EXPO,QBV,K)
                  C
                  C  ***************************************
                  C     COMPUTATION OF SEDIMENT DISCHARGE
                  C        (VOLUME BASIS) BY USING
                  C        EINSTEIN-BROWN'S EQUATION
                  C  ***************************************
                  C
ISN        2            REAL K
ISN        3            FSI=U*U/((SP-1)*CH*CH*DS)
ISN        4            IF(FSI.LE.0.047)THEN
ISN        5              FHI=0.0
ISN        6            ELSE IF(FSI.LE.0.0562)THEN
ISN        7              FHI=(4*FSI-0.188)**1.5
ISN        8            ELSE IF(FSI.LE.2.0)THEN
ISN        9              FHI=40.0*FSI**3
ISN       10            ELSE
ISN       11              FHI=SEC*FSI**EXPO
ISN       12            ENDIF
ISN       13            QBV=FHI*K*((SP-1)*9.8*DS**3)**0.5
ISN       14            RETURN
ISN       15            END
```

```
ISN        1            SUBROUTINE COY2YT(NOF1,B2S,ZS,CHS,NMS,SS,QS,Y2C)
                  C
                  C ****************************************
                  C     COMPUTATION OF NORMAL DEPTH
                  C ****************************************
                  C
ISN        2            REAL NMS
ISN        3            IF(NOF1.EQ.1)GO TO 3571
                  C
                  C NEWTON-RAPHSON METHOD
                  C
ISN        4            IF(NMS.EQ.0.0)THEN
ISN        5              Y2S=((QS/(CHS*B2S))**2/SS)**(1./3.)
ISN        6            ELSE
ISN        7              Y2S=(1.44*NMS*NMS*QS*QS/(B2S**2.67*SS))**(1./3.)
ISN        8            ENDIF
ISN        9     3532   IF(NMS.NE.0.0)CHS=((B2S+ZS*Y2S)*Y2S/(B2S+2*Y2S*
                  1     (1+ZS**2)**0.5))**(1./6.)/NMS
ISN       11            FY=QS*SQRT(B2S+2*Y2S*SQRT(1+ZS**2))-CHS*((B2S+ZS*Y2S)
                  1     *Y2S)**1.5*SQRT(SS)
ISN       12            FPY=QS*SQRT((1+ZS**2)/(B2S+2*SQRT(1+ZS**2)*Y2S))-
                  1     1.5*CHS*SQRT(SS*(B2S+ZS*Y2S)*Y2S)*(B2S+2*ZS*Y2S)
ISN       13            Y2C=Y2S-FY/FPY
ISN       14            IF(ABS(Y2C-Y2S).LE.0.005)GO TO 3580
ISN       15            Y2S=Y2C
ISN       16            GO TO 3532
                  C
                  C FIXED POINT ITERATION METHOD
                  C
ISN       17     3571   Y2S=0.001
ISN       18     3572   IF(NMS.NE.0.0)CHS=((B2S+ZS*Y2S)*Y2S/(B2S+2*Y2S*
                  1     (1+ZS**2)**0.5))**(1./6.)/NMS
ISN       20            Y2C=(QS*QS*(B2S+2*Y2S*(1+ZS**2)**0.5)/(CHS*CHS*
                  1     (B2S+ZS*Y2S)**3*SS))**(1./3.)
ISN       21            IF(ABS(Y2C-Y2S).LE.0.005)GO TO 3580
ISN       22            Y2S=Y2C
ISN       23            GO TO 3572
ISN       24     3580   RETURN
ISN       25            END
```

```
ISN        1            SUBROUTINE CCQB2(H2,Z2,B2,ZT,NOF1,B2S,ZS,CHS,NMS,SS,
                       1   QB2,Z2MIN,SUBM,QOU2,QSP2,HB)
                  C
                  C ***************************************
                  C     COMPUTATION OF QB2 AND TAILWATER
                  C        EFFECTS DUE TO SUBMERGENCE
                  C ***************************************
                  C
ISN        2            REAL NMS
ISN        3            INTEGER SUBM
ISN        4            IF(Z2.LE.Z2MIN)Z2=Z2MIN
ISN        6            IF(H2-Z2.GT.0.0)GO TO 3410
ISN        7            QB2=0.0
ISN        8            GO TO 3418
ISN        9     3410   QB2=1.45*B2*(H2-Z2)**1.5+1.15*ZT*(H2-Z2)**2.5
ISN       10            QS=QB2+QOU2+QSP2
                  C
                  C CHECK FOR SUBMERGENCE
                  C
ISN       11            CALL COY2YT(NOF1,B2S,ZS,CHS,NMS,SS,QS,YT)
ISN       12            IF(YT+HB-Z2.LE.0.67*(H2-Z2))GO TO 3418
ISN       13            QB2=QB2*(1-27.8*((YT+HB-Z2)/(H2-Z2)-0.67)**3)
ISN       14            SUBM=1
ISN       15            GO TO 3420
ISN       16     3418   SUBM=0
ISN       17     3420   RETURN
ISN       18            END
```

APPENDIX C: LISTING OF BED-II MICROCOMPUTER PROGRAM

```
10 '
20 ' ************************************************************************
30 '
40 '                P R O G R A M     B E E D    II
50 '
60 '
70 '                    - V E R S I O N   2 B A S I C -
80 '
90 ' ************************************************************************
100 '
110 ' ************************************************************************
120 '
130 '                    M A I N    P R O G R A M
140 '
150 ' ************************************************************************
160 '
170 ' ***************************************
180 '     D A T A   P R O C E S S I N G
190 ' ***************************************
200 '
210 OPTION BASE 1
220 DIM HVL(20),VOL(20),HSP(20),QSP(20),HOU(20),QOU(20),TIF(20),INF(20),THYD(100
0),HYD(1000),QIN(1000),QTT(500,2),BV(200),ZV(200),CHV(200),NMV(200),SV(200),DIST
(200),PRT(200),PRST(20),QTTPT(20),QMA(M(200),TTRAV(200),TTTP(200),ITTP(200)
230 READ CH,DS,SB,P,NIU,PHI,COH
240 READ LB,LT,LC,HTD,HB
250 READ H1T,Z1T,Z2MIN,DTB
260 READ L1MIN,SEC,EXPO,X,ZT
270 READ NOF1
280 READ TSIM,DTP
290 READ DYMIN
300 '
310 ' READ DATA FOR FLOOD ROUTING AND DEFINE INTERMEDIATE SECTIONS
320 '
330 J=1
340 READ BV(J),ZV(J),CHV(J),NMV(J),SV(J),DIST(J),PRT(J)
350 READ BV2,ZV2,CHV2,NMV2,SV2,DIST2,PRT2
360 IF BV2=9999 THEN 500
370 IF DIST2-DIST(J) DYMIN THEN NINT=INT((DIST2-DIST(J))/DYMIN)+1 ELSE NINT=1
380 J1=J
390 JT=J+NINT-1
400 FOR J=J1 TO JT
410 BV(J+1)=BV(J1)+(BV2-BV(J1))*(J+1-J1)/NINT
420 ZV(J+1)=ZV(J1)+(ZV2-ZV(J1))*(J+1-J1)/NINT
430 CHV(J+1)=CHV(J1)+(CHV2-CHV(J1))*(J+1-J1)/NINT
440 NMV(J+1)=NMV(J1)+(NMV2-NMV(J1))*(J+1-J1)/NINT
450 SV(J+1)=SV(J1)+(SV2-SV(J1))*(J+1-J1)/NINT
460 DIST(J+1)=DIST(J1)+(DIST2-DIST(J1))*(J+1-J1)/NINT
470 PRT(J+1)=0
480 NEXT J
490 PRT(JT+1)=PRT2:J=J1+NINT:GOTO 350
500 NS=J
```

```
510 '
520 ' READ INITIAL DISCHARGE AT LAST SECTION
530 '
540 READ QTTLS
550 '
560 ' READ VOLUME STORED BY THE RESERVOIR
570 '
580 I=1
590 READ HVL(I),VOL(I):IF HVL(I)  9999 THEN I=I+1:GOTO 590
600 '
610 ' READ SPILLWAY DISCHARGE
620 '
630 I=1
640 READ HSP(I),QSP(I):IF HSP(I)  9999 THEN I=I+1:GOTO 640
650 '
660 ' READ OUTLET DISCHARGE
670 '
680 I=1
690 READ HOU(I),QOU(I):IF HOU(I)  9999 THEN I=I+1:GOTO 690
700 '
710 ' READ INFLOW HYDROGRAPH TO THE RESERVOIR
720 '
730 I=1
740 READ TIF(I),INF(I):IF TIF(I)  9999 THEN I=I+1:GOTO 740
750 '
760 ' PRINT HEADINGS
770 '
780 LPRINT:LPRINT
790 LPRINT "DTB [S]=";DTB,:LPRINT "ITF [H]=";ITF:LPRINT
800 LPRINT "SEC=";SEC,:LPRINT "EXPO=";EXPO,:LPRINT "CH=";CH,:LPRINT "DS=";DS:LPRI
NT
810 LPRINT "PHI=";PHI,:LPRINT "COH=";COH,:LPRINT "ZT=";ZT,:LPRINT "Y=";Y:LPRINT
820 LPRINT "H1T=";H1T,:"Z1T=";Z1T:LPRINT
830 LPRINT "DXMIN=";DXMIN:LPRINT
840 LPRINT "BREACH EROSION SIMULATION":LPRINT
850 LPRINT
860 LPRINT "  TT (H)  QBR (M^3/S)  HD (EL)   ZD(EL)  BRHT (M)   BD (M)  TD? (M)"
870 LPRINT
880 '
890 ' ************************************************************************
900 '
910 '                              BREACH EROSION SIMULATION
920 '
930 ' ************************************************************************
940 '
950 ' *************************************
960 '       I N I T I A L   V A L U E S
970 ' *************************************
980 '
990 ' TT      =TIME
1000 ' DTB     =BASIC TIME INTERVAL
1010 ' DT      =VARIABLE TIME INTERVAL
```

```
1020 ' DZ1    =BREACH EROSION AT THE TOP OF THE DAM DURING DT
1030 ' DZ2    =BREACH EROSION AT THE DOWNSTREAM FACE DURING DT
1040 ' DZT1   =BREACH DEPTH AT THE TOP
1050 ' DZT2   =BREACH DEPTH AT THE DOWNSTREAM FACE
1060 ' H2     =RESERVOIR LEVEL
1070 ' Z2     =BREACH BOTTOM LEVEL
1080 ' AA     =UPSTREAM FACE ANGLE WITH THE HORIZONTAL
1090 ' BB     =DOWNSTREAM FACE ANGLE WITH THE HORIZONTAL
1100 ' F      =EINSTEIN-BROWN'S EQUATION COEFFICIENT
1110 ' A      =DUMMY VARIABLE USED TO COMPUTE B2
1120 ' B2     =BREACH BOTTOM WIDTH
1130 ' HYD(I) =OUTFLOW HYDROGRAPH
1140 ' NT     =NUMBER OF TIME STEPS USED FOR HYD(I)
1150 '
1160 H2=H1T:Z2=Z1T:DZT1=H1T-Z2:DZT2=H1D-Z2:Z1=Z2
1170 AA=ATN((H1D-HB)/LT):BB=ATN((H1D-HB)/(LB-LT-LL))
1180 F=Z*NU*(1/(9.8*DS^3*(SR-1)))^.5*...
1190 '
1200 ' COMPUTE SPILLWAY,OUTLET &INFLOW DISCHARGES
1210 '
1220 TCI=T1:GOSUB 4500:QTT2=QSPL:QOUL=QOUT:INF2=INFL
1230 QMAX=.0001
1240 A=H2-Z2:B2=Y*A
1250 '
1260 ' COMPUTE QB2 AND CHECK FOR TAILWATER EFFECTS
1270 '
1280 GOSUB 4890
1290 NT=INT(3600*TSIM/DTB):QTT2=QSP2+QOU2+QB2:HYD(1)=QTT2
1300 '
1310 ' ****************************************************
1320 '           LOOP TO COMPUTE HYD(I) -BEGINNING
1330 ' ****************************************************
1340 '
1350 FOR I=1 TO NT
1360 '
1370 ' ************************************
1380 '        VALUES FROM LAST ITERATION
1390 ' ************************************
1400 '
1410 ' COMPUTE BREACH BOTTOM WIDTH
1420 '
1430 IF H2-Z2>A THEN A=H2-Z2
1440 B2=Y*A
1450 IF QMAX<QB2 THEN QMAX=QB2
1460 DT=DTB
1470 H1=H2:Z1=Z2:DZT1=DZT1+DZ1:DZT2=DZT2+DZ2:HS=H1:GOSUB 4400:VOL1=V1:QB1=QB2:QTT1=QTT2
1480 '
1490 ' IF QB1/QMAX<0.005,DEFINE QB2 BY INTERPOLATION AND DO NOT COMPUTE BREACH EROSION
1500 '
1510 IF(QB1/QMAX<.005)THEN 1880
```

```
1520 QB2=.0005*QMAX+(QB1-.0005*QMAX)*(3600*TSIM-TT-DT)/(3600*TSIM-TT)
1530 H2=Z2+(QB2/(1.45*B2))^(2/3)
1540 '
1550 ' U1=WATER VELOCITY AT THE TOP OF THE DAM
1560 '
1570 U1=QB2/((B2+ZT*(H2-Z2))*(H2-Z2)):GOTO 2470
1580 IF DZT1>HTD-Z2MIN THEN DZT1=HTD-Z2MIN:GOTO 1740
1590 '
1600 ' L1=BREACH LENGTH AT THE TOP OF THE DAM
1610 '
1620 L1=LC+DZT1*(1/TAN(AA)+1/TAN(BB))-DZT2/SIN(BB)
1630 IF L1<0 THEN L1=L1MIN:DZT1=(L1-LC+DZT2/SIN(BB))/(1/TAN(AA)+1/TAN(BB))
1640 IF DZT1>HTD-Z2MIN THEN DZT1=HTD-Z2MIN:L1=0:DZT2=SIN(BB)*(LC+DZT1*(1/TAN(AA)
+1/TAN(BB))-L1)
1650 '
1660 ' L2=BREACH LENGTH AT THE DOWNSTREAM FACE
1670 '
1680 L2=(HTD-HB-DZT1)/SIN(BB)
1690 '
1700 ' ***********************************************
1710 '     LOOP TO COMPUTE H2  -BEGINNING
1720 ' ***********************************************
1730 '
1740 H2T=H2
1750 '
1760 ' ***********************************************
1770 '     LOOP TO COMPUTE DZ1  -BEGINNING
1780 ' ***********************************************
1790 '
1800 DZ=DZ1:Z2=HTD-DZT1-DZ1:IF Z2<=Z2MIN THEN Z2=Z2MIN:GOTO 2070
1810 '
1820 ' COMPUTE QB2 AND CHECK FOR SUBMERGENCE
1830 '
1840 GOSUB 4890
1850 '
1860 ' ***************************************
1870 '           DETERMINATION OF DZ1
1880 ' ***************************************
1890 '
1900 U1=QB2/((B2+ZT*(H2-Z2))*(H2-Z2))
1910 '
1920 ' COMPUTE SEDIMENT DISCHARGE (VOLUME BASIS)
1930 '
1940 U=U1:GOSUB 4770
1950 FSI1=FSI:IF Z2=Z2MIN THEN QBV1=0:DZ1=0:GOTO 1990
1960 QBV1=QBV
1970 DZ1=QBV1*DT/(L1*(1-P))
1980 IF DZ1>1' THEN DT=DT/10:GOTO 1970
1990 IF ABS(DZ1-DZ)<.005 THEN 1800
2000 '
2010 ' ***************************************
2020 '      COMPUTATION OF H2
2030 ' ***************************************
```

```
2040 '
2050 ' COMPUTE VOLUME STORED BY THE RESERVOIR
2060 '
2070 IF ABS(H1-H2)<.01 THEN HSV=H1-2! ELSE HSV=H2
2080 GOSUB 4400:VOL2=VL
2090 '
2100 ' COMPUTE SPILLWAY,OUTLET &INFLOW DISCHARGES
2110 '
2120 TSI=TT+DT:GOSUB 4500:QSP2=QSPL:QOU2=QOUT:INF2=INFL
2130 '
2140 ' COMPUTE QB2 AND CHECK FOR TAILWATER EFFECTS
2150 '
2160 GOSUB 4890
2170 H2C=H1+DT*.5*(INF1+INF2-QTT1-QSP2-QOU2-QB2)*(HSV-H1)/(VOL2-VOL1)
2180 IF ABS(H2C-H2)>.005 THEN H2=H2C:GOTO 2070
2190 IF ABS(H2-H2T)>.01 THEN 1740
2200 '
2210 ' ****************************************
2220 '      LOOP TO COMPUTE H2  -END
2230 ' ****************************************
2240 '
2250 ' ****************************************
2260 '     DETERMINATION OF DZ2
2270 ' ****************************************
2280 '
2290 IF SUBM=1! THEN U2=0:GOTO 2370
2300 B2S=B2:CHS=CH:NMS=0!:SS=(HTD-HB)/(LB-LT-LC)
2310 ZS=ZT1*DZT1/DZT2:QS=QB2
2320 '
2330 ' COMPUTE Y2 AND U2 ALONG THE DOWSTREAM FACE OF THE DAM
2340 '
2350 GOSUB 5060:Y2=Y2C
2360 U2=QB2/((B2+ZS*Y2)*Y2)
2370 U=U2
2380 '
2390 ' COMPUTE SEDIMENT DISCHARGE (VOLUME BASIS)
2400 '
2410 GOSUB 4770
2420 FSI2=FSI:IF Z2=Z2MIN THEN U2=0:QBV2=0:DZ2=0:GOTO 2470
2430 QBV2=QBV:DZ2=QBV2*DT/(L2*(1-P))
2440 '
2450 ' PRINT RESULTS
2460 '
2470 TT=TT+DT
2480 QTT2=QSP2+QOU2+QB2
2490 TTH=TT/3600
2500 RH2=(H2-HB)/(H1T-HB)
2510 RZ2=(Z2-HB)/(Z1T-HB)
2520 BRHT=HTD-Z2
2530 B2T=B2+2!*ZT*BRHT
2540 LPRINT USING " ##.##  ";TTH;:LPRINT USING " ######.# ";QB2;RH2;RZ2;BRHT;B2;
B2T
2550 '
```

```
2560 ' ****************************************
2570 '    DETERMINATION OF LATERAL SLOPE
2580 ' ****************************************
2590 '
2600 IF QB2/QMAX<=.005 THEN 2740
2610 AP=ATN(1/ZT)
2620 AP=AP-5/57.29578
2630 IF AP<0 THEN 2740
2640 LSS1=(HTD-Z2)*(1/TAN(AP)-ZT):LSS2=(H1T-Z2)*(1/TAN(AP)-ZT):LSS3=(H2-Z2)*ZT
2650 H4=LSS2*(H1T-H2)*TAN(AP)/(H2-Z2+(H1T-H2)*(1-ZT*TAN(AP)))
2660 A1=.5*(LSS1*(HTD-Z2)-LSS2*(H1T-Z2)):A2=.5*LSS2*H4:A3=.5*LSS2*(H1T-Z2)-A2
2670 A4=.5*LSS3*(H1T-H2-H4)
2680 FG=9800*(SR*A1+(SR+F)*A2+(SR-(1-F))*A3-A4):FH=4900*(H1T-H2)*(H2-Z2)
2690 NORM=FG*COS(AP)-FH*SIN(AP):IF NORM<>0 THEN NORM=0
2700 LHS=FG*SIN(AP)+FH*COS(AP):RHS=NORM*TAN(PHI/57.29578)+COH*(HTD-Z2)/SIN(AP)
2710 IF LHS<>RHS THEN 2620
2720 ZT=1/TAN(AP)
2730 LPRINT "ZT NEW=";ZT
2740 IF J*DTB<TT THEN 1430
2750 HYD(J+1)=QTT1+(J*DTB-TT+DT)*(QTT2-QTT1)/DT
2760 NEXT J
2770 '
2780 ' ****************************************
2790 '    LOOP TO COMPUTE HYD(J)  -END
2800 ' ****************************************
2810 '
2820 LPRINT:LPRINT
2830 LPRINT "HYDROGRAPH AT THE DAM SITE"
2840 LPRINT "  T [H]  QTT [M3/S]   T [H]  QTT [M3/S]   T [H]  QTT [M3/S]   T [H]
  QTT [M3/S]"
2850 LPRINT
2860 FOR J=1 TO NT+1
2870 THYD(J)=(J-1)*DTB/3600
2880 LPRINT USING "######.## ";THYD(J);HYD(J);
2890 NEXT J
2900 '
2910 ' ********************************************************************************
2920 '
2930 '                    F L O O D    R O U T I N G
2940 '
2950 ' ********************************************************************************
2960 '
2970 ' PRINT HEADINGS
2980 '
2990 LPRINT:LPRINT:LPRINT
3000 LPRINT "   FLOOD ROUTING":LPRINT
3010 LPRINT "   T [H]                QTT [M3/S] AT STATION # ":LPRINT
3020 '
3030 ' ****************************************
3040 '          INITIAL CONDITIONS
3050 ' ****************************************
```

```
3060 '
3070 ' HYDROGRAPH IN SECTION 1
3080 '
3090 NR=INT(TSIM/DTR)
3100 I=2
3110 FOR N=1 TO NR
3120 I=I-1
3130 IF I*DTB-N*3600*DTR<=-.001 THEN 3150
3140 I=I+1:GOTO 3130
3150 QIN(N)=HYD(I)+(HYD(I+1)-HYD(I))*(N*3600*DTR-(I-1)*DTB)/DTB
3160 NEXT N
3170 '
3180 ' DEFINITION OF THE SECTIONS TO BE PRINTED
3190 '
3200 M=1:FOR J=1 TO NS
3210 IF PRT(J)=0 THEN 3230
3220 PRST(M)=PRT(J):M=M+1
3230 NEXT J
3240 LPRINT "    ---     ";
3250 MT=M-1
3260 FOR M=1 TO MT
3270 LPRINT USING "     ##     ";PRST(M);
3280 NEXT M
3290 LPRINT
3300 '
3310 ' INITIAL DISCHARGE AT EVERY SECTION (BY LINEAR INTERPOLATION)
3320 '
3330 FOR J=1 TO NS:QTT(J,2)=QTTLS+(HYD(1)-QTTLS)*(NS-J)/(NS-1)
3340 QTT(J+1,2)=QTTLS+(HYD(1)-QTTLS)*(NS-J-1)/(NS-1)
3350 QMAXM(J)=.001:NEXT J
3360 '
3370 ' ************************************************
3380 '           LOOP THROUGH TSIM  -BEGINNING
3390 ' ************************************************
3400 '
3410 ' ALPHA1=KINEMATIC WAVE APPROXIMATION COEFFICIENT AT
3420 '         SECTIONS (J,N) AND (J,N+1)
3430 ' ALPHA2=KINEMATIC WAVE APPROXIMATION COEFFICIENT AT
3440 '         SECTION (J+1,N)
3450 ' BETHA =KINEMATIC WAVE APPROXIMATION EXPONENT
3460 ' CA    =FLOOD WAVE CELERITY AT SECTION (J,N)
3470 ' CB    =FLOOD WAVE CELERITY AT SECTION (J,N+1)
3480 ' CC    =FLOOD WAVE CELERITY AT SECTION (J+1,N)
3490 '
3500 FOR N=1 TO NR
3510 QTT(1,2)=QIN(N)
3520 '
3530 ' ************************************************
3540 '           LOOP ALONG CHANNEL  -BEGINNING
3550 ' ************************************************
3560 '
3570 FOR J=1 TO NS-1
```

```
3580 IF NMV(J)=0 THEN ALPHA1=CHV(J)*SQRT(SV(J)):ALPHA2=CHV(J+1)*SQRT(SV(J+1)):BE
THA=1.5:GOTO 3600
3590 ALPHA1=SQRT(SV(J))/NMV(J):ALPHA2=SQRT(SV(J+1))/NMV(J+1):BETHA=5/3
3600 CA=BETHA*ALPHA1^(1/BETHA)*(QTT(J,2)/BV(J))^((BETHA-1)/BETHA)
3610 CB=BETHA*ALPHA1^(1/BETHA)*(QTT(J,3)/BV(J))^((BETHA-1)/BETHA)
3620 CC=BETHA*ALPHA2^(1/BETHA)*(QTT(J+1,2)/BV(J+1))^((BETHA-1)/BETHA)
3630 '
3640 ' COMPUTE FLOOD WAVE CELERITY AND UNIT WIDTH DISCHARGE
3650 '
3660 C=(CA+CB+CC)/3!
3670 QM=(Q(J,2)/BV(J)+Q(J,3)/BV(J)+Q(J+1,2)/BV(J+1))/3!
3680 '
3690 ' COMPUTE PARAMETERS FOR MUSKINGUM METHOD
3700 '
3710 IF C=0 THEN QTT(J+1,3)=QTT(J+1,2):GOTO 3850
3720 K1=(DIST(J+1)-DIST(J))/C
3730 X=.5*(1-2!*QM/((SV(J)+SV(J+1))*C*(DIST(J+1)-DIST(J))))
3740 IF X<0! THEN X=0!
3750 '
3760 ' COMPUTE COEFFICIENTS
3770 '
3780 C4=3600*DTR/K1+2!*(1-X)
3790 C1=(3600*DTR/K1+2!*X)/C4
3800 C2=(3600*DTR/K1-2!*X)/C4
3810 C3=(2!*(1-X)-3600*DTR/K1)/C4
3820 QTT(J+1,3)=C1*QTT(J,2)+C2*QTT(J,3)+C3*QTT(J+1,2)
3830 IF QMAXM(J+1)<QTT(J+1,3) THEN QMAXM(J+1)=QTT(J+1,3)
3840 IF QTT(J+1,3)<0! THEN LPRINT "J=";J:LPRINT "DIST(J)=";DIST(J):LPRINT "QTT(J
+1,3)=";QTT(J+1,3):LPRINT "MODIDY DXMIN AND/OR DTR":STOP
3850 NEXT J
3860 '
3870 ' ******************************************
3880 '       LOOP ALONG CHANNEL  -END
3890 ' ******************************************
3900 '
3910 ' CTRAV=MEAN WAVE CELERITY
3920 ' TTRAV=ACCUMULATED TIME OF TRAVEL OF THE WAVE
3930 '
3940 TR=N*DTR
3950 M=1
3960 FOR J=1 TO NS
3970 IF PRT(J)=0 THEN 3990
3980 QTTPT(M)=QTT(J,3):M=M+1
3990 NEXT J
4000 LPRINT USING "  ###.##  ";TR;
4010 FOR M=1 TO MT:LPRINT USING " ######.# ";QTTPT(M);:NEXT M:LPRINT
4020 FOR J=1 TO NS:QTT(J,1)=QTT(J,2):QTT(J,2)=QTT(J,3):NEXT J
4030 NEXT N
4040 TTTR(1)=0!
4050 FOR J=1 TO NS-1
4060 CTRAV=BETHA*(SQRT(SV(J))/NMV(J))^(1!/BETHA)*(.5*QMAXM(J)/BV(J))^((BETHA-1!/B
ETHA)
```

```
4070 TTRAV(J+1)=(DIST(J+1)-DIST(J))/CTRAV
4080 TTTR(J+1)=0':NEXT J
4090 FOR J=1 TO NS-1
4100 FOR I=1 TO J:TTTR(J+1)=TTTR(J+1)+TTRAV(I+1):NEXT I:NEXT J
4110 LPRINT " --- LAG TIMES ---"
4120 M=1
4130 FOR J=1 TO NS
4140 IF PRT(J)=0' THEN 4160
4150 TTTR(M)=TTTR(J):M=M+1
4160 NEXT J
4170 LPRINT USING "  ###.## ";TR;
4180 FOR M=1 TO MT:LPRINT USING " ######.# ';TTTR(M);:NEXT M:;LPRINT
4190 '
4200 ' ****************************************
4210 '       LOOP THROUGH TSIM  -END
4220 ' ****************************************
4230 '
4240 STOP
4250 '
4260 ' ********************************************************************************
4270 '
4280 '                E N D   O F   T H E   M A I N   P R O G R A M
4290 '
4300 ' ********************************************************************************
4310 '
4320 END
4330 '
4340 ' ********************************************************************************
4350 '
4360 '                    S U B R O U T I N E S
4370 '
4380 ' ********************************************************************************
4390 '
4400 ' ***************************************
4410 '   DETERMINATION OF RESERVOIR VOLUME
4420 ' ***************************************
4430 '
4440 I=1
4450 IF HSV HVL(I) THEN VL=0:GOTO 4480
4460 IF HSV HVL(I+1) THEN I=I+1:GOTO 4450
4470 VL=VOL(I)+(VOL(I+1)-VOL(I))*(HSV-HVL(I))/(HVL(I+1)-HVL(I))
4480 RETURN
4490 '
4500 ' ***************************************
4510 '   DETERMINATION OF SPILLWAY,OUTLET
4520 '         AND INFLOW DISCHARGES
4530 ' ***************************************
4540 '
4550 ' COMPUTE SPILLWAY DISCHARGE
4560 '
4570 I=1
4580 IF H2 HSP(I) THEN QSPL=0:GOTO 4640
```

```
4590 IF H2>HSP(I+1) THEN I=I+1:GOTO 4590
4600 QSPL=QSP(I)+(QSP(I+1)-QSP(I))*(H2-HSP(I))/(HSP(I+1)-HSP(I))
4610 '
4620 ' COMPUTE OUTLET DISCHARGE
4630 '
4640 I=1
4650 IF H2<HOU(I) THEN QOUT=0:GOTO 4710
4660 IF H2>HOU(I+1) THEN I=I+1:GOTO 4660
4670 QOUT=QOU(I)+(QOU(I+1)-QOU(I))*(H2-HOU(I))/(HOU(I+1)-HOU(I))
4680 '
4690 ' COMPUTE INFLOW DISCHARGE
4700 '
4710 I=1
4720 IF TSI<TIF(I) THEN INFL=INF(I):GOTO 4750
4730 IF TSI>TIF(I+1) THEN I=I+1:GOTO 4730
4740 INFL=INF(I)+(INF(I+1)-INF(I))*(TSI-TIF(I))/(TIF(I+1)-TIF(I))
4750 RETURN
4760 '
4770 ' ****************************************
4780 '   COMPUTATION OF SEDIMENT DISCHARGE
4790 '         (VOLUME BASIS) BY USING
4800 '        EINSTEIN-BROWN'S EQUATION
4810 ' ****************************************
4820 '
4830 FSI=U*2/((SR-1)*CH*2*DS):IF FSI<=.047 THEN FHI=0:GOTO 4860
4840 IF FSI<=.0562 THEN FHI=(4*FSI-.188)^1.5:GOTO 4860
4850 IF FSI<=2! THEN FHI=40*FSI^3 ELSE FHI=SEC*FSI^EXPO
4860 QBV=FHI*U*((SR-1)*9.8*DS^3)^.5
4870 RETURN
4880 '
4890 ' ****************************************
4900 '    COMPUTATION OF QB2 AND TAILWATER
4910 '      EFFECTS DUE TO SUBMERGENCE
4920 ' ****************************************
4930 '
4940 IF Z2<=Z2MIN THEN Z2=Z2MIN
4950 IF H2-Z2<=0! THEN QB2=0:GOTO 5030
4960 QB2=1.45*B2*(H2-Z2)^1.5+1.15*ZT*(H2-Z2)^2.5
4970 '
4980 ' CHECK FOR SUBMERGENCE
4990 '
5000 B2S=BV(1):ZS=ZV(1):NMS=NMV(1):SS=SV(1):QS=QB2+QOU2+QSP2:CHS=CHV(1):NMS=NMV(
1)
5010 GOSUB 5060:YT=Y2C
5020 IF YT+HB-Z2<.67*(H2-Z2) THEN QB2=QB2*(1-27.8*((YT+HB-Z2)/(H2-Z2)-.67)^3):SU
BM=1:GOTO 5040
5030 SUBM=0!
5040 RETURN
5050 '
5060 ' ****************************************
5070 '    COMPUTATION OF Y2,YT
5080 ' ****************************************
```

```
5090 IF NOF1=1 THEN 5230
5100 '
5110 ' NEWTON-RAPHSON METHOD
5120 '
5130 IF NMS=0 THEN Y2S=((QS/(CHS*B2S))^2/SS)^(1/3) ELSE Y2S=(1.44*NMS^2*QS^2/(B2
S^2.67*SS))^(1/3)
5140 IF NMS<>0 THEN CHS=((B2S+ZS*Y2S)*Y2S/(B2S+2*Y2S*(1+ZS^2)^.5))^(1/6)/NMS
5150 FY=QS*(B2S+2*Y2S*(1+ZS^2)^.5)^.5-CHS*((B2S+ZS*Y2S)*Y2S)^1.5*SS^.5
5160 FPY=QS*(1+ZS^2)^.5/(B2S+2*(1+ZS^2)^.5*Y2S)^.5-1.5*CHS*(SS*(B2S+ZS*Y2S)*Y2S)
^.5*(B2S+2*ZS*Y2S)*SS^.5
5170 Y2C=Y2S-FY/FPY
5180 IF ABS(Y2C-Y2S)<.005 THEN Y2S=Y2C:GOTO 5140
5190 GOTO 5270
5200 '
5210 ' FIXED POINT ITERATION METHOD
5220 '
5230 Y2S=.001
5240 IF NMS<>0 THEN CHS=((B2S+ZS*Y2S)*Y2S/(B2S+2*Y2S*(1+ZS^2)^.5))^(1/6)/NMS
5250 Y2C=(QS^2*(B2S+2*Y2S*(1+ZS^2)^.5)/(CHS^2*(B2S+ZS*Y2S)^3*SS))^(1/3)
5260 IF ABS(Y2C-Y2S)<.005 THEN Y2S=Y2C:GOTO 5240
5270 RETURN
5280 '
5290 '
5300 ' ****************************************
5310 '      D A T A
5320 ' ****************************************
5330 '
5340 DATA  50,0.0030,2.5,0.20,1E-6,40,49000
5350 DATA 533.4,290.0,10.0,1625.19,1532.23
5360 DATA 1613.95,1612.95,1532.23,300
5370 DATA 1.0,139.99,1.2,0.5,0.25
5380 DATA 1
5390 DATA 36,0.0833333
5400 DATA 1000.0
5410 DATA     300.0,     1,     0.0,    0.032,    0.0025,       0,     1
5420 DATA     470.0,     0,     0.0,    0.035,    0.0018,    7240,     2
5430 DATA    4400.0,     0,     0.0,    0.032,    0.0012,   10458,     3
5440 DATA    4600.0,     0,     0.0,    0.030,    0.0027,   14803,     4
5450 DATA   10200.0,     0,     0.0,    0.037,    0.0042,   26388,     0
5460 DATA    5200.0,     0,     0.0,    0.042,    3.2E-4,   36363,     6
5470 DATA    5200.0,     0,     0.0,    0.040,    7.6E-4,   52453,     0
5480 DATA    3900.0,     0,     0.0,    0.037,    0.0014,   62590,     8
5490 DATA    1300.0,     0,     0.0,    0.035,    0.0014,   71761,     0
5500 DATA     260.0,     0,     0.0,    0.033,    0 0014,   75945,    10
5510 DATA     140.0,     0,     0.0,    0.040,    0.0014,   90748,     0
5520 DATA     200.0,     0,     0.0,    0.035,    0.0014,   97827,     0
5530 DATA     170.0,     0,     0.0,    0.035,    0.0014,  103298,    13
5540 DATA    9999  ,     0,     0.0,    0.0  ,    0.0  ,       0,     0
5550 DATA 700.0
5560 DATA 1532.23, 0
5570 DATA 1529.24, 2.2E6
```

```
5580 DATA 1546.86, 11.01E6
5590 DATA 1560.58, 38.33E6
5600 DATA 1569.72, 61.68E6
5610 DATA 1577.34, 88.11E6
5620 DATA 1584.96, 123.35E6
5630 DATA 1591.06, 160.80E6
5640 DATA 1598.68, 202.65E6
5650 DATA 1606.30, 251.11E6
5660 DATA 1622.76, 383.27E6
5670 DATA 9999, 0
5680 DATA 1616.96, 0
5690 DATA 1618.71, 991.2
5700 DATA 1621.54, 5097.60
5710 DATA 1625.19, 5097.60
5720 DATA 9999, 0
5730 DATA 1566.45, 0
5740 DATA 1569.72, 566.40
5750 DATA 1579.52, 718.11
5760 DATA 1601.29, 849.60
5770 DATA 1620.88, 960.86
5780 DATA 1622.76, 960.86
5790 DATA 9999, 0
5800 DATA     0, 28.32
5810 DATA  1800, 84.96
5820 DATA  3600, 158.59
5830 DATA  7200, 212.40
5840 DATA 10800, 192.58
5850 DATA 14400, 130.27
5860 DATA 21600, 67.97
5870 DATA 28800, 42.48
5880 DATA 36000, 28.32
5890 DATA 99000, 28.32
5900 DATA 9999,0
```

APPENDIX D: NOTATION

A	Wetted cross section of flood channel
A_b	Wetted cross section of dam breach
A_s	Surface water area within reservoir
$A_{( )}$	Partial area of sliding wedge
b	Bottom width of the breach
B	Top width of the breach
B_D	Top width of the dam
c_o	Wave celerity
C	Cohesion
C_h	Chezy's coefficient of friction
C_i	Muskingum-Cunge coefficients (i = 1, 5)
C_i^*	Broad-crested weir discharge coefficients (i = 1, 2)
C_I	Integration constant
$C^{\pm}$	Wave characteristics
d	Depth of the breach
D_s	Representative size of sediment particles
D_{50}	Median size of sediment particles
e_i	Erodibility index
F	Breach Froude number
F_H	Seepage force
g	Acceleration due to gravity
G	Weight of sliding wedge
h	Hydraulic head
H	Reservoir water level
H_o	Initial reservoir water level
i	Imaginary number
I	Inflow into a channel segment
I_o	Inflow discharge
$J^{\pm}$	Riemann's quasi-invariants
K	Muskingum parameter
K_c	Erosion proportionality constant
K_E	Einstein-Brown formula constant
ℓ	Length of breach in the flow direction

ℓ_s	Minimum breach horizontal length
m	Number of nodes of each finite element
M	Mass of eroded material
n	Manning's coefficient of friction
N_i	Shape function (i = 1, 2, 3, 4)
$\emptyset$	Outflow from a channel segment
p	Soil porosity
q	Unit width discharge
q_{bw}	Bed-load discharge in weight per unit width
q_o	Lateral inflow
Q	Total outflow discharge
Q_b	Breach outflow discharge
Q_o	Crest overtopping discharge
Q_p	Peak outflow discharge
Q_s	Sediment discharge
Q_{sp}	Outflow discharge from spillway and powerhouse outlet
R_h	Hydraulic radius
s	Side slope (1V:sH)
S	Reach storage
S_f	Energy gradient
S_F	Breach shape factor
S_o	Slope of the channel
t	Time
t_d	Dam failure duration time
T	Top width of flood channel
u	Water velocity
V	Reservoir water storage capacity
¥	Water volume stored in reservoir
x	Distance
x_p	Horizontal projection of the sliding wedge
y	Water depth in flood channel
y_c	Critical depth
y_o	Depth of tailwater section
Z	Breach bottom elevation
Z_o	Initial dam height
α	Weighting factor in Muskingum method

α_1 Coefficient of discharge formula

α_2 Coefficient of erosion rate formula

β_1 Exponent of discharge formula

β_2 Exponent of erosion rate formula

γ Specific weight of water

γ_s Specific weight of soil

γ_1 Specific weight of saturated soil

γ_2 Specific weight of submerged soil

Δt Time step

Δx Length of channel segment

ΔZ Depth of scour

ζ Angle between shearing plane and horizontal

θ Angle between breach sides and vertical

ν Kinematic viscosity of water

τ Shear stress

ϕ Angle of repose of the soil

Φ Sediment transport rate function

$\chi^{(e)}$ Unknown variable within a finite element

χ_i Unknown variable at nodal point

Ψ Inverse of Shields dimensionless shear stress